MOUNTAIN-PLAINS CONSORTIUM

MPC 19-373 | Z. Carnahan, M. Mingo, M. Tazarv and N. Wehbe

Development of Alternative Bridge Superstructures for South Dakota Local Roads

MOUNTAIN-PLAINS CONSORTIUM REGION 8

A University Transportation Center sponsored by the U.S. Department of Transportation serving the Mountain-Plains Region. Consortium members:

Colorado State University
North Dakota State University
South Dakota State University
University of Colorado Denver
University of Denver
University of Utah
Utah State University
University of Wyoming

Development of Alternative Bridge Superstructures for South Dakota Local Roads

Zachary Carnahan
Michael Mingo
Mostafa Tazarv
Nadim Wehbe

Department of Civil and Environmental Engineering
South Dakota State University
Brookings, South Dakota

February 2019

Achnowledgements

This work was performed under the direction of the SD2014-14 Technical Panel:

Cody Axlund..... Local Government Assistance
Ron Bren..... Local Government Assistance
Aaron Breyfogle .....Research
Mark Clausen.....Federal Highway Administration
Justin Cook .....Research
Hadly Eisenbeisz ..... Bridge Design
Harvey Fitzgerald .....Research
Kevin Heiman ..... Yankton Office
Thomas Herman..... Road Design
Marc Hoelscher. Federal Highway Administration
Tom Kallemeyn ..... Bridge Design
Aaron Litka .....Research
Gregory Vavra ..... SDLTAP

The present study was jointly funded by the South Dakota Department of Transportation (SDDOT) and the US Department of Transportation (USDOT) through the Mountain-Plains Consortium (MPC) - University Transportation Center (UTC). Their support and guidance are greatly appreciated. The authors would like to thank Gage Brothers Concrete Products, Gruen-Wald Engineered Laminates, Inc., and Headed Reinforcement Corporation for their support and contributions throughout the project. The authors acknowledge the assistance and valuable feedback of Aaron Breyfogle of the Research Office at the South Dakota Department of Transportation, Jared Gusso of Journey Group Companies, and Zachary Gutzmer of South Dakota State University (SDSU).

ABSTRACT

The South Dakota Department of Transportation (SDDOT) allows the use of precast double-tee bridges in counties because they are economical and fast in construction. Alternative durable prefabricated bridge systems are needed to provide more options to local governments. The present study was carried out to investigate the feasibility of alternative prefabricated bridge systems that can be incorporated in South Dakota. The project technical panel approved testing of two superstructure bridge systems: (1) precast full-depth deck panels on prestressed inverted tee girders and (2) glulam timber bridges. The present report includes the design, construction, testing methods, and recommendations for the selected bridge alternatives. Three full-scale bridges, one fully precast and two glulam timber, were tested under fatigue and ultimate loading. The precast bridge specimen was 50-ft long by 9.5-ft wide. No significant damage beyond the prior-to-testing shrinkage cracks was observed throughout the entire fatigue test, and the overall bridge stiffness did not deteriorate. The strength load testing showed that the load amplitude at the first crack was higher than the AASHTO Service and Strength I limit state loads, indicating sufficient performance. Based on the construction, testing, and cost analysis, it was concluded that the precast full-depth deck panels on prestressed inverted tee girder bridge is a viable alternative to the double-tee girder bridge. The full-scale glulam girder bridge test model was 50-ft long and 9.25-ft wide. The full-scale glulam slab bridge was 16.5-ft long and 8-ft wide. Both timber bridge types showed minimal damage during fatigue testing. The only damage to the girder timber bridge was cracking of tongue-and-groove deck-to-deck connections, which can be eliminated using flat-end panels. Ultimate testing of the two bridge systems confirmed that the AASHTO design method for timber bridges is adequate. Girders of glulam bridges should be designed as fully non-composite members. Based on the construction, testing, and cost analysis, it was concluded that both types of glulam timber bridges are viable alternatives to the double-tee girder bridges.

TABLE OF CONTENTS

LIST OF TABLES

LIST OF FIGURES

TABLE OF ACRONYMS

Acronym	Definition
AASHTO	American Association of State Highway and Transportation Officials
ABC	Accelerated Bridge Construction
ACM	Advanced Composite Material
ADT	Average Daily Traffic
ADTT	Average Daily Truck Traffic
AFRP	Aramid Fiber Reinforced Polymer
AITC	American Institute of Timber Construction
ANSI	American National Standards Institute
ASD	Allowable Stress Design
AWC	American Wood Council
CFCC	Carbon Fiber Composite Cable
CFRP	Carbon Fiber Reinforced Polymer
CIP	Cast-in-Place
COF	Coefficient of Friction
DOT	Department of Transportation
FE	Finite Element
FHWA	Federal Highway Administration
ft	Foot or feet
FDDP	Full-Depth Deck Panels
HSS	Hollow Structural Steel
in.	Inch or Inches
kip	Kilo Pound = 1000 Pounds
klf	Kip per Linear Foot
ksi	Kip per Square Inch
lbs	Pounds
LMC	Latex Modified Concrete
LRFD	Load and Resistance Factor Design
LTAP	Local Transportation Assistance Program
LVDT	Linear Voltage Differential Transformer
m	Meter
mm	Millimeter
NBI	National Bridge Inventory
NCHRP	National Cooperative Highway Research Program

Acronym	Definition
NDS	National Design Specification for Wood Construction
PCI	Precast/Prestressed Concrete Institute
psi	Pound per Square Inch
SD	South Dakota
SDDOT	South Dakota Department of Transportation
SDSU	South Dakota State University
SLT	Stress-Laminated Timber
UHPC	Ultra-High Performance Concrete
VDOT	Virginia Department of Transportation
VHPC	Very-High Performance Concrete

1. EXECUTIVE SUMMARY

1.1 Introduction

The precast prestressed double-tee girder bridge system is commonly used on South Dakota's local roads due to its economical and rapid construction. However, many double-tee bridges have been deteriorating faster than the 75-year design life. Furthermore, the double-tee bridge system has only one supplier in South Dakota. Alternative durable precast or prefabricated bridge systems are needed to provide more options to local governments when designing a new bridge. Alternatives will also give local governments more flexibility to select the best system by comparing performance, availability, durability, and cost of various options. This study was carried out to investigate the feasibility and structural performance of three alternative prefabricated bridge systems that could be incorporated in South Dakota.

1.2 Problem Description

Many U.S. bridges are in need of replacement. Of the 5,870 bridges in South Dakota, 1,208 are structurally deficient and 237 are functionally obsolete according to the Federal Highway Administration (FHWA, 2012). The South Dakota Department of Transportation (SDDOT) owns approximately 30% of South Dakota bridges, and the rest are owned by local governments. Although 90% of state-owned bridges are not deficient, a large portion of bridges owned by local governments are either structurally deficient or functionally obsolete mainly due to inadequate maintenance. Local governments rely on SDDOT to help replace them, but with limited resources, SDDOT can only help replace about 30 bridges statewide each year, causing a backlog of local bridges in need of replacement.

The most common bridge type on South Dakota local roads is the double-tee girder bridge with more than 700 currently in service in the state. Bridges are often designed for a service life of 75 years, but many of current double-tee bridges in South Dakota are deteriorating or are in need of replacement after only 40 years of service.

Double-tee bridges are used because of their ease of construction, reduced construction time, and relatively low cost. With only one double-tee bridge supplier in the state, alternative systems are needed to provide local governments more options when designing a new bridge or replacing a deteriorated one. Alternative systems and suppliers allow local governments to select the best system by comparing performance, availability, durability, and cost of different options. Feasibility and performance of three full-scale prefabricated bridge systems, one precast concrete bridge and two glued laminated (glulam) timber bridges, were investigated in the present study.

1.3 Research Work

Three full-scale prefabricated bridge specimens were tested at the Lohr Structures Laboratory at South Dakota State University (SDSU): (1) a fully precast bridge consisting of two precast inverted tee girders supporting five precast full-depth deck panels, (2) a glulam timber bridge consisting of three glulam girders and 13 glulam deck panels connected using epoxy, and (3) a glulam timber bridge consisting of two glulam deck panels placed in the longitudinal direction of the bridge connected together incorporating three glulam stiffeners. Each specimen represented approximately one lane of traffic. The main objective of the laboratory tests was to evaluate the structural performance of the proposed systems under fatigue and ultimate loading.

Each specimen was subjected to cyclic loading representative of the American Association of State Highway and Transportation Officials (AASHTO) Fatigue II limit state, then tested to failure under increasing monotonic loads. Fatigue II loading was included in this study to investigate the effect of the

maximum stress ranges that could result from an average daily truck traffic (ADTT) of 15 for 75 years of service. Stiffness tests were performed after every 10,000 or 50,000 fatigue load cycles to investigate bridge deterioration. Finally, a strength test was carried out for each specimen to study the bridge performance under AASHTO service and strength limit states, and to understand the bridge failure mode.

1.4 Research Findings

The following is a summary of the experimental findings, constructability, and cost estimate for the three bridge systems considered in this study.

1.4.1 Fully Precast Bridge (Full-Depth Deck Panels on Inverted Tee Girders)

- The design of the proposed bridge system was simple, and the bridge assembly was easy and fast without the need for advanced technologies or skilled labor.
- The proposed bridge system did not exhibit any sign of deterioration or water leakage through 500,000 Fatigue II load cycles (equivalent to 91 years of service) and an additional 150,000 Fatigue II load cycles adjacent to the middle panel transverse joints (equivalent to 27 years of service). The overall stiffness of the proposed bridge system essentially remained the same throughout the fatigue testing.
- Shrinkage cracks were observed at 125,000 load cycles in almost all of the full-depth shear pockets, all of the transverse joints, and the grouted haunch. These cracks were shallow since there was no water seepage when the deck was tested for water leaks.
- The first horizontal shear cracks in the grouted haunch region were observed at an actuator load of 200 kips, which was higher than the equivalent AASHTO Strength I limit state load of 131 kips.
- Both inverted U-shape shear studs and double-headed shear studs performed adequately through the entire fatigue testing and the ultimate test.
- The hidden pocket detail was found to be a better alternative than the full-depth pockets since they provided a better durability. Shrinkage cracks were observed in almost all full-depth pockets, but none in the hidden pockets.
- The bridge girders did not crack until the applied load exceeded the equivalent Strength I limit state load, indicating adequate design and performance.
- The superstructure materials and fabrication cost for the proposed system for a 50-ft long by 34.5-ft wide bridge was estimated to be 11% higher than that for a double-tee bridge with the same geometry.

Overall, it was concluded from the design, construction, testing, and cost estimate that the proposed bridge system—full-depth deck panels supported on inverted tee girders—is a viable alternative to precast double-tee girder bridges.

1.4.2 Glulam Timber Girder Bridge

- Construction of a glulam girder bridge is fast and does not require any advanced technology or skilled labor.
- The girder bridge did not exhibit any signs of deterioration throughout the 500,000 AASHTO Fatigue II load cycles (equivalent to 91 years of service), and the bridge overall stiffness essentially remained constant throughout the fatigue testing.

- Damage of tongue-and-groove deck-to-deck connections was observed at 250,000 load cycles (equivalent to 45 years of service). The damage can be eliminated by connecting flat deck panels with epoxy, instead of using a tongue-and-groove connection.
- Although there was partial composite action between the glulam girders and the glulam deck panels, it was not sufficient to warrant composite design. Glulam timber girders should be designed as fully non-composite sections.
- The epoxy connection between the glulam deck and the glulam girder performed adequately throughout fatigue and strength testing.
- The girder bridge did not meet the AASHTO service and strength limit state requirements under strength testing because, by mistake, a wrong grade of wood was used in the fabrication. Furthermore, the girders were designed assuming a partial composite action. A calculation of the bridge capacity assuming the non-composite behavior, and using the as-built material properties and bridge geometry, led to accurate estimations of the bridge test model capacities. Therefore, the current AASHTO method of design for this type of bridge is valid.
- The superstructure cost for a 50-ft long by 34.5-ft wide glulam timber girder bridge was estimated to be 70% of that for a double-tee bridge with the same geometry.

1.4.3 Glulam Timber Slab Bridge

- Construction of a glulam slab bridge is fast and does not require any advanced technology or skilled labor.
- The slab bridge did not exhibit any signs of deterioration through the 550,000 AASHTO Fatigue II load cycles (equivalent to 50 years of service). The bridge overall stiffness essentially remained constant throughout the fatigue testing.
- No damage was observed during the ultimate testing at an actuator load of 270 kips, which was three times higher than the AASHTO Strength I limit state load of 85.7 kips. The test was stopped due to setup limitations.
- The current AASHTO method of design for this type of bridge is valid.
- The superstructure cost per square foot for a 16.5-ft long by 34.5-ft wide glulam slab bridge was estimated to be only 50% of that for a typical double-tee bridge.

Overall, it was concluded from the design, construction, testing, and cost estimate that both types of the glulam timber bridges are viable alternatives to the precast double-tee girder bridges. The AASHTO method of design for timber bridges can be utilized for the design of these types of bridges.

1.5 Recommendations

Based on the findings of this study, the research team offers the following recommendations.

1.5.1 Recommendation 1: Precast Full-Depth Deck Panel Bridges

The guidelines, as detailed in Section A.1 of Appendix A, should be adopted for the construction of "precast full-depth deck panel bridges." A span length of 40 ft to 70 ft is recommended for this bridge type.

Precast full-depth deck panel bridges generally consist of precast inverted tee girders and precast full-depth deck panels. The test results of a full-scale 50-ft long precast full-depth deck panel bridge showed that this bridge type is a viable alternative to double-tee girder bridges, which are common in South Dakota. To minimize durability issues due to cold joints, (1) only hidden pocket detailing was allowed, (2) all bridge deck reinforcement was recommended to be epoxy coated, and (3) hollow structural steel sections, which are used to reduce the splice length, was recommended to be galvanized. These precast bridges with the recommended span lengths are constructible in South Dakota and may cost slightly more than double-tee bridges.

1.5.2 Recommendation 2: Glulam Timber Girder Bridges

The guidelines, as detailed in Section A.2 of Appendix A, should be adopted for the construction of "glulam timber girder bridges." A span length of 30 ft to 70 ft is recommended for this bridge type.

Glulam timber girder bridges generally consist of glulam girders, glulam deck panels, and diaphragms. The test results of a full-scale 50-ft long glulam girder bridge showed that this bridge type is a viable alternative to double-tee girder bridges. Glulam timber bridges with the recommended span lengths can be fabricated in South Dakota and will be more cost-effective than double-tee bridges.

1.5.3 Recommendation 3: Glulam Timber Slab Bridges

The guidelines, as detailed in Section A.3 of Appendix A, should be adopted for the construction of "glulam timber slab bridges." A span length of 30 ft or less is recommended for this bridge type.

Glulam timber slab bridges generally consist of glulam deck panels and glulam stiffeners. The test results of a full-scale 16.5-ft long glulam slab bridge showed this bridge type is a viable alternative to double-tee girder bridges. Currently, glulam slab bridges with a span length of 20 ft can be fabricated in South Dakota, and will be more cost-effective than double-tee or glulam timber bridges.

2, INTRODUCTION

2.1 Problem Description

Numerous bridges in the South Dakota local highway system are in need of replacement. South Dakota has 5,870 bridges, of which 1,208 are structurally deficient and 237 are functionally obsolete according to the Federal Highway Administration (FHWA, 2012). This equates to 24.6% of bridges in the state being structurally deficient or functionally obsolete. There are more than 700 bridges in South Dakota with precast double-tee girder systems. This type of bridge is very common since it is economical and quick to construct. Bridges are designed for a service life of 75 years, but many double-tee bridges have not met that expectation because of deterioration or the need for replacement after about half the expected service live.

The main problem associated with the currently used precast double-tee bridge in South Dakota (Fig. 2.1) is that it is prone to reflective cracking along the longitudinal joints. The cause is an inadequate longitudinal joint detail that utilizes discrete welded plates to transfer shear forces through the joint. The reflective cracking provides a pathway for water and deicing agents to seep through the joint, spall the concrete, and sometimes reach the girder topmost prestressing steel tendon. Deterioration is initiated when the joint cracks, followed by corrosion of steel plates and girder top reinforcement.

There is currently only one double-tee girder supplier in the state. Alternative durable bridge systems are needed to provide more design options to local governments. Different alternatives will also give local governments more flexibility to select the best system by comparing the performance, availability, durability, and cost. The present study was carried out to investigate the feasibility and structural performance of three alternative prefabricated bridge systems that can be deployed in South Dakota: fully precast superstructure consisting of inverted tee girders and full-depth deck panels, glulam girder, and glulam slab bridges.

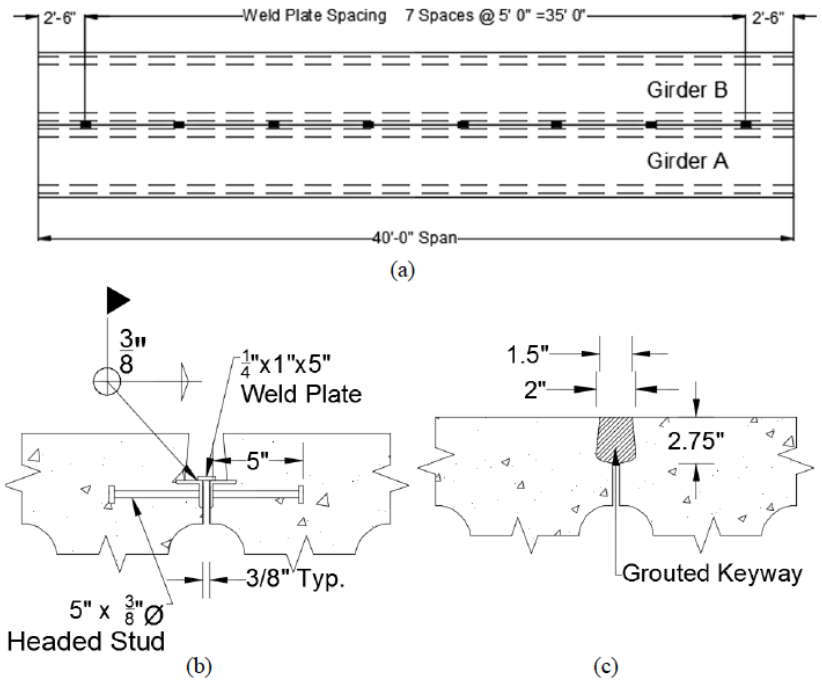

Figure 2.1 Current Double-Tee Bridge Longitudinal Joint Detailing (Konrad, 2014)

2.2 Research Objectives

The main research objectives and activities carried out to achieve these goals are briefly discussed in this section.

2.2.1 Identify Alternatives to Double-Tee Bridges

Determine bridge system alternatives to the double-tee precast girder system meeting HL93 load requirements and 75-year design life for single span bridges of less than 70 feet.

An extensive review of the literature and practice at the state and national levels was performed, and local precast companies were consulted to find feasible alternatives to the double-tee bridges. Based on the typical properties of local bridges, a few criteria were selected to narrow down the literature review to alternatives that (1) are suitable for single-span bridges with a length of 70 ft or less, (2) can withstand the AASHTO HL93 load, (3) are designed for a service life of at least 75 years, and (4) incorporate accelerated bridge construction (ABC) techniques. Nine bridge systems were identified, and a summary of findings was submitted for discussion with the project technical panel. The panel selected two bridge systems for further investigation: a fully precast bridge model and two types of glulam timber bridges.

2.2.2 Experimental Programs

Perform ultimate and fatigue load testing on alternative bridge system(s).

Three full-scale prefabricated bridge specimens were tested at the Lohr Structures Laboratory at South Dakota State University (SDSU): (1) a fully precast bridge consisting of two precast inverted tee girders supporting five precast full-depth deck panels, (2) a glulam timber girder bridge consisting of three glulam girders and 13 glulam deck panels connected using epoxy, and (3) a glulam timber slab bridge consisting of two glulam deck panels placed in the longitudinal direction of the bridge connected together incorporating three glulam stiffeners. Each specimen represented approximately one lane of a typical bridge. The main objective for the laboratory tests was to evaluate the structural performance of the proposed systems under fatigue and ultimate loading.

2.2.3 Evaluation of Different Bridge Alternatives

Compare cost, construction process, and performance of alternative bridge system(s) to the revised double-tee girder system from SD2013-01.

The constructability, structural performance, and costs of the three alternative bridge systems were compared with those of the modified and original double-tee bridges. Comparisons were made with the results obtained from project SD2013-01. Detailed design and construction guidelines were proposed to facilitate the implementation of the new bridges.

3. LITERATURE REVIEW

A comprehensive review of literature and practice was performed. Nine bridge systems were identified as potential candidates for implementation in South Dakota: (1) full-depth deck panels supported by precast girders, (2) voided slab bridges, (3) ultra-high performance concrete (UHPC) waffle deck panels, (4) carbon fiber composite cable-prestressed decked tee beams, (5) bridge decks reinforced with aramid fiber reinforced polymer, (6) stress-laminated timber bridge decks, (7) glulam timber bridges, (8) advanced composite material bridges, and (9) recycled plastic bridges. Among those nine choices of bridge systems, a full-depth precast panel on precast girders and two glulam designs were selected by the technical panel for testing. This section presents the findings of the literature review on the selected bridges systems. Information regarding the other bridge systems can be found in Mingo (2016) and Carnahan (2017).

3.1 Full-Depth Deck Panels Supported on Prefabricated Girders

The main components of a full-depth deck panel (FDDP) system are typically precast full-depth concrete deck slabs, prestressed concrete or steel girders, transverse joints, longitudinal joints, shear pockets, and horizontal shear reinforcement. The findings of the literature review on these components are briefly discussed.

3.1.1 Transverse Joints

Different connection details have been developed for transverse joints of FDDP systems. The detailing usually incorporates longitudinal post-tensioning to aid in moment and shear transfer and to prohibit reflective cracking. However, post-tensioning was not preferred in the present study, since many local counties may not have the technology and skilled labor to utilize post-tensioning.

It is also common to splice the longitudinal steel reinforcement of precast deck panels to avoid post-tensioning. Badie and Tadros (2008) reported that some highway agencies (e.g., the Alaska and New Hampshire DOTs) did not use any reinforcement crossing the transverse joint (Fig. 3.1). The Alaska DOT has not reported any significant joint cracking or leakage on simply supported bridges on low-volume traffic roads when there was no reinforcement in the transverse joints (Badie and Tadros, 2008).

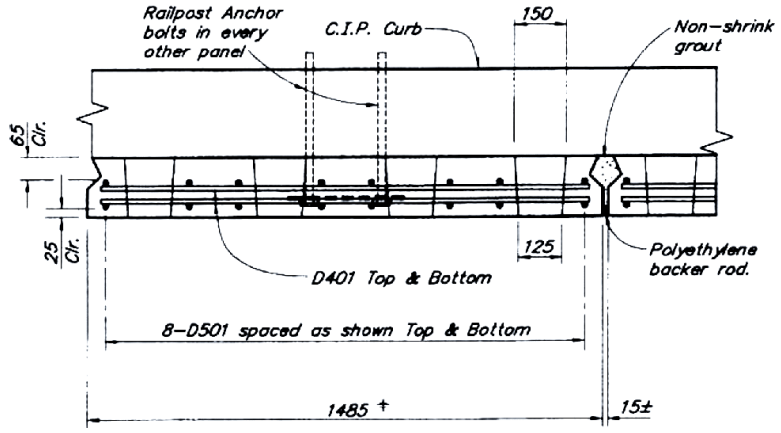

Figure 3.1 Transverse Joint Detailing for Precast Deck Panel Bridges in Alaska (Badie and Tadros, 2008)

3.1.1.1 Shear Key Types

Various shear key details exist for FDDP systems (Fig. 3.2). Shear keys transfer both shear forces and bending moments. The shear force transfer is achieved through a combination of bearing against the concrete-grout surfaces and the bond between the concrete-grout surfaces.

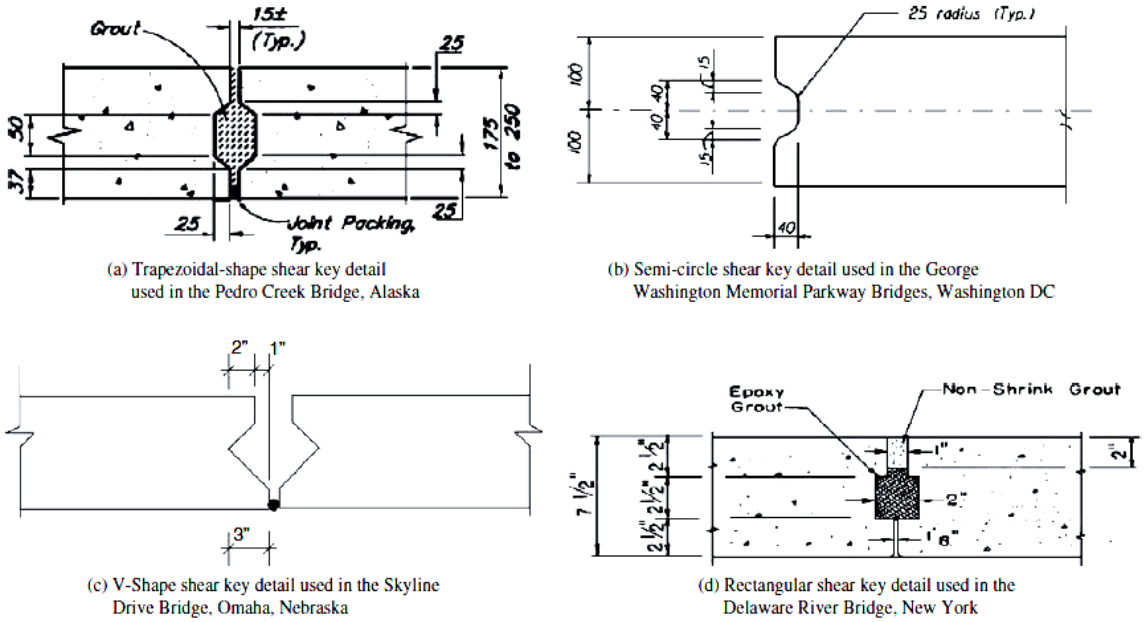

(a) Trapezoidal-shape shear key detail used in the Pedro Creek Bridge, Alaska

(b) Semi-circle shear key detail used in the George Washington Memorial Parkway Bridges, Washington DC

(c) V-Shape shear key detail used in the Skyline Drive Bridge, Omaha, Nebraska

(d) Rectangular shear key detail used in the Delaware River Bridge, New York

Figure 3.2 Grouted Female-to-Female Shear Key Details for Transverse Joints (Badie and Tadros, 2008)

Two methods have been used to contain the grout poured into the shear keyways: inserting a polyethylene backer rod toward the bottom of the keyway, and using wood formwork placed from under the panel. Badie and Tadros (2008) recommended roughening the surface of the shear key for deck systems that do not include post-tensioning.

3.1.1.2 Block-out with Tied-in Lap Splice and Spiral Confinement

For block-out with tied-in lap splice and spiral confinement configurations, the transverse joint detail consists of a series of block-outs along the joint (Fig. 3.3). Bridge deck longitudinal reinforcement extends from panels into the block-outs, and a steel bar is tied to the deck longitudinal reinforcement. Steel spirals are used to confine the concrete, shorten the lap splice length by 40% to 50%, and simplify the construction, since deck steel does not extend into the transverse joint (Badie and Tadros, 2008).

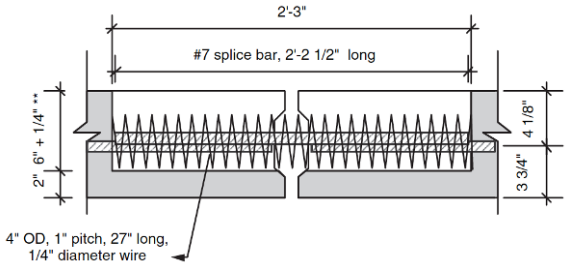

(a) Detailing of Block-out with Tied-in Lap Splice and Spiral Confinement (Badie and Tadros, 2008)

(b) Photogram of Block-out with Tied-in Lap Splice and Spiral Confinement (Badie et al., 1998)

Figure 3.3 Spiral Confinement Detailing for Transverse Joints

3.1.1.3 Hollow Structural Steel Confinement

Badie and Tadros (2008) developed two new FDDP transverse joints with external confinement (Figs. 5.4 and 5.5) in which hollow structural steel (HSS) tubes are embedded in the FDDP decks adjacent to the transverse joint. Figure 3.4 shows the detailing for one of the joints. Deck steel bars are extended out the transverse joint on one side of the slab and are inserted into the HSS tube in the adjacent slab during construction.

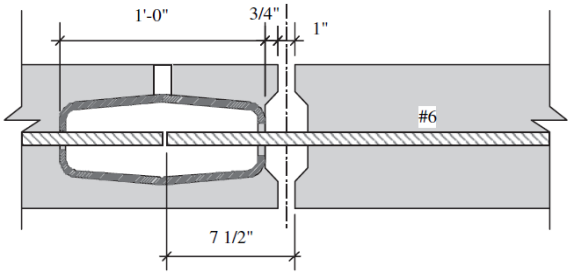

(a) HSS Tube Confinement Detail

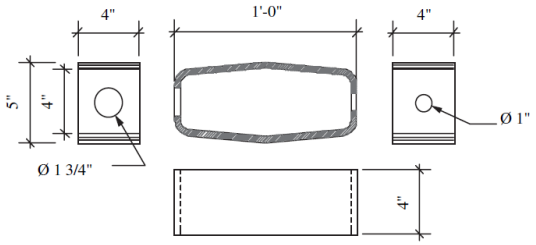

(b) Galvanized Bulged HSS 4x12x3/8 in.

Figure 3.4 HSS Tube Confinement Details for Transverse Joints (Badie and Tadros, 2008)

Figure 3.5 shows the detailing for another joint, in which HSS tubes are embedded in both adjacent panel transverse joints. Deck steel bars are extended into the HSS tubes. The main difference with respect to the first detailing is that the top portion of the HSS tube is open to allow placement of deck steel bars in the HSS tubes. It should be noted that these types of joints have a tight construction tolerance.

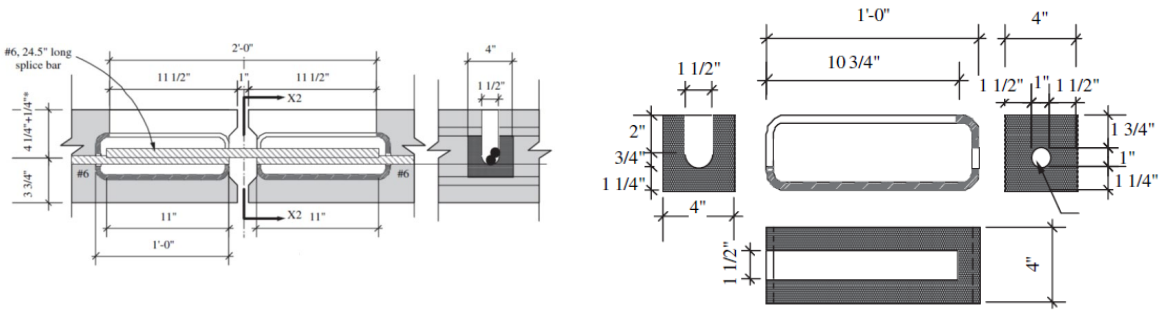

(a) HSS Tube Confinement Detail (b) Galvanized Bulged HSS 4x12x3/8 in.

Figure 3.5 Adjacent HSS Tube Confinement Details for Transverse Joints (Badie and Tadros, 2008)

3.1.1.4 UHPC for Transverse Joints

Graybeal (2010) tested various transverse joint details incorporating ultra-high performance concrete (UHPC) as joint filler. One detail consisted of non-contact headed mild-steel reinforcement extending from the bridge deck into the joints. Figure 3.6 shows the layout and rebar plan of the connection. Two No. 5 bars were placed along the length of the connection between the heads. Another connection consisted of epoxy-coated No. 4 hairpin bars extending from the deck into the joint (Fig. 3.7). Two No. 5 bars were placed inside the hairpins along the length of the joint. The third detail consisted of straight lapped No. 5 mild-steel reinforcement extending from the deck into the joint (Fig. 3.8). Two No. 5 bars were placed along the length of the connection between the top and bottom layer of joint reinforcement.

No cracking between the UHPC and the precast panels was observed during cyclic loading. Furthermore, no rebar de-bonding occurred in the joints of the test specimens. Cracks propagated perpendicular to the transverse joints when subjected to ultimate loading. The joint details tested by Graybeal (2010) are expected to perform sufficiently in the field.

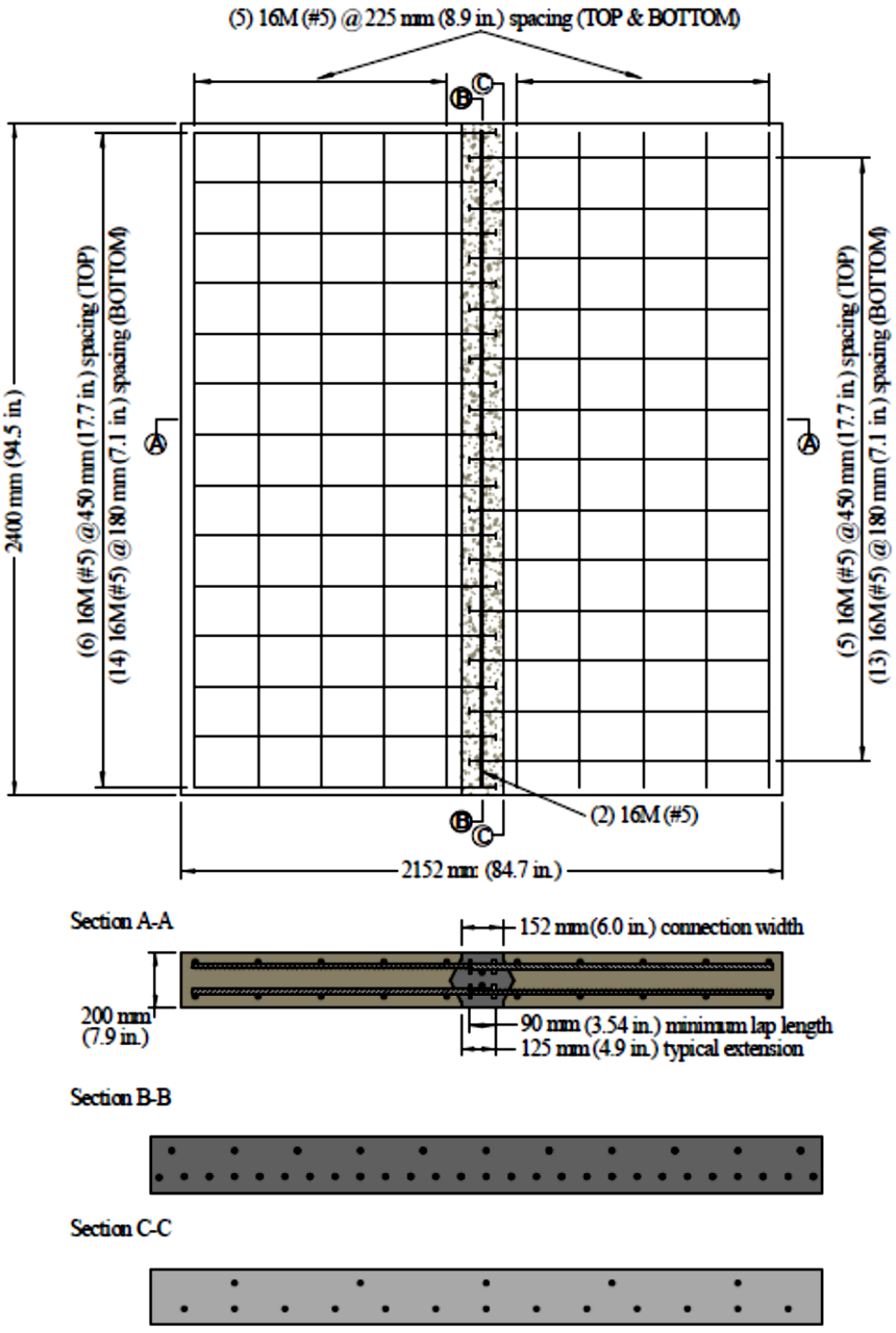

Figure 3.6 UHPC and Headed Steel Bars for Transverse Joints (Graybeal, 2010)

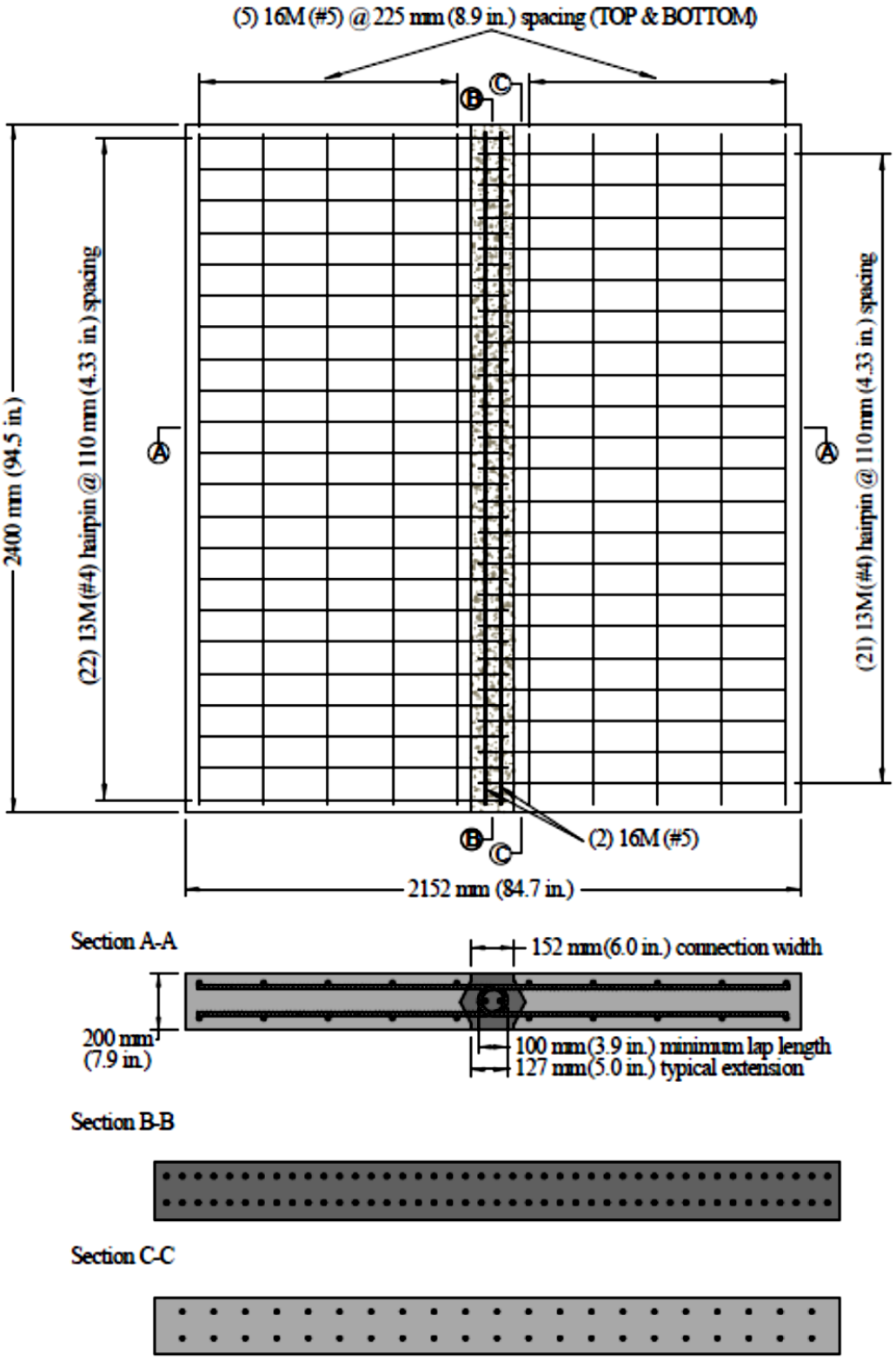

Figure 3.7 UHPC and Hairpin Steel Bars for Transverse Joints (Graybeal, 2010)

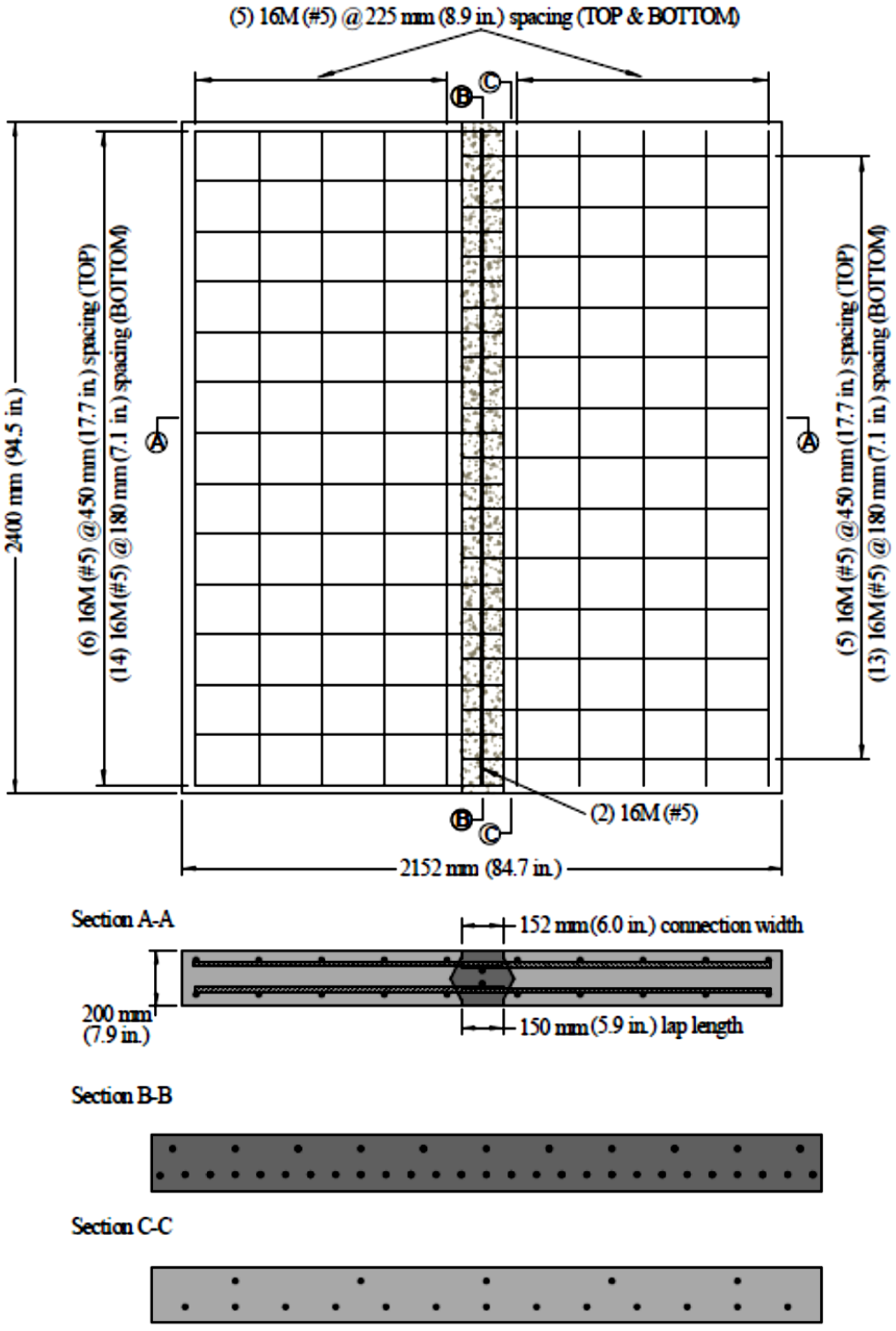

Figure 3.8 UHPC and Straight Lapped Steel Bars for Transverse Joints (Graybeal, 2010)

3.1.2 Longitudinal Joint

For FDDP systems, a longitudinal joint is usually used at the centerline of the bridge in the direction of traffic to allow the bridge to be crowned for water drainage. Typically, U-shape steel bars are extended from two adjacent panels to splice the panels and to provide reinforcement continuity to resist bending moments and shear forces. Longitudinal steel bars are installed along the length of the bridge inside the U-shape bars to increase the bond strength. The Bill Emerson Bridge in Missouri is an example of such longitudinal joint detail (Fig. 3.9).

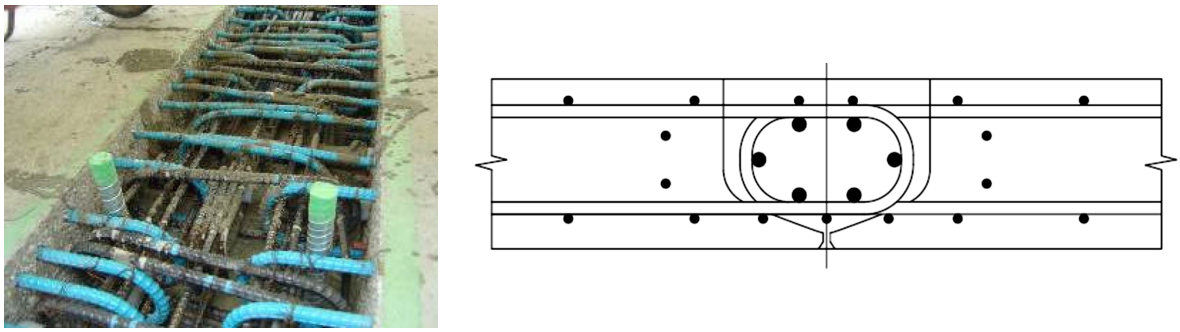

(a) Photograph of Longitudinal Joint (b) Detailing of Longitudinal Join

Figure 3.9 Longitudinal Joint Detail of Bill Emerson Memorial Bridge, Missouri DOT (Badie and Tadros, 2008)

Aaleti and Sritharan (2014) developed a UHPC waffle deck panel system with a longitudinal joint consisting of 1-in. diameter straight dowel bars extending from the deck into the joint and bars running along the length of the joint to aid in development of the dowel bars. Figure 3.10 shows the longitudinal joint detailing for the UHPC waffle deck panel system.

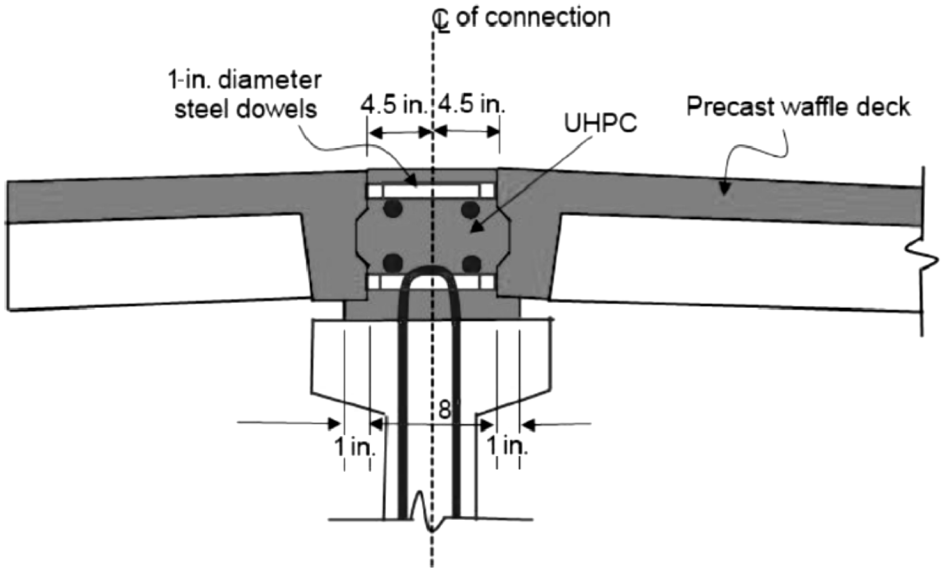

Figure 3.10 Longitudinal Joint Detailing for UHPC Waffle Deck Panel System (Aaleti and Sritharan, 2014)

3.1.3 Shear Pockets

The shear pockets connect the concrete panels to the girder to create composite action. Scholz (2007) performed a shear pocket connections study, which was funded by the Virginia DOT. Eight various grout types were investigated to determine the best grout. This study also investigated the bond between the girder-grout and grout-deck interfaces. Flow and workability, horizontal shear strength with two planes of shear, various shear pocket reinforcement types, grout compressive and tensile strength, shrinkage, and bond strength between the grout-to-concrete interface were measured. Both grout and extended grout with pea gravel were utilized. Inverted U-shape stirrups and headed shear studs were tested through push-off tests.

Two grouts were found to be suitable for use in an FDDP system based on this research: Five Star® Highway Patch and Set® 45 Hot Weather. Two types of shear reinforcement between the precast concrete I-beams and bridge deck panels were tested, and they provided adequate shear resistance. These included two No. 4 or No. 5 bars extending from the I-beam into the shear pocket and headed shear studs, which were welded to steel plates embedded in the I-beams.

Badie et al. (2006) developed two types of shear pockets that can be used in FDDP systems: partial-depth and full-depth shear pockets (Figures 3.11 and 3.12, respectively). The partial-depth shear pocket was recommended when no overlay is used to protect the deck from water leakage at the grout and surrounding concrete interface.

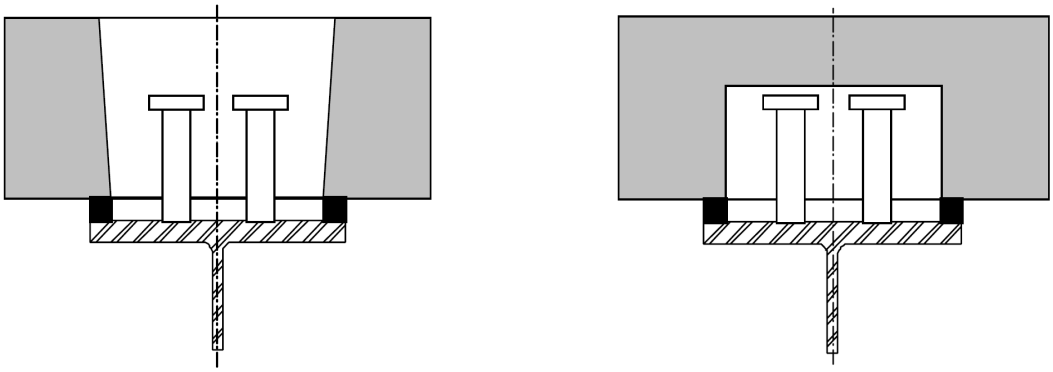

Figure 3.11 Shear Pocket Details (Badie et al., 2006)

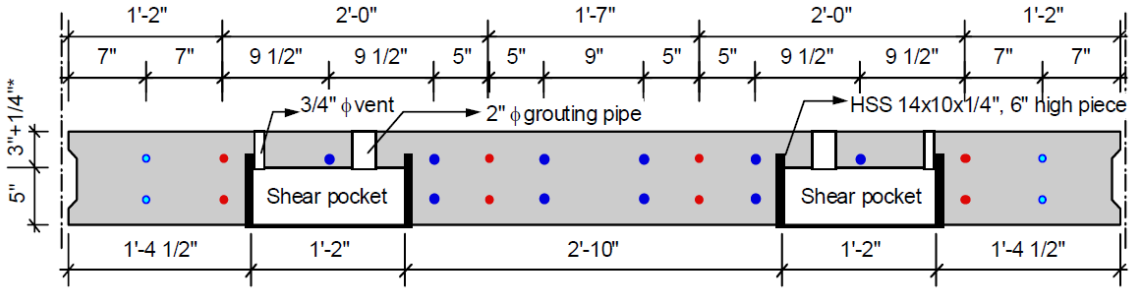

Figure 3.12 FDDP System with Partial-Depth Shear Pockets (Badie et al., 2006)

3.1.4 Horizontal Shear Reinforcement

Two types of reinforcement detailing were previously used to transfer horizontal shear forces between the girder and the deck: inverted U-shape bars and headed shear studs (Figures 3.13 - 3.15). The U-shape bars placed transversely minimize the length of shear pockets, and the U-shape bars placed longitudinally can be used in girders with small web widths. The headed shear stud detail (Fig. 3.15) proposed by Badie and Tadros (2008) requires welding of shear studs to a steel plate and embedding the plate in the top flange of the prestressed concrete girder.

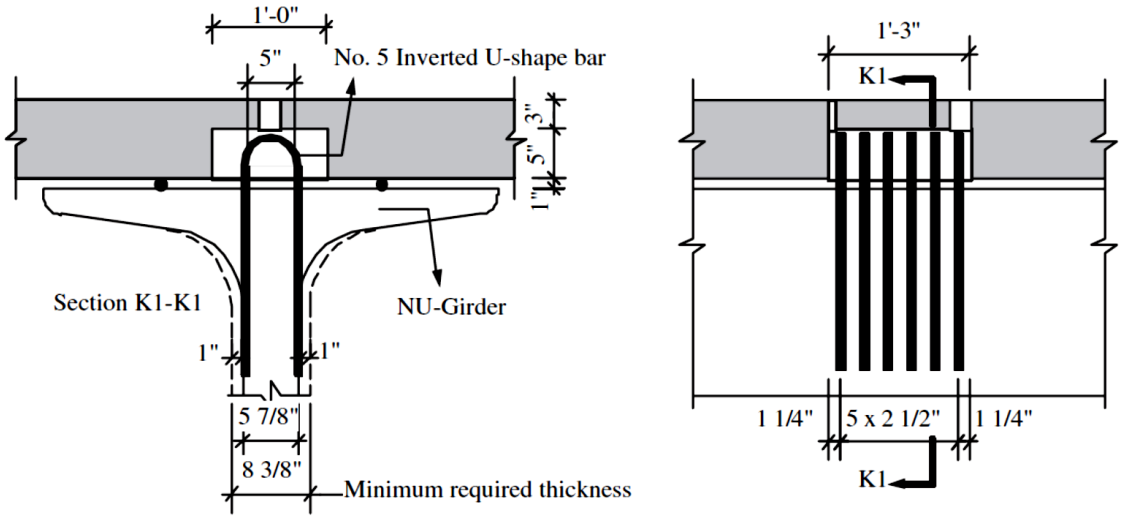

Figure 3.13 Inverted U-shape Horizontal Shear Reinforcement Placed Transversely (Badie and Tadros, 2008)

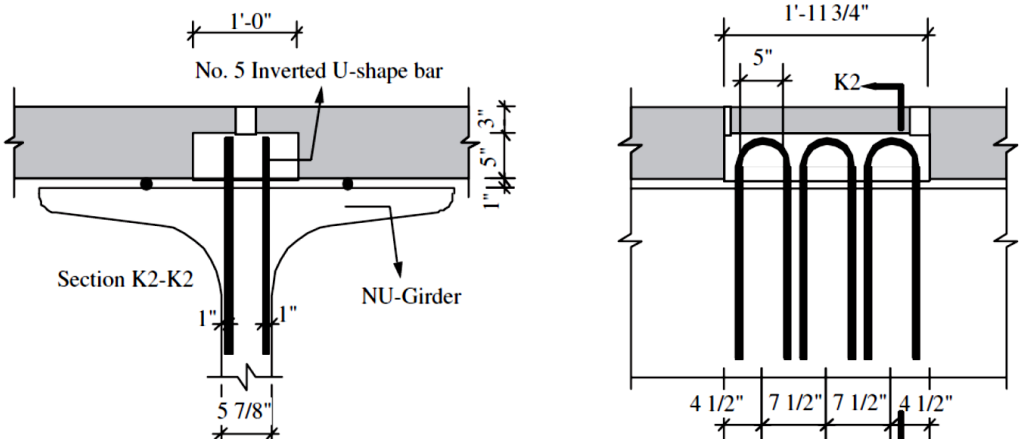

Figure 3.14 Inverted U-shape Horizontal Shear Reinforcement Placed Longitudinally (Badie and Tadros, 2008)

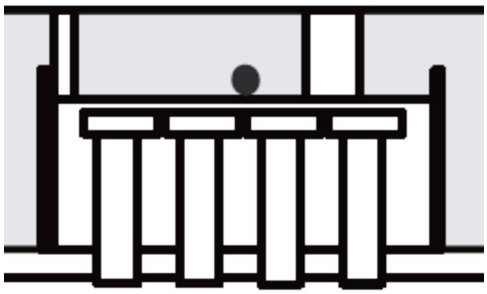

Figure 3.15 Headed Stud Horizontal Shear Reinforcement (Badie and Tadros, 2008)

3.2 Glulam Timber Bridges

This section includes a summary of findings in the literature review on the feasibility, performance, and past application of two different glulam timber bridge systems.

3.2.1 Overview of Glulam Timber Bridges

Glulam timber bridges (Fig. 3.16) are constructed of glulam members manufactured from lumber laminations bonded together on their wide faces with waterproof structural adhesives. According to Ritter (1990), glulam is the most common material used for the fabrication of timber bridges because glulam members can be manufactured to any size and shape. In general, the span length of glulam bridges ranges from 20 to 80 ft, but construction of longer bridges with span lengths of 140 ft or longer is possible (Ritter, 1990). Important design and construction considerations, such as design method, wearing surfaces, railing systems, and abutments, are discussed in the following sections.

Figure 3.16 Glulam Timber Bridge in Buchanan County, Iowa

Wood is a renewable material readily available in South Dakota. Ritter (1990) states that glulam timber bridges are very economical, light-weight, easy to fabricate, and environmentally friendly. Construction of glulam timber bridges is relatively simple and usually can be done without highly skilled labor. Since they can be fabricated off-site and installed in place in a short period of time, glulam bridges are suitable for accelerated bridge construction (ABC) and can be installed in most weather conditions.

Glulam timber bridges are not very common; therefore, data on the long-term performance of such bridges is scarce. Timber bridges will deteriorate rapidly if exposed to moisture for a long duration;

therefore, frequent inspection and retreating are needed. Early detection of moisture is critical in extending the life of timber bridges (Ritter 1990).

3.2.2 Types of Glulam Timber Bridges

Two main types of glulam timber bridges have been used in the field: longitudinal glulam deck bridges (Fig. 3.17a), and transverse glulam deck bridges (Fig. 3.17b). The former type consists of glulam deck panels, which are typically 4-ft wide, spanning in the longitudinal direction of the bridge. These panels are held together by transverse stiffeners, which cannot be spaced more than 8-ft apart. The longitudinal glulam deck bridges can only span up to 38 ft (Wacker and Smith, 2001). The latter type of glulam bridge consists of transverse glulam deck panels supported by stringers placed in the longitudinal direction of the bridge. The deck panels are typically 4-ft wide and the stringers are typically spaced at 4-ft intervals. These bridges typically span up to 80 ft.

(a) Longitudinal Glulam Deck (Slab Bridge) (b) Transverse Glulam Deck (Girder Bridge)

Figure 3.17 Glulam Timber Bridge Types

3.2.3 Timber Bridge Structural Components

The material and various structural components of a glulam timber bridge including girders, deck panels, connections, and stiffeners, are discussed herein.

3.2.3.1 Glulam Materials

Timber is a nonhomogeneous and brittle material as evidenced by bending and axial compressive behavior (Fig. 3.18). The strength of glulam timber is evaluated (rated) either mechanically or visually. Design values for typical glulam timber are specified in section 8 of AASHTO LRFD Bridge Design Specifications (AASHTO, 2013). Other glulam materials and species are allowed by the code, however. These design values are then adjusted by correction factors as specified by AASHTO, accounting for several parameters affecting the behavior of wood, such as wet service conditions, temperature, member size, member volume, and load duration.

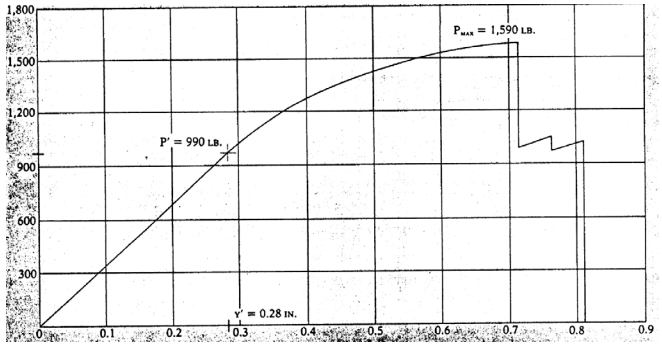

Vertical Axis = Load (lb)
Horizontal Axis = Displacement (in.)

(a) Force-Displacement Relationship under Bending

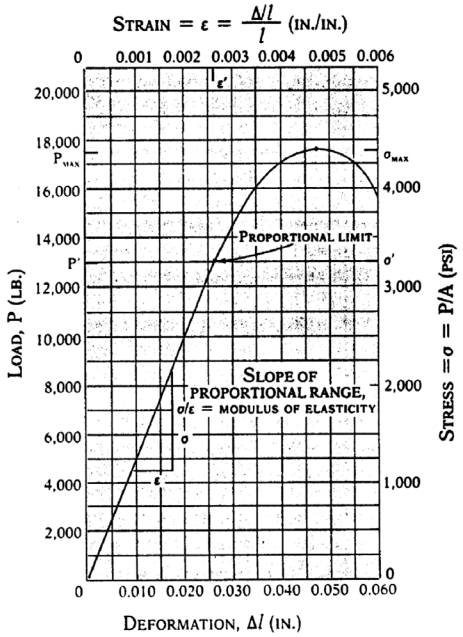

(b) Axial Compressive Behavior

Figure 3.18 Force-Displacement Relationship for Wood (after Hoadley, 1980)

3.2.3.2 Girders (Stringers)

The size of glulam girders varies based on the bridge span length, the girder spacing, lamination species, and design loads. The nominal width of a glulam girder typically ranges from 8 to 12 in. The nominal depth of a glulam girder can vary from 12 to 60 in. The lamination species is selected based on the availability of the material and the cost. Southern Pine is the most commonly used species for wood bridge girders in South Dakota.

3.2.3.3 Deck Panels

The deck panels for the girder bridges are typically 4-ft wide. A weaker species of wood, rather than Southern Pine, may be used in the panels due to low stress demands. The panels should have a minimum nominal depth of 6 in. to meet AASHTO (2013) LRFD standards. The deck panels for the slab bridges are typically 4-ft wide. The strong, inexpensive, and easily available wood material is normally used due to high stress demands on the slab. The nominal depth of a deck panel varies from 6 to 16 in. Nominal depths greater than 12 in. are not common.

3.2.3.4 Stiffeners

For glulam slab bridges, stiffeners are required to unify the deformation of the individual panels and to make the panels act as one system. One stiffener must be placed at the mid-span of the bridge, and the additional stiffeners should be placed no more than 8 ft apart on the remainder of the span length according to AASHTO LRFD (2013). AASHTO (2013) Section 9.9.4.3.1 also requires that the rigidity, defined as the product of the modulus of elasticity and the moment of inertia (*EI*), of a stiffener beam shall not be less than 80,000 kip-in^2. Any size and material can be used as long as it satisfies the rigidity standard.

3.2.3.5 Diaphragms

AASHTO LRFD (2013) currently specifies that either solid diaphragms (Fig. 3.19a) or steel cross braces (Fig. 3.19b) be installed on the timber bridges to improve the stability of the bridge. The feasibility and performance of glulam cross braces was investigated in the present study (Fig. 3.20).

(a) Solid Glulam Diaphragm (Hosteng, 2013)

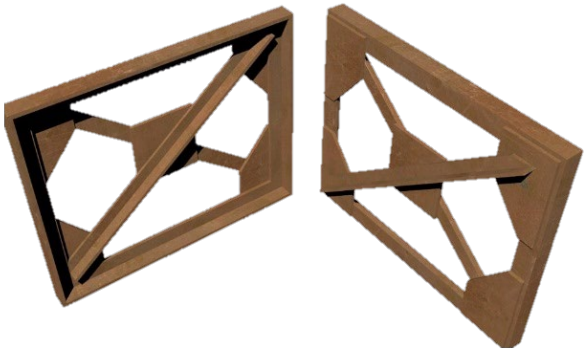

(b) Steel Cross Braces (etraxx.com)

Figure 3.19 Diaphragm Types for Girder Timber Bridges

Figure 3.20 Glulam Cross Braces for Girder Timber Bridges

3.2.3.6 Deck to Stringer Connections

Currently, two methods are primarily used to connect deck panels to stringers. One method is to install lag bolts from the top of the deck through the entire panel into the top of the beam (Fig. 3.21). One of the disadvantages of using lag bolts is their large size, requiring field boring for installation. Since it is impractical to drill lag bolt holes before the pressure treatment of the lumber, the bridge is more susceptible to decay due to water penetration. Furthermore, it is not possible to retighten these bolts if they loosen since the wearing surface will cover them.

Figure 3.21 Lag Bolt Deck-to-Stringer Connection for Timber Bridges (Hosteng, 2013)

Another connection detailing uses brackets (Fig. 3.22). Aluminum brackets usually have small teeth that bite into a routed slot cut into the girder. The top portion of the bracket is then bolted to the deck. The deck bracket connection offers a tight connection that can be retightened if needed. Deck bracket connections also do not affect the deck preservative treatment, since lag bolts can be placed from the bottom of the deck. Disadvantages of this type of connection are that several brackets are required and the slots require removal of a large volume of the wood to accommodate the size of the bolt head. Furthermore, many holes are drilled into the deck if bolts are installed from the top of the bridge.

Figure 3.22 Aluminum Clip Deck-to-Stringer Connection for Timber Bridges (Hosteng, 2013)

The third deck-to-stringer connection incorporated in the Cedar Rock Bridge in Buchanan County, Iowa (Fig. 3.16), is made through the use of epoxy (Fig. 3.23). Epoxy provides a strong bond between the deck and the stringer. This connection reduces the areas where water can seep into the deck, since only small

structural screws are needed to hold the deck panels to the stringers as the epoxy cures. The performance of this type of deck-to-stringer connection was investigated in the present study.

Figure 3.23 Epoxy Deck-to-Stringer Connection

3.2.4 Long-Term Performance of Glulam Timber Bridges

Ritter (1990) states that while timber has been used as a bridge material for hundreds of years, the application of treated timber was very rare until the early 1900s. Numerous untreated timber bridges performed well in the past, but untreated timber bridge numbers have declined in the modern era, due to the reduction in naturally weather resistant North American wood species once used in bridge construction. It is no longer feasible or economical to cover bridges for protection against moisture if the wood is untreated.

Brashaw et al. (2013) investigated the long-term performance of many different types of bridges, including five glulam timber bridges. The study included the National Bridge Inventory (NBI) ratings for those five bridges in Faribault County, Minnesota (Table 3.1). Figures 3.24 to 3.28 show these five bridge conditions in 2016. It can be concluded that glulam timber bridges can last more than 60 years if properly maintained.

Table 3.1 Glulam Timber Girder Bridges in Minnesota (Brashaw et al., 2013)

Bridge ID	Year Built	Span (ft)	Average Daily Traffic	Width (ft)	Wearing Surface	NBI Condition Rating - Deck	NBI Condition Rating- Superstructure
22508	1968	33.5	95	33.3	Bituminous	7	7
22514	1968	40	35	26	Gravel	6	7
22518	1969	38.5	70	33.1	Gravel	7	7
22519	1969	33.5	539	32	Bituminous	6	7
9967	1951	36.2	175	27.4	Bituminous	7	6

Figure 3.24: Glulam Timber Bridge No. 22508 in Faribault County, Minnesota

Figure 3.25 Glulam Timber Bridge No. 22514 in Faribault County, Minnesota

Figure 3.26 Glulam Timber Bridge No. 22518 in Faribault County, Minnesota

Figure 3.27 Glulam Timber Bridge No. 22519 in Faribault County, Minnesota

Figure 3.28 Glulam Timber Bridge No. 9967 in Faribault County, Minnesota

3.2.5 Wearing Surface for Timber Bridges

According to Ritter (1990), a wearing surface is the top layer placed on the bridge deck to form the road surface. The main purpose of a wearing surface is to improve safety, provide a smoother surface, improve skid resistance, and protect the deck. Typically, a wearing surface for a timber bridge can consist of (1) an asphalt overlay, (2) an asphalt chip seal, (3) sacrificial lumber covering the entire deck, (4) cover steel plates, (5) cover lumber planks, and (6) aggregate overlay. In the case that no wearing surface is used, routine inspections must be performed to ensure the deck remains properly sealed to maintain the acceptable condition.

Asphalt is the most commonly used wearing surface since it provides a smooth and skid-resistant surface. Asphalt provides a tight waterproof layer that protects the timber deck from abrasion. The only negative aspect of using asphalt is that reflective cracks can form, allowing water to seep into the wood and decreasing the service life of the bridge. Geotextile fabrics are highly recommended to help prevent reflective cracking and to improve the bond between the glulam deck and the asphalt wearing surface. To prevent any moisture from reaching the deck, the asphalt needs to be maintained. The asphalt approaches must be paved a minimum of 75 ft beyond the ends of the bridge to prevent the formation of potholes at the ends of the bridge. Examples of the asphalt wearing surface on timber bridge decks are shown in Figures 5.24, 5.27, and 5.28 where the surfaces performed reasonably well with minor cracks and potholes.

Another commonly used wearing surface is asphalt chip seal (Ritter, 1990), which is formed by placing a layer of aggregate onto liquid asphalt. Like the asphalt wearing surface, chip seal is smooth and skid-resistant. The main advantage of asphalt chip seal compared with regular asphalt is that the chip seal is thinner and more flexible with fewer reflective cracks. Two 3/4-in thick layers of chip seal are recommended to seal the deck. Geotextile fabric is also recommended for an asphalt chip seal wearing surface.

The use of an aggregate wearing surface is not common. Two examples are given in Figures 5.25 and 5.26. Both bridges with the aggregate wearing surface were in reasonable condition in 2016. They might need some grading soon to remove the ruts from daily traffic.

The remaining wearing surface types were not recommended by Ritter (1990), since they can trap water. These types of wearing surfaces are typically used on very low volume of traffic roads when no other options are feasible.

A new wearing surface was recently used on the Cedar Rock Bridge in Buchanan County, Iowa (Fig. 3.29). The bridge deck was flooded with epoxy to fill all the gaps in the wood. Then very small rocks were imbedded into the epoxy to improve traction. The epoxy is typically applied in three layers of 3/8-in thickness each. The life of the epoxy depends on its exposure. This wearing surface was applied in 2015, which is too recent for full performance evaluation.

Figure 3.29 Epoxy with Embedded Grit Wearing Surface for Glulam Timber Bridge in Buchanan County, Iowa

3.2.6 Preservative Treatment of Wood

All wood used in the construction of glulam bridges must be treated with preservatives, as required by AASHTO (2013) LRFD specifications (Section 8.4.3). Water repellents are used to slow the absorption of water and to keep the moisture content low, which helps prevent decay and slows the weathering process. Wood preservatives are used to prevent biological deterioration. These preservatives are applied to the wood by vacuum-pressure treatment (FHWA, 2012a).

Fire retardant treatments are generally not recommended by AASHTO (2013), since the large-sized timber components used in bridge construction have inherent fire resistance characteristics. A fire retardant should not be applied unless it is compatible with the preservative treatment used in the wood. The strength and stiffness of fire treated wood should be reduced, as recommended by the product manufacturer (AASHTO, 2013, Article 8.4.3.4).

3.2.7 Maintenance and Inspection Required for Glulam Timber Bridges

Since dry wood lasts longer than wood that has been exposed to moisture, it is necessary to perform routine maintenance on glulam timber bridges to keep the wearing surface and other exposed areas in good condition. It is also highly recommended that timber bridges be inspected every two years, and any exposed wood be retreated every six years (Ritter, 1990). Retreatment can be done by applying the preservative with a brush.

According to Ritter (1990), several methods can be utilized for timber bridge inspection. Visual inspection is the most convenient method. An inspector looks over the bridge for signs of deterioration, decay, mold, fungi, insect activity, or any other abnormal changes in the wood. Probing is another inspection method usually performed as part of the visual inspection. A moderately pointed tool is used to probe for any soft spots in the wood. The third, and the most common inspection method for wood, is to use sounding in which the bridge inspector strikes the wood with a mallet or another object. The inspector can determine if there is decay by listening to the sound feedback. If decay is suspected, the inspector then must drill or core the area for further inspection. If decay is found, a plan of action must be made to fix the distressed region.

Preventative maintenance is crucial for long-term serviceability of timber bridges. For example, resealing the exposed wood can prevent decay and deterioration by keeping out moisture. Remedial maintenance should be performed when decay is present. However, remedial maintenance is only applicable where the distress is not severe enough to affect the overall performance of the bridge. In this case, a small section of a timber bridge can be replaced. Major maintenance is usually performed when deterioration results in strength degradation. In that case, a few members of the bridge have to be replaced to increase the bridge's load-carrying capacity. When the deterioration is severe, the bridge has to be replaced.

3.2.8 Railing Systems

A bridge railing system must be positioned to safely contain an impacting vehicle without allowing it to pass over, under, or through the rail elements. A proper railing system must be free of features that may catch on the vehicle or cause it to overturn or decelerate too rapidly. Any crash-tested railing configuration or any railing designed according to Section 13.7 of AASHTO LRFD (2013) can be used for timber bridges. The connecting components should be designed adequately. The rail material can be timber, metal, or concrete. One example of a timber railing is shown in Fig. 3.30.

Figure 3.30 Railing on a Glulam Bridge (laminatedconcepts.com)

3.2.9 Timber Bridge Abutments

Many studies note that existing abutment detailing can be used for glulam timber bridges (Ritter, 1990). Timber bridge abutments are typically constructed using either timber or concrete (Fig. 3.31). The connections should be designed to resist appropriate design loads.

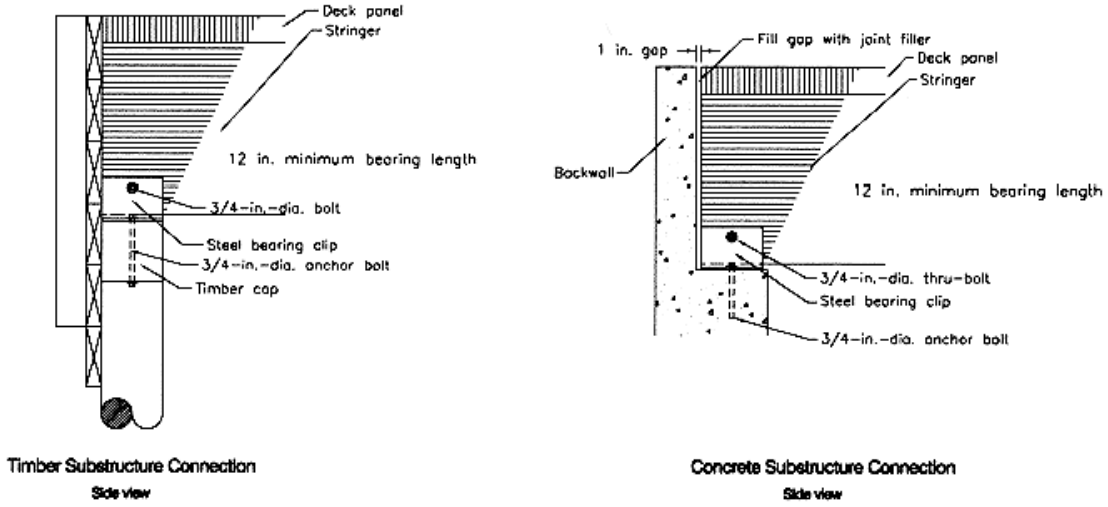

Figure 3.31 Glulam Timber Bridge Abutment Connections (Wacker and Smith, 2001)

3.2.10 Timber Bridge Fabrication

One of the advantages of glulam timber bridges is they can be completely prefabricated offsite and shipped to the project site for installation (Fig. 3.32). This feature is in line with Accelerated Bridge Construction (ABC), which has been recently emphasized in the United States. For wide timber bridges, the bridge can be prefabricated in segments of one or two lanes to be shipped and assembled onsite.

Figure 3.32 Erie Canal Bridge Being Placed in Port Byron, NY, in 2014 (laminatedconcepts.com)

For onsite construction of glulam girder timber bridges, assembly is typically started by placing the center girder, followed by the placing of the other girders, working outwards. Subsequently, the deck panels are placed; then curbs and railings are installed. Once the bridge superstructure is completed, the substructure back-walls can be placed and the approach can be backfilled. The last step is the wearing surface application. The entire construction process for a 60-ft long bridge can be completed in 60 hours or less (Ritter, 1990). The construction time for prefabricated timber bridges is expected to be significantly less than that for timber bridges built onsite.

4. EXPERIMENTAL FINDINGS

Full-scale experiments were conducted in the present study to evaluate the structural performance of the selected bridge systems: (1) precast full-depth deck panel supported on inverted precast prestressed tee girder bridge, (2) glulam timber girder bridge, and (3) glulam timber slab bridge. This section covers design, fabrication, test setup, instrumentation, test procedures, and test results for the three test specimens.

4.1 Precast Full-Depth Deck Panel Bridge Specimen

The structural performance of a full-scale bridge specimen incorporating precast full-depth deck panels supported on inverted tee girders was experimentally evaluated under fatigue and ultimate loading. A summary of the experimental program and findings are presented. An in-depth discussion can be found in Mingo (2016).

4.1.1 Precast Bridge Test Specimen

4.1.1.1 Design of Precast Bridge Test Specimen

A full-scale 50-ft long by 34.5-ft wide prototype bridge was selected for experimental studies. The bridge was designed for HL-93 loading according to AASHTO (2013), which includes both the design truck or tandem load and the design lane load. Because of test setup limitations, only a 10-ft width of the prototype bridge could be tested in the Lohr Structures Laboratory at SDSU. Therefore, two interior girders of the prototype bridge were selected for further investigation. The full-scale bridge test specimen consisted of five precast full-depth deck panels with a 9.5-ft total width (in the bridge transverse direction) and a 10-ft length (in the bridge longitudinal direction) and two 50-ft long prestressed precast inverted tee girders spaced 4.67 ft on center.

The main objective of the laboratory tests was to assess the bridge system performance under fatigue and strength loading. A summary of the design and detailing of the girders and the panels are presented.

Inverted Tee Girders

A software, PS Beam (Ericksson Technologies, 2011), was used to design the prestressed inverted tee girders according to AASHTO (2013). A total of 20 Grade 270 low-relaxation prestressing strands with a diameter of 0.6 in. were used in the inverted tee girders to meet the design requirements (Fig. 4.1). Two of the strands were harped to avoid concrete cracking at the girder ends. The girders were transversely reinforced with ASTM A615 Grade 60 No. 4 bars at a spacing varying from 6 to 18 in.

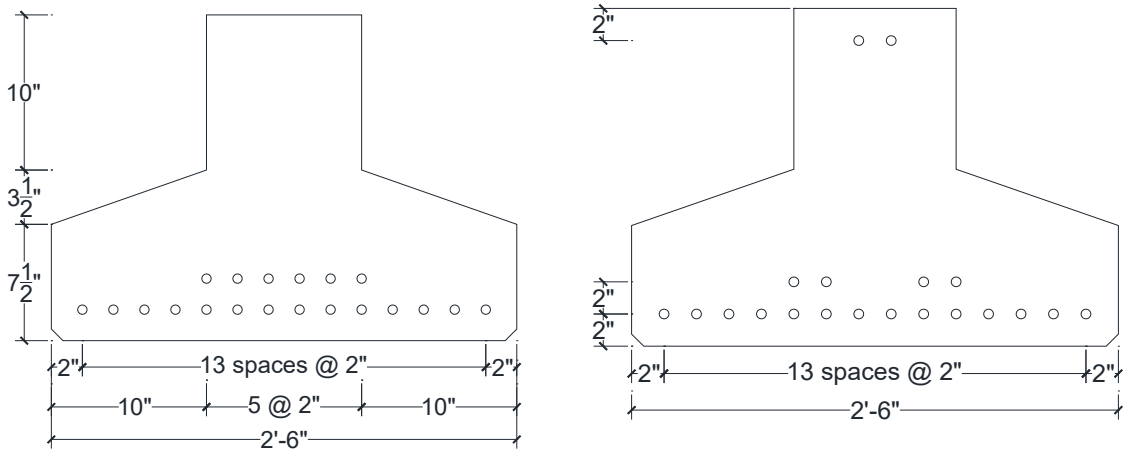

Figure 4.1 Inverted Tee Girder Cross Section with Two Harped Strands

Full-Depth Deck Panels for Precast Bridge

The full-depth deck panel top and bottom reinforcement in the transverse direction of the bridge was designed using table A4-1 in AASHTO (2013), which provides maximum live load moments per unit width for both positive and negative transverse deck moments. The tabulated values are based on the equivalent strip method. The deck longitudinal reinforcement was designed to accommodate creep and shrinkage requirements and to allow splicing of reinforcement at transverse joints to provide adequate shear and moment transfer between the transverse joints. The deck longitudinal steel was placed in one layer at 4.25 in. below the deck surface to allow for splicing of the steel at the transverse joints.

Shear Pockets for Precast Bridge. The precast girders and panels were connected using shear studs extending from the girder web into the panel shear pockets to make the deck-girder system composite. The deck system will be composite since horizontal shear stresses were transferred through the bond in the haunch region as well as the shear studs when the grout was cured.

Two types of shear pockets were incorporated in the test bridge: (1) full-depth pocket, in which the full-depth of the deck was open (Fig. 4.2), and (2) hidden pocket, in which the large portion of the pocket was covered with 3 in. of concrete (Fig. 4.3). Grout can be poured from the top of the pockets into the full-depth pocket or through pipes in the hidden pocket. Figure 4.4 shows the location of the two pocket types in the bridge test model.

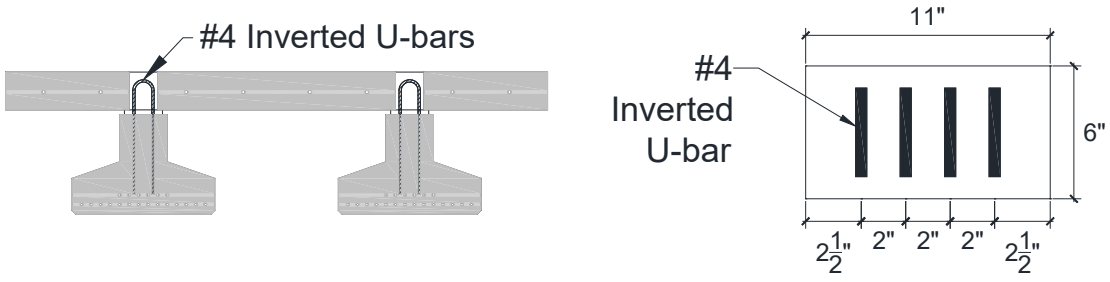

Figure 4.2 No. 4 Inverted U-Shape Bars in Full-Depth Shear Pockets

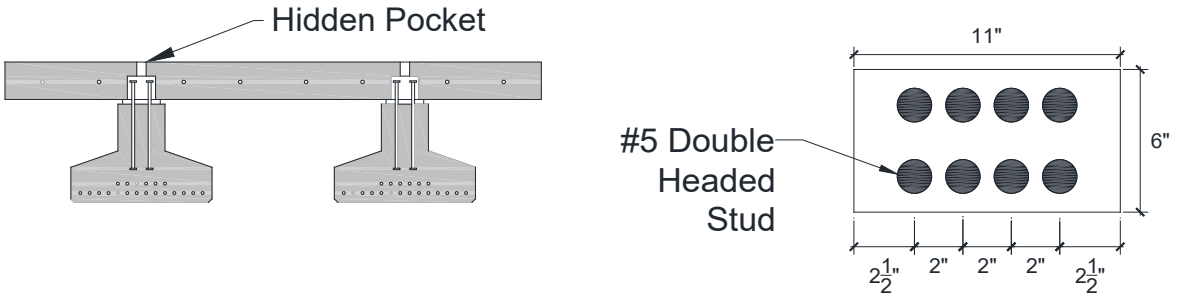

(a) Test Girder Cross Section (b) Hidden Pocket Plan View

Figure 4.3 No. 5 Double Headed Studs in Hidden Shear Pockets

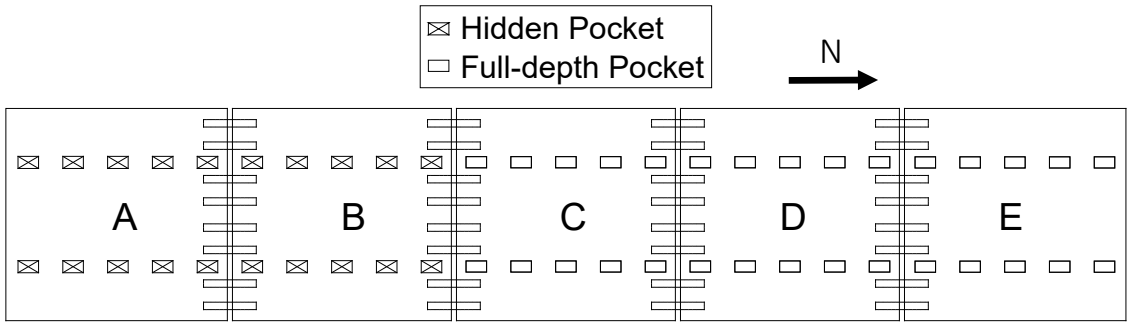

Figure 4.4 Test Bridge Shear Pocket Locations

Horizontal Shear Studs for Precast Bridge. Two types of horizontal shear studs were incorporated in this study: (1) inverted U-shape bars in the full-depth pockets (Fig. 4.2), and (2) double headed studs in the hidden pockets (Fig. 4.3). ASTM A615 Grade 60 No. 4 bars were used to form the inverted U-shape studs. Each full-depth pocket contained eight legs of No. 4 inverted U-shape bars and was spaced 2 ft on center. The double headed studs were made of ASTM A615 Grade 60 No. 5 bars. Eight double headed studs were used in the hidden pockets, and the pockets were spaced 2 ft on center. Horizontal shear studs were designed based on AASHTO (2013) standards.

Transverse Joint for Precast Bridge. The full-depth deck panel (FDDP) transverse joints consisted of (1) female-to-female grouted shear keys (Fig. 4.5) in the transverse direction of the bridge, and (2) dowel bars in the bridge longitudinal direction to be embedded in hollow structural steel (HSS) members (Fig. 4.6). The gap between the two adjacent precast deck slabs in the bridge longitudinal direction is usually 1 in. to 1.5 in. for a typical FDDP transverse joint. However, a 2.75-in. wide transverse joint was used to allow a transverse steel bar to be placed in the joint to meet maximum rebar spacing requirements of 18 in. and to allow 1 in. of clear cover from the face of the joint. Two No. 5 bars were placed beneath HSS sections to meet creep and shrinkage requirements (Fig. 4.6c).

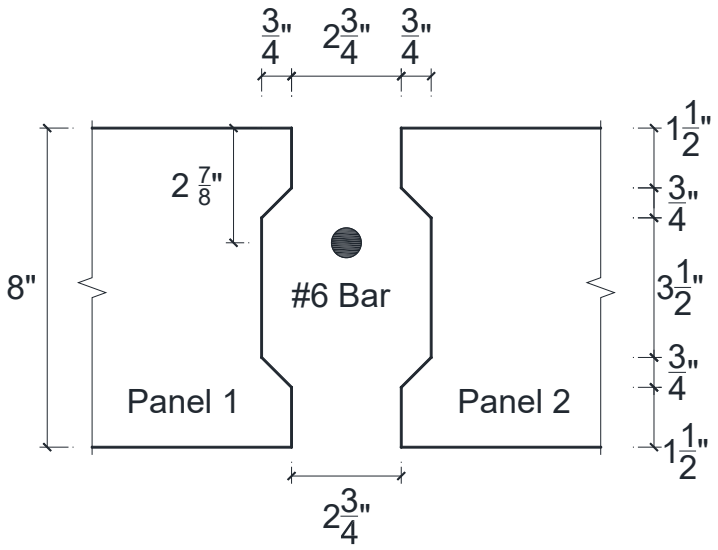

Figure 4.5 Female-to-female Transverse Deck-to-Deck Joint Detailing

The deck longitudinal reinforcing bars were spliced using 25.75-in. long No. 6 ASTM A615 Grade 60 dowels, which were inserted into HSS from the top of the deck after the panels were placed. ASTM A500 Grade B steel was used to form HSS. The HSS will increase the confinement, resulting in a shorter lap-splice for dowels.

Two types of failure can be assumed for the proposed transverse joint: bearing and vertical shear. Modified shear friction theory was used to check the strength of the transverse joints with the longitudinal dowels (Badie and Tadros, 2008).

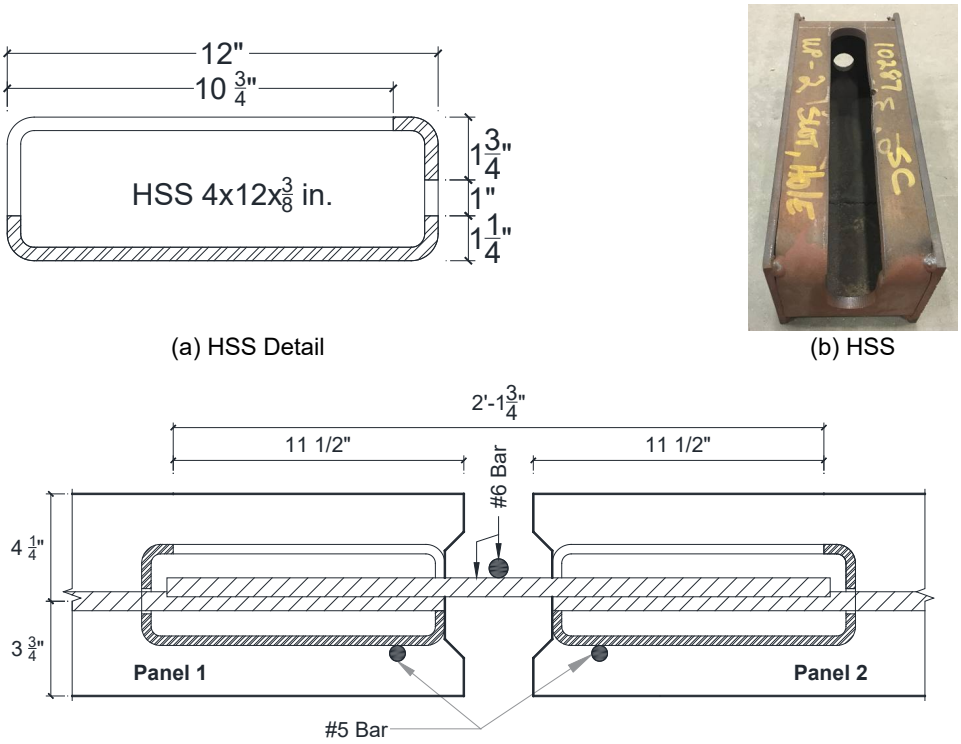

Figure 4.6 Transverse Joint Reinforcement for Full-Depth Precast Panels

4.1.1.2 Fabrication and Assembly of Precast Bridge Test Specimen

The girders and panels for the test bridge specimen were fabricated at Gage Brothers Concrete Products in Sioux Falls, SD. This section includes the fabrication of bridge members and construction stages for the bridge test specimen.

Inverted Tee Girders

The inverted tee girders were prepared and cast on a single bed (Fig. 4.7). Low relaxation Grade 270 prestressing strands were initially tensioned to 10,000 lbs. to eliminate slacks and to straighten tendons for instrumentation. Then the girder shear reinforcement and shear studs were installed. Strain gauge data from strands were obtained before tensioning. Finally, each strand was tensioned to 44,000 lbs., equivalent to 75% of the ultimate stress. Strain gauge readings were also taken during jacking.

The girders were cast in two consecutive days. The one-day concrete compressive strengths of the first and the second girders were 6,820 and 6,190 psi, respectively. Since the specified concrete strength at the time of tendon release was 6,000 psi, the strands were concurrently cut one day after casting. Strains were also measured during the tendon release.

(a) Placement of Bars and Prestressing Strands

(b) Formwork Removal

Figure 4.7 Fabrication of Inverted Tee Girders

The test girders were shipped to the Lohr Structures Laboratory at SDSU after releasing the tendons. The girders were unloaded using a 15-ton overhead crane and placed on concrete reaction blocks (Fig. 4.8).

(a) Girder Unloading

(b) Girder Placement on Abutments

Figure 4.8 Unloading and Positioning of Test Girders

Full-Depth Deck Panels

Five precast panels were fabricated in an indoor construction site (Fig. 4.9). Three interior panels were 9.5-ft wide in the transverse direction of the bridge and 9.77-ft long in the longitudinal direction, and two exterior panels had the same width, but were 9.89-ft long. Each of the five panels contained 10 pockets. Three panels (C, D, and E in Fig. 4.4) had full-depth pockets (Fig. 4.2), while the remaining two panels (A and B) had hidden pockets (Fig. 4.3). The full-depth pocket forms were constructed using cut-out hardboard insulation in stacked layers (Fig. 4.9b). The hidden pocket forms were constructed using plywood for the pockets (Fig. 4.9c). The PVC pipes were installed to form the grouting vents. Four leveling bolts were placed in each panel (Fig. 4.9d). Leveling bolt forms consisted of a nut tack-welded to a vertical steel pipe, and a 2-in. by 4-in. lumber piece to form a blockout at the top of the steel pipe.

(a) Panel Formwork

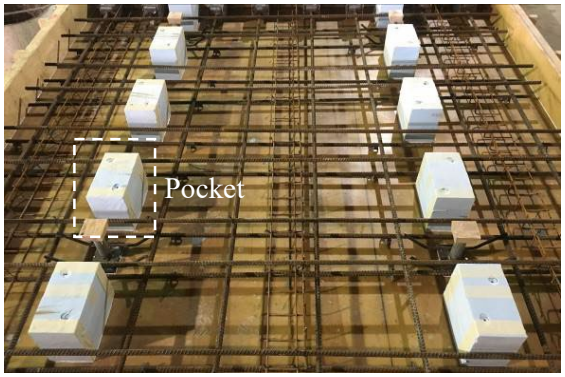

(b) Full-Depth Pocket Formwork

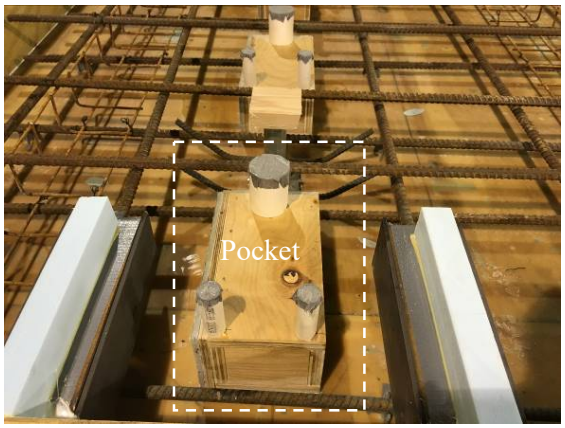

(c) Hidden Pocket Formwork

(d) Leveling Bolt

Figure 4.9 Fabrication of Full-depth Deck Panels

The full-depth deck panels were shipped to the Lohr Structures Laboratory and unloaded using a 15-ton overhead crane. The pockets, joints, and embedded hollow structural steel members were cleaned to avoid any bonding issues. Petroleum jelly was applied to the leveling bolt shaft at the bottom end to allow bolt removal after pouring the grout in the haunch. Next, the panels were placed (Fig. 4.10) starting from one end of the bridge specimen (the south end) toward the other end (the north end). Then the leveling bolts were adjusted with a wrench to level the deck panels. The target grouted haunch depth was 1 in. at the mid-span, which was achieved using the leveling bolts.

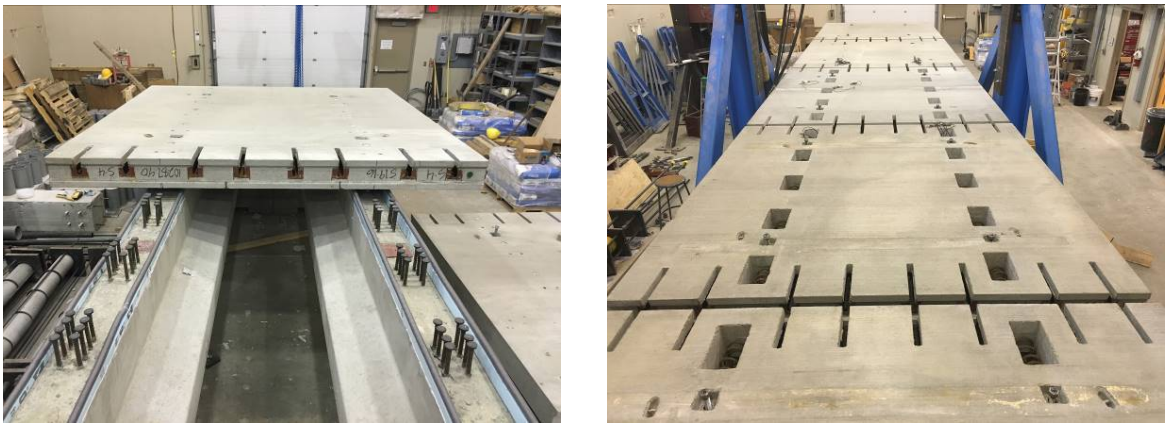

Figure 4.10 Installation for Full-depth Deck Panels on Precast Girders

Plywood was attached at the bottom of the transverse joints using tie wires (Fig. 4.11), which were tied to the transverse joint reinforcement. The plywood and tie wires were installed from the top of the bridge. Silicone was then applied around the concrete-plywood edges from the top of the bridge to create watertight joints. A No. 6 bar was placed and centered on the spliced bars of each transverse joint (Fig. 4.11).

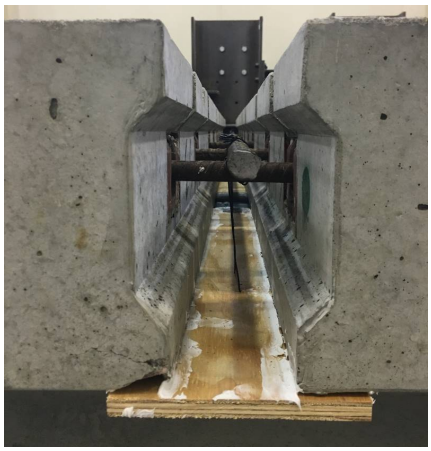

Figure 4.11 Transverse Joint Formwork

Figure 4.12 Grout Hunch Region Formwork

The grouted haunch dam was formed using ¾-in. thick plywood and 2-in. by 4-in. nominal dimension lumber (Fig. 4.12). The lumber was used as a strut to hold the plywood in place. For the exterior of the girders, longitudinal lumber was clamped to the deck and was used as a reaction block for the transverse struts.

Two types of filler materials were incorporated into the grouted haunch, shear pockets, and transverse joints: conventional non-shrink grout and latex modified concrete (LMC). As previously discussed, two types of pockets were used in the test specimen: (1) hidden, and (2) open (full-depth). Since durability of the open pockets was a concern, LMC was proposed as an alternative filler material for this type of pocket because the durability of LMC is better than conventional grout (Wenzlick, 2006; BASF, 2011; Baer, 2013). Half of the open pockets were filled with LMC, and the remaining pockets were cast with conventional grout, as shown in Fig. 4.13. Figure 4.14 shows the grout pour in the hidden and open pockets.

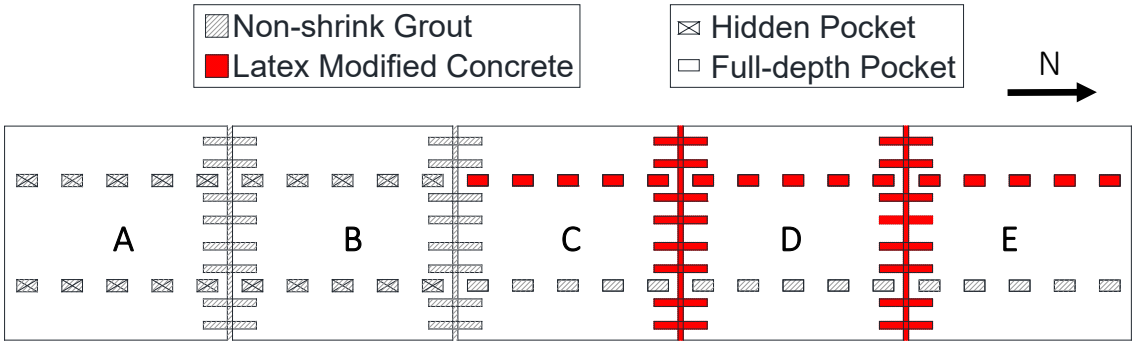

Figure 4.13 Filler Materials and Shear Pocket Locations

(a) Pouring in Hidden Pockets (b) Pouring in Open Pockets

Figure 4.14: Filling Shear Pockets, Haunch Region, and Transverse Joints

4.1.1.3 Precast Bridge Test Setup

The test bridge was placed in a vertical loading frame so that a 146-kip hydraulic actuator was at the centerline of the bridge at the mid-span. The girders were supported on concrete reaction blocks. A 6-in. by 6-in. elastomeric bearing pad was placed between each girder and the reaction block. The effective span length of the test bridge was 49.13 ft. Water ponds were formed on the top of the pockets and joints to investigate the integrity of the precast joint detailing during fatigue testing.

Fatigue testing was performed in two phases: (1) Phase I, in which the bridge overall performance was investigated, and (2) Phase II, in which the performance of the transverse joint was emphasized. In Phase I, a single point load was applied at the centerline of the bridge at the mid-span using a 146-kip actuator (Fig. 4.15a). The load was applied to a 10-in. by 20-in. steel plate to simulate AASHTO (2013) design truck tire bearing area. A 0.5-in. thick layer of plaster was poured beneath the steel plate to ensure a level and uniform bearing surface.

(a) Single Point Load in Phase I (b) Two-Point Loads in Phase II

Figure 4.15 Test Setup for the Precast Bridge Specimen

An 8-ft long W12x93 steel spreader beam was used in Phase II to spread the load directly to the transverse joints and to maximize the shear transfer from panel to panel (Fig. 4.15b). Two 10-in. by 20-in. steel plates were positioned at the ends of the spreader beam and were leveled. The center-to-center distance between the two loading plates was 7.5 ft.

After the completion of the fatigue testing, an ultimate test was conducted using a 328-kip actuator. A W12x93 steel beam was used to spread the load over the two girder centerlines at the mid-span to avoid punching shear failure of the deck. Figure 4.16 shows the test setup for the strength test.

Figure 4.16 Ultimate Test Setup for the Precast Bridge Specimen

4.1.1.4 Instrumentation Plan for the Precast Bridge Specimen

The test bridge was heavily instrumented with axial strain gauges, shear strain gauges, linear variable differential transducers (LVDTs), and load cells. The instrumentation plan is briefly discussed.

Strain Gauges Used in the Precast Bridge

Three types of strain gauges were used on different materials: (1) surface-mounted axial strain gauges were used to measure axial strains in mild and prestressing reinforcement; (2) surface-mounted shear strain gauges were used to capture shear strain data on mild steel bars; and (3) embedded concrete strain gauges were used to measure the concrete strain.

Figure 4.17 shows the bridge strain gauge plan at the mid-span. Five axial strain gauges were mounted to the top surface of the deck longitudinal mild steel bars. Two axial strain gauges were installed on the prestressing tendons at the bottom layer of each girder. One embedded concrete strain gauge per girder was installed slightly above the composite bridge section neutral axis. A total of nine axial strain gauges and two embedded concrete strain gauges were used at the mid-span.

Strain gauges were installed on the studs in four of the shear pockets. Of which, two were hidden pockets with No. 5 double-headed studs and filled with non-shrink grout; the other two were full-depth pockets with No. 4 inverted U-shape bars (one filled with non-shrink grout and the other with latex modified concrete). Eight studs/legs were extended into each pocket to resist horizontal shear. Two axial strain gauges were mounted to the pocket corner studs in a diagonal pattern, and two shear strain gauges were mounted on the opposite two diagonal studs. The combination of one axial and two shear strain gauges enabled the measurement of strains in three different directions. Thus, principal strains and stresses of shear studs could be measured.

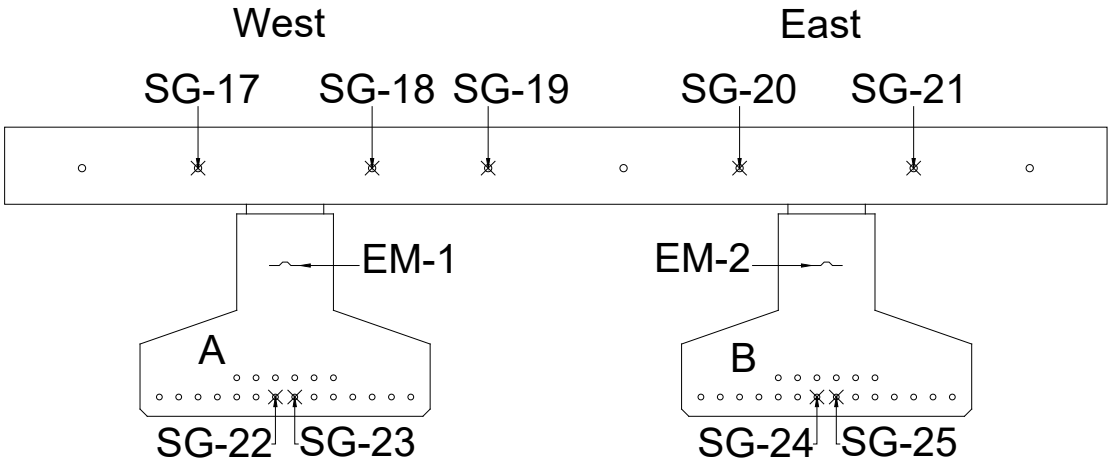

Figure 4.17 Strain Gauge Configuration at Mid-span of the Precast Bridge Specimen

Linear Variable Differential Transformers Used for the Precast Bridge Specimen

Thirteen linear variable differential transformers (LVDTs) were attached to the test specimen to measure deflections and rotations in various directions (Fig. 4.18).

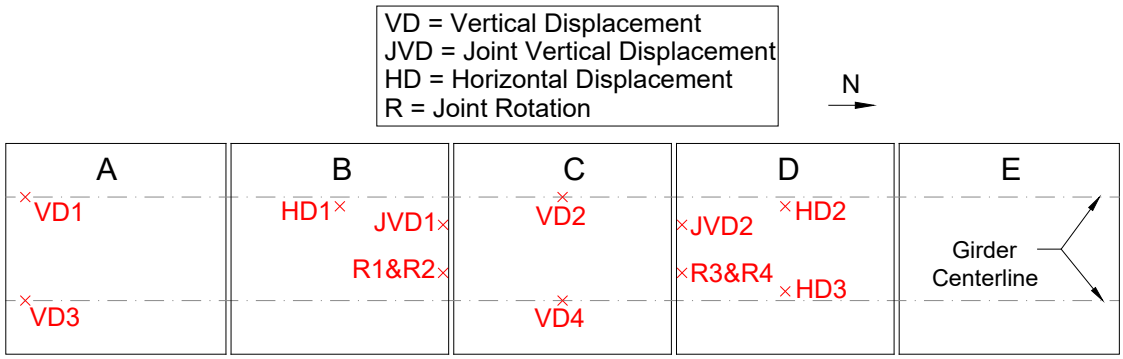

Figure 4.18 LVDT Installation Plan for the Precast Bridge Specimen

Vertical deflections were measured both at the mid-span of the bridge as well as the girder ends using LVDTs. The difference between the girder mid-span and the girder end displacements was reported as actual (net) girder deflections to account for compression of the elastomeric bearing pads.

Deck-to-girder slippage was measured using horizontal LVDTs mounted to the top of the girder. They were mounted at three locations to observe the performance of (1) full-depth pockets with latex modified concrete and No. 4 inverted U-shape bars, (2) full-depth pockets with non-shrink grout and No. 4 inverted U-shape bars, and (3) hidden pockets with non-shrink grout and No. 5 double headed studs. Each HD LVDT was installed 15 ft away from the mid-span.

Joint rotations were also measured with LVDTs mounted adjacent to the two transverse joints of the middle panel. Each joint had an LVDT mounted horizontally in the longitudinal direction of the bridge on the top and bottom of the deck at the same section. The LVDTs were offset 13 in. from the longitudinal centerline of the bridge to allow ponding of the joint.

The relative vertical deflection across the two transverse joints of the middle panel was measured with a single vertical LVDT mounted adjacent to each joint. Similar to the previous measurement, these LVDTs were offset 13 in. from the longitudinal centerline of the bridge to allow ponding of the joint.

Load Cells Used in the Precast Bridge Specimen

Four load cells were placed under the south end of the girders to measure support reactions. Two load cells were utilized per girder, offset 6.25 in. from the girder centerline to enhance overall stability, and offset 6 in. from the girder end to provide sufficient seat length. Steel plates with a dimension of 6 in. by 6 in. by 1 in. were placed at the top and the bottom of the load cells to create a level bearing surface. Elastomeric bearing pads were placed on top of the steel plates to allow the girders to freely rotate.

Data Acquisition System

A 128-channel data acquisition device was used, which could record between 10 and 2,048 readings per second. Stiffness and ultimate tests were scanned at a rate of 10 readings per second. For the fatigue testing, cyclic data was recorded at a scan rate of 100 points per second for 30 load cycles at the beginning and the end of each fatigue test.

4.1.1.5 Test Procedure for the Precast Bridge Specimen

The full-scale bridge was tested under fatigue, stiffness, and ultimate loading. Fatigue testing was performed by applying cyclic loads either at the mid-span (phase I) or close to the transverse joints (phase II). Stiffness tests, which consisted of applying a monotonic point load or loads, were performed at intervals of 50,000 cycles to determine the effect of fatigue on the bridge performance and to measure the bridge overall stiffness. The ultimate test was carried out by applying point loads to the girders at the mid-span with a monotonic loading protocol.

Fatigue Testing of the Precast Bridge Specimen

For Phase I, a 27.7-kip point load was applied at the center of the bridge at the mid-span at a loading rate of 1 cycle per second. The actuator was controlled by force to ensure the cyclic load magnitude remained the same even if the bridge stiffness degraded. The magnitude of the point load was calculated according to AASHTO (2013) Fatigue II limit state load combination.

Since the proposed bridge will be used on local South Dakota roads, the average daily traffic (ADT) was assumed to be 100 vehicles per day with a 15% truck density (ADTT = 15). Therefore, 410,625 trucks would cross the bridge over a 75-year design life. The test bridge was subjected to at least 500,000 load cycles to account for the possibility of increased truck traffic.

After the completion of Phase I loading, fatigue testing was continued with two point loads adjacent to the transverse joints. The distance between the two point loads was 7.5 ft on center. The same load magnitude as that of Phase I was applied to the beam resulting in a 13.9-kip load at each end of the spreader beam. The load magnitude was determined by matching the girder shear demand in the test girder from Phase I loading. The test was terminated at 150,000 cycles since no stiffness degradation was observed.

Stiffness Testing of the Precast Bridge Specimen

Stiffness tests were performed at the beginning of the testing and then at every 50,000-load cycle increment thereafter. The stiffness load magnitude was 55.4 kips, which was applied monotonically using a displacement-control loading protocol. The load was calculated according to the AASHTO (2013) Fatigue I limit state. Displacements were applied with an interval of 0.01 in. with a speed of 0.007 in./sec.

Strength Testing of Precast Bridge

A point load at the mid-span of the bridge was monotonically applied to a beam placed in the transverse direction of the bridge to spread the load to the two girders. The girders were loaded under a displacement-control loading protocol, in which displacements were applied with an increment of 0.02 in. and a rate of 0.007 in./sec.

4.2.1 Material Properties of the Precast Bridge Specimen

Different materials were incorporated in different bridge components. In this section, the following mix design and mechanical properties are presented: (1) concrete used in the deck, (2) concrete used in the girders, (3) conventional non-shrink grout used in the joints, (4) latex modified concrete used in the joints, (5) deck mild steel, (6) inverted U-shape shear studs, (7) double headed shear studs, and (8) prestressing strands used in the girders.

4.2.1.1 Properties of Concrete Used in the Precast Bridge Specimen

The design concrete compressive strength at 28 days was 6,000 psi and 8,000 psi for the full-depth deck panels and the prestressed inverted tee girders, respectively. The properties of the fresh concrete used in the full-depth deck panels and inverted tee girders were measured in accordance with ASTM C143 and C231 standards (2010).

Standard 6 in. by 12 in. cylinders were used for concrete sampling. The cylinders were first placed next to the deck panels and girders for 24 hours. Molded girder samples were stored in the Lohr Structures Laboratory while deck concrete samples were unmolded and placed in a moist cure room. Note that both methods are acceptable by ASTM standards. Compressive strength tests were performed in accordance with ASTM C39 standard (2010).

4.2.1.2 Properties of Grout Used in the Precast Bridge Specimen

Fifteen standard 2 in. by 2-in. cube samples were collected for each mix of conventional non-shrink grout and LMC, which were used as filler materials in different precast joints. The non-shrink grout had a 28-day strength of approximately 9 ksi, and the latex modified concrete had a 28-day strength of approximately 7.5 ksi. The detailed measured material properties can be found in Mingo (2016).

4.2.1.3 Properties of Prestressing Strands Used in the Precast Bridge Specimen

Low-relaxation Grade 270 prestressing strands with a diameter of 0.6 in. were used in this project. The mechanical properties of the strands are summarized in Table 4.1.

Table 4.1 Mechanical Properties of Prestressing Strands Used in the Precast Bridge Specimen

Cross-Sectional Area (in.^{2})	Modulus of Elasticity (ksi)	Yield Stress (ksi)	Ultimate Stress (ksi)
0.22	29,000	254.4 at 1% extension	287.8 at 7.4% extension

4.2.1.4 Properties of Horizontal Shear Studs Used in Precast Bridge

Dog-bone samples were prepared for the tensile testing of reinforcement used as horizontal shear studs in accordance with ASTM 370. This section includes a summary of the measured data.

Inverted U-shape Bars Used in Precast Bridge

No. 4 inverted U-shape bars that extended from the girder top into the full-depth shear pockets were made of ASTM A615 Grade 60 reinforcing steel bars. Table 4.2 presents the measured mechanical properties for the inverted U-shape bars.

Table 4.2 Mechanical Properties of Inverted U-shape Bar Used in Precast Bridge

Bar Size	ASTM Type	Yield Strength, f_y (ksi)	Ultimate Strength, f_u (ksi)	Strain at Peak Stress (%)	Strain at Fracture (%)
No. 4	A615 Grade 60	74.9	113.6	7.0	13.4

Note: Measured data were based on the average of two tensile tests.

Double Headed Studs Used in Precast Bridge

No. 5 ASTM A706 Grade 60 double headed reinforcing steel bars were used in the hidden shear pockets as shear studs. Table 4.3 presents the mechanical properties of the double headed stud according to the mill certificate provided by the manufacturer.

Table 4.3 Mechanical Properties of Double Headed Stud Used in Precast Bridge

Cross-Sectional Area (in.^{2})	Yield Stress (ksi)	Ultimate Stress (ksi)	Strain at Fracture (%)
0.31	69.9	90.7	17

4.2.1.5 Properties of Reinforcement in Panels and Joints Used in Precast Bridge

Tensile tests were performed on dog-bone samples of steel bars used in the test bridge transverse joints and deck panels. A summary of the test data is presented in Table 4.4 and Table 4.5.

Table 4.4 Mechanical Properties of Transverse Joint Reinforcement Used in Precast Bridge

Bar Size	ASTM Type	Yield Strength, f_y (ksi)	Ultimate Strength, f_u (ksi)	Strain at Peak Stress (%)	Strain at Fracture (%)
No. 6	A615 Grade 60	71.5	112.5	7.4	14.8

Note: Measured data were based on the average of two tensile tests.

Table 4.5 Mechanical Properties of Deck Reinforcement Used in Precast Bridge

Bar Size	ASTM Type	Yield Strength, f_y (ksi)	Ultimate Strength, f_u (ksi)	Strain at Peak Stress (%)	Strain at Fracture (%)
No. 6	A615 Grade 60	63.4	107.3	7.2	14.9

Note: Measured data were based on the average of two tensile tests.

4.2.1.6 Properties of Elastomeric Neoprene Bearing Pads Used in Precast Bridge

A 6-in. by 6-in. by 3/8-in. elastomeric neoprene pad was tested in a compression machine to determine the force-deformation relationship of the bearing pads used at the supports. The stiffness of the linear portion of the force-displacement relationship was 1,128 kip/in.

4.2.2 Test Results for Precast Bridge

As mentioned, the precast bridge specimen was first tested under 500,000 cycles of the Fatigue II loading using a point load applied at the mid-span. Then it was subjected to 150,000 cycles using two point loads applied adjacent to the middle panel (Panel C) transverse joints. Finally, it was loaded monotonically to failure.

4.2.2.1 Phase I – Fatigue II Loading of Precast Bridge

A Phase I testing results summary for the precast prestressed bridge, including observed damage, stiffness degradation, and joint rotation and slippage, is presented in this section.

Observed Damage

At 25,000 load cycles, which corresponds to 4.6 years of service, a vertical hairline crack was observed on the grouted haunch of Girder A, located approximately 4.2 ft south of the mid-span in one of the LMC joints. One of the water ponds was on top of this joint. Since (1) the crack width did not change over the entire fatigue test (Fig. 4.19), (2) the pond did not lose water from this leak, and (3) this joint was the last one filled with LMC (which sets in approximately 30 minutes), it was concluded that the leak was because of construction issues but not structural degradation due to fatigue. Furthermore, there was no change in bridge overall stiffness due to this crack.

(a) Observed Crack at 25,000-Load Cycle

(b) Close Up of Crack

(c) Pocket and Water Pond from Bridge Top

(d) Crack Condition after 650,000 Load Cycle

Figure 4.19 Observed Damage in LMC Full-Depth Pocket of Girder A

At 125,000 load cycles, which corresponds to 22.8 years of service, vertical hairline cracks were observed along the length of the grouted haunch of both girders, approximately evenly spaced between 2 in. and 4 in. (Fig. 4.20). Both the conventional non-shrink grout and the latex modified concrete exhibited vertical hairline cracking in the haunch area. Also, hairline shallow cracks were observed in all transverse joints (Fig. 4.21) and most shear pockets (Fig. 4.22). Since (1) water did not leak through these cracks, (2) the crack width did not increase over time, and (3) there was no change in the bridge overall stiffness, it was concluded that these hairline cracks were caused by shrinkage, not fatigue loading.

(a) Shrinkage Cracks in Haunch Region of Girder A Filled with Latex Modified Concrete

(b) Close Up of Girder A Haunch Region Filled with Latex Modified Concrete

(c) Shrinkage Cracks in Haunch Region of Girder B Filled with Non-Shrink Grout

(d) Close Up of Girder B Haunch Region Filled with Non-Shrink Grout

Figure 4.20: Haunch Region Shrinkage Cracks at 125,000 Load Cycle

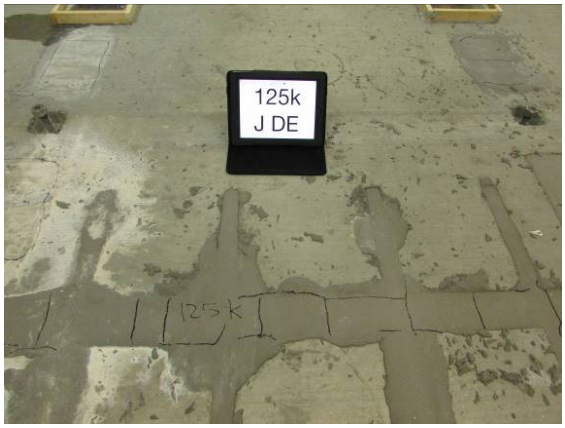

(a) Latex Modified Concrete at 125,000 Cycle

(b) Latex Modified Concrete at 650,000 Cycle

Figure 4.21 Transverse Joint Cracks in the Precast Bridge Specimen

(a) Non-Shrink Grout at 125,000 Cycle

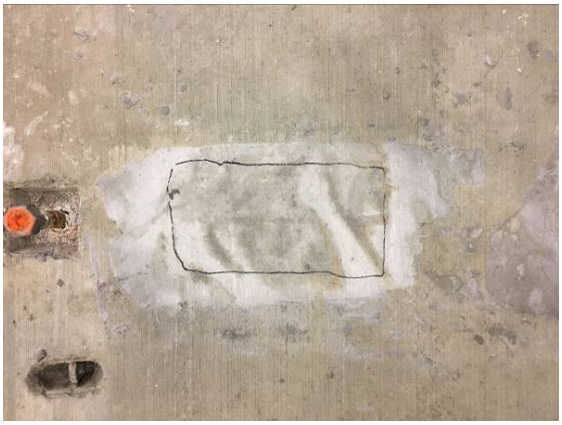

(b) Non-Shrink Grout at 650,000 Cycle

(c) Latex Modified Concrete at 125,000 Cycle

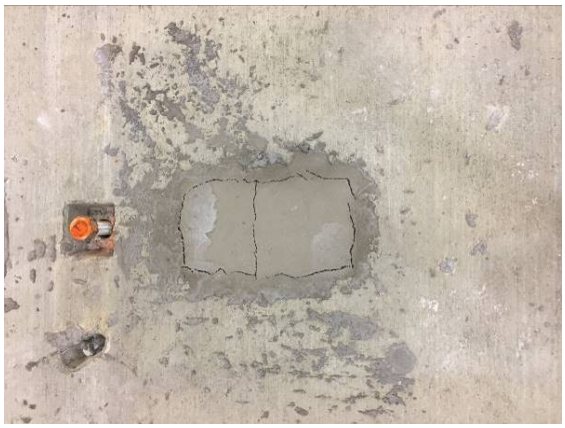

(d) Latex Modified Concrete at 650,000 Cycle

Figure 4.22 Full-Depth Shear Pocket Cracks in the Precast Bridge Specimen

Stiffness Degradation and Joint Integrity

The measured force-displacement relationship for each stiffness, which was test performed after every 50,000 load cycles, is shown in Fig. 4.23. The measured effective stiffness (EI) of the bridge versus the number of load cycles is shown in Fig. 4.24. The stiffness was measured based on the applied loads and the average girder net mid-span deflections. It can be seen that the bridge overall stiffness essentially remained the same throughout the fatigue testing, indicating sufficient detailing for the proposed bridge system.

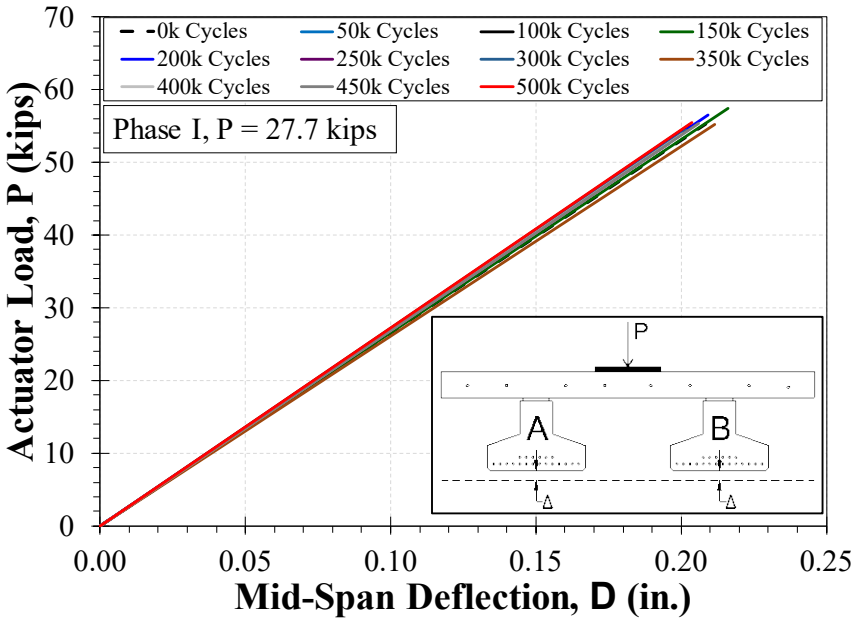

Figure 4.23 Measured Stiffness During Phase I Fatigue Loading – Precast Bridge Specimen

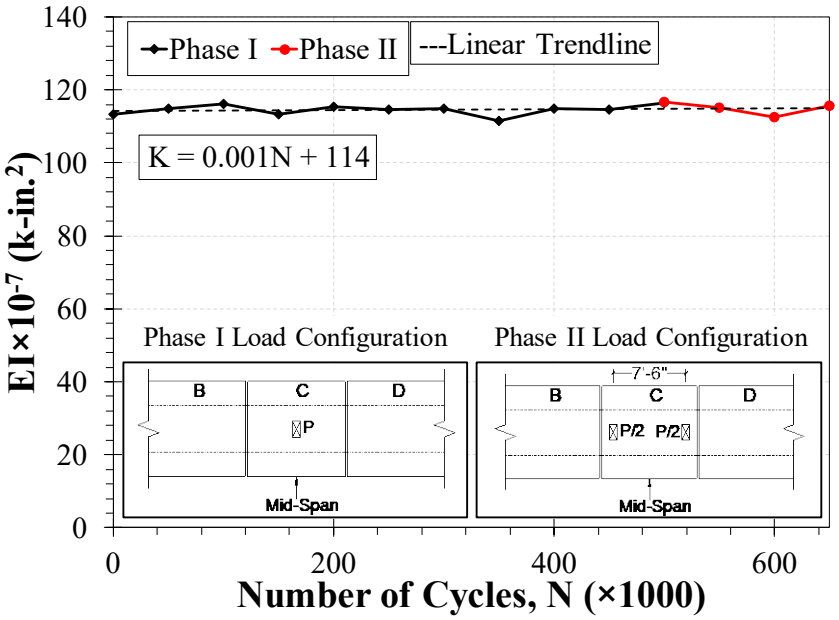

Figure 4.24 Stiffness Degradation During Fatigue Testing – Precast Bridge Specimen

Figure 4.25 shows the measured joint relative deflections versus the number of load cycles for the two joints of Panel C. The joint's relative deflections were negligible and remained essentially constant through all 500,000 load cycles of Phase I fatigue testing. Figure 4.26 shows the measured joint rotations versus number of load cycles for the two joints of Panel C. The joint rotations were negligible and remained essentially constant through all 500,000 load cycles of Phase I fatigue testing.

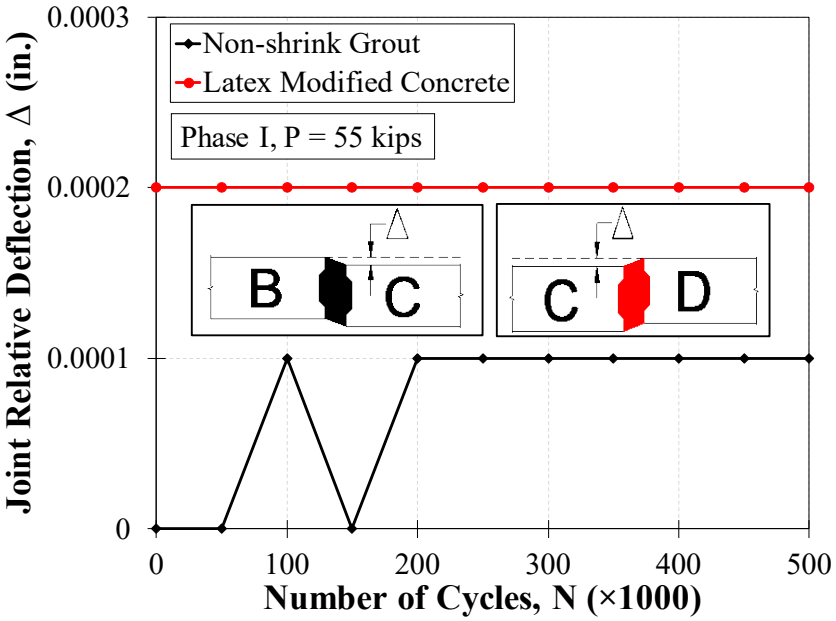

Figure 4.25 Transverse Joint Relative Deflection During Phase I Fatigue Testing – Precast Bridge Specimen

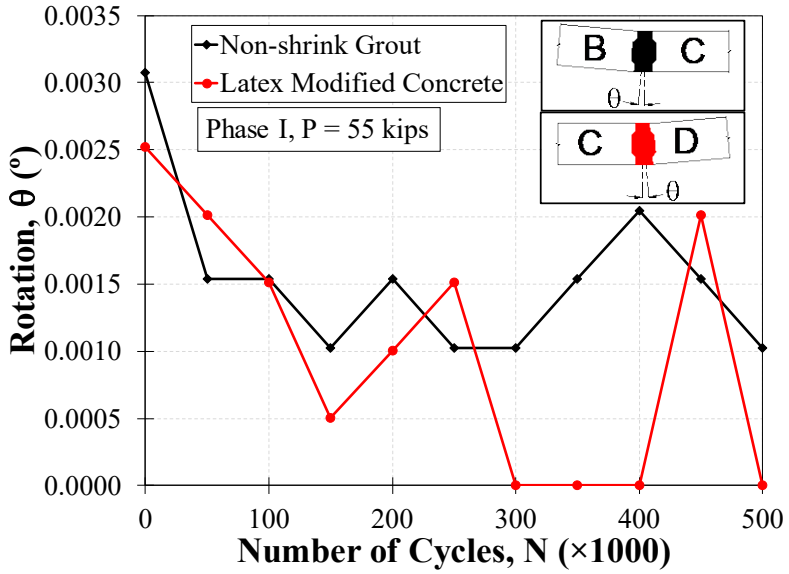

Figure 4.26 Transverse Joint Rotation During Phase I Fatigue Testing – Precast Bridge Specimen

The relative displacement between the girder top flange and the deck bottom (deck-to-girder slippage) was measured during each stiffness test (Fig. 4.27). The slippage was negligible and remained essentially constant through all 500,000 load cycles of Phase I fatigue testing.

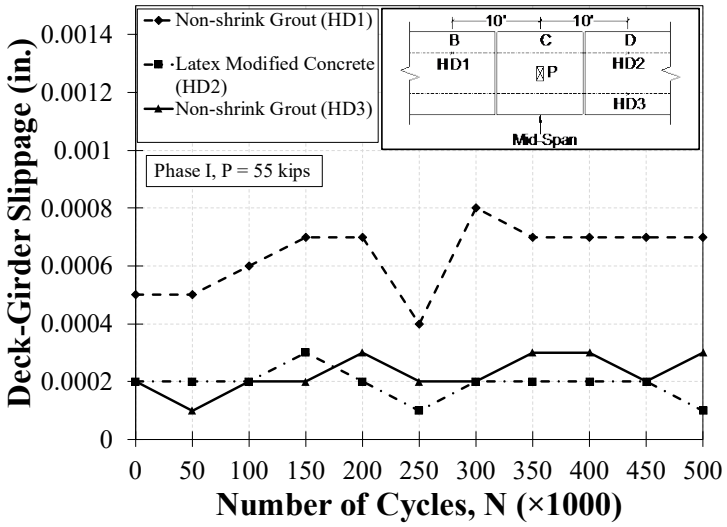

Figure 4.27 Deck-to-Girder Slippage During Phase I Fatigue Testing – Precast Bridge Specimen

4.2.2.2 Phase II – Joint Loading of Precast Bridge

A summary of the Phase II testing results for the precast prestressed bridge, including observed damage, stiffness degradation, and joint rotation and slippage, is presented in this section.

Observed Damage

Figure 4.28 shows the middle panel transverse joints with either non-shrink grout or latex modified concrete after applying 150,000 cycles of joint loading. All joints remained watertight through the fatigue loading. No significant damage of the bridge components, in addition to what was reported in Phase I testing, was observed.

(a) Joint with Non-Shrink Grout – Deck Underneath

(b) Joint Latex Modified Concrete – Deck Underneath

Figure 4.28 Transverse Joint Damage During Phase II Fatige Testing – Precast Bridge Specimen

Stiffness Degradation and Joint Integrity

Figure 4.29 shows the measured force-displacement relationship for each stiffness test performed at every 50,000 load cycles during Phase II fatigue testing. The stiffness was measured based on the applied loads and the girder net mid-span deflections. It can be seen that the bridge overall stiffness essentially remained the same throughout the transverse joint fatigue testing, indicating sufficient transverse joint detailing for the proposed bridge system.

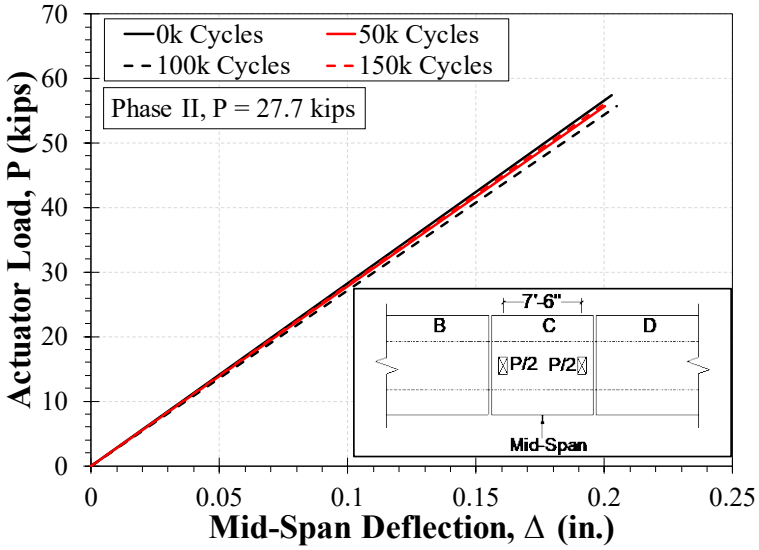

Figure 4.29 Measured Stiffness During Phase II Fatigue Loading – Precast Bridge Specimen

Figure 4.30 shows the measured joint relative deflections versus number of load cycles for both joints of Panel C during Phase II testing. The joint relative deflections were negligible and remained essentially constant through all 150,000 load cycles. Figure 4.31 shows the measured joint rotations versus number of load cycles for both joints of Panel C under the Phase II loading. The joint rotations were negligible.

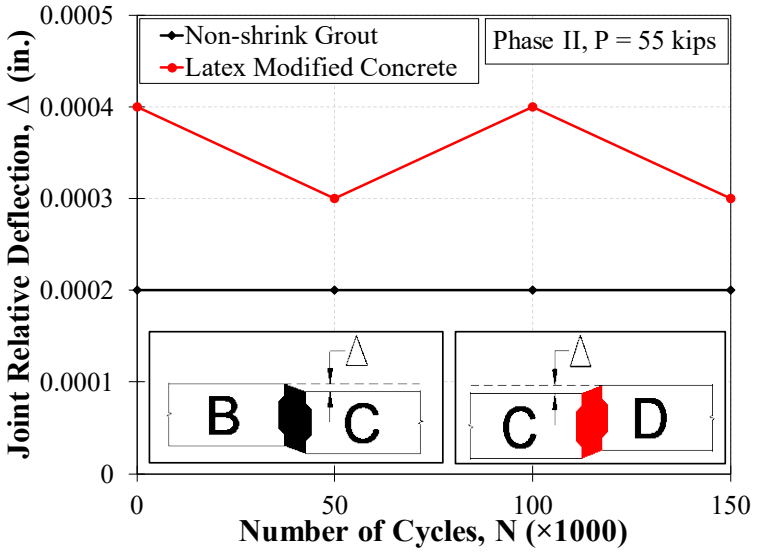

Figure 4.30 Joint Relative Deflection During Phase II Testing – Precast Bridge Specimen

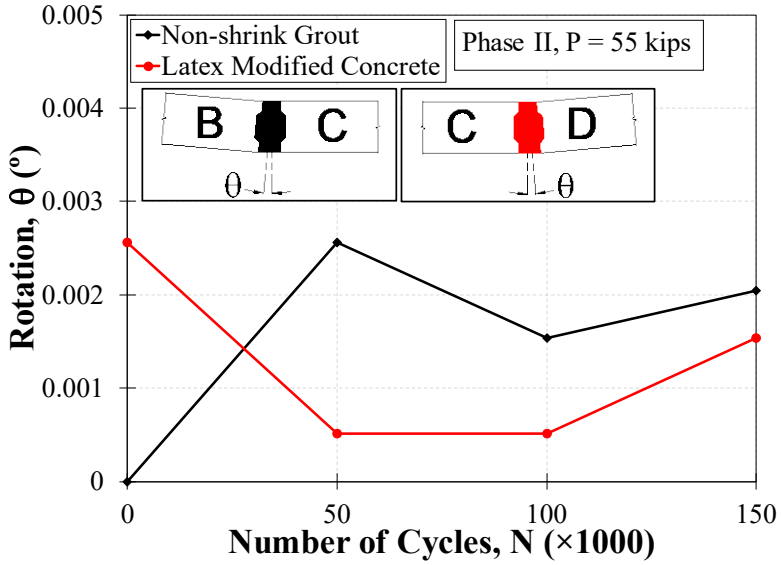

Figure 4.31 Joint Rotation During Phase II Testing – Precast Bridge Specimen

Figure 4.32 shows the deck-to-girder slippage versus number of load cycles. It can be seen that the slippage was negligible through all 150,000 load cycles of Phase II testing.

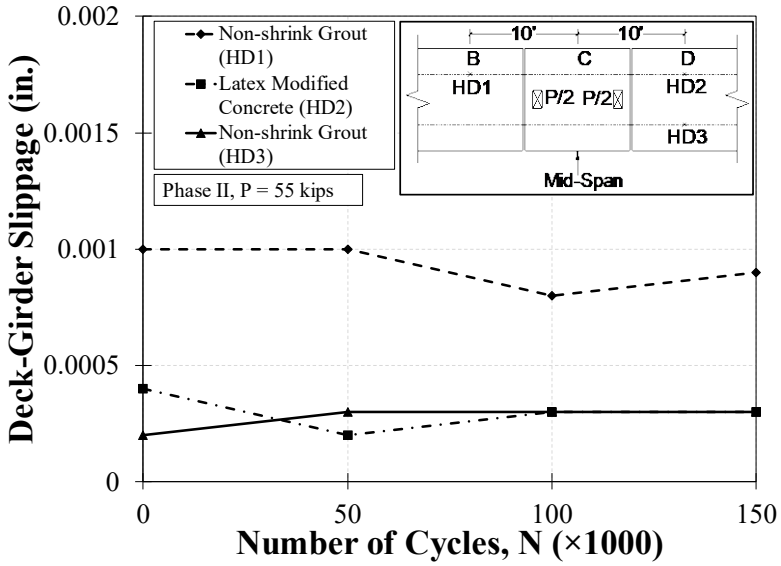

Figure 4.32 Deck-to-Girder Slippage During Phase II Testing – Precast Bridge Specimen

4.2.2.3 Strength Testing Used in the Precast Bridge Specimen

A summary of the strength test results for the precast prestressed bridge, including observed damage, force-displacement relationship, strain profiles, and joint performance, is presented in this section.

Observed Damage

The first crack in the girder was observed at the mid-span at an actuator load of 149 kips (Fig. 4.33a). Subsequently, more cracks were developed on both girders close to the mid-span at higher loads, as shown in Figs. 4.33b to 4.33d.

(a) First Crack, Mid-Span of Girder A at P = 251 kips

(b) First Crack, Mid-Span of Girder B at P = 251 kips

(c) Crack Pattern for Girder A at P = 263 kips

(d) Crack Pattern for Girder B at P = 263 kips

Figure 4.33 Girder Cracks During Strength Testing of the Precast Bridge Specimen

The first horizontal shear crack in the grouted haunch region of the precast bridge (Fig. 4.34) was observed at an actuator load of 200 kips, which corresponds to a girder load of approximately 100 kips. However, horizontal shear stud strain gauge data suggests that cracking occurred at lower loads. Additional shear cracks appeared at an actuator load of 226 kips (Fig. 4.35). Note that shear cracks did not form under an equivalent strength I limit state load for this bridge, which was 131.4 kips, indicating that the shear reinforcement detailing was sufficient.

(a) 14-ft North of Mid-Span (Girder A)

(b) 14-ft South of Mid-Span (Girder A)

Figure 4.34 Haunch Region Horizontal Shear Cracks at an Actuator Load of 200 kips During Strength Testing of the Precast Bridge Specimen

(a) 16-ft North of Mid-Span (Girder B)

(b) 14-ft South of Mid-Span (Girder B)

Figure 4.35 Haunch Region Horizontal Shear Cracks at an Actuator Load of 226 kips During Strength Testing of the Precast Bridge Specimen

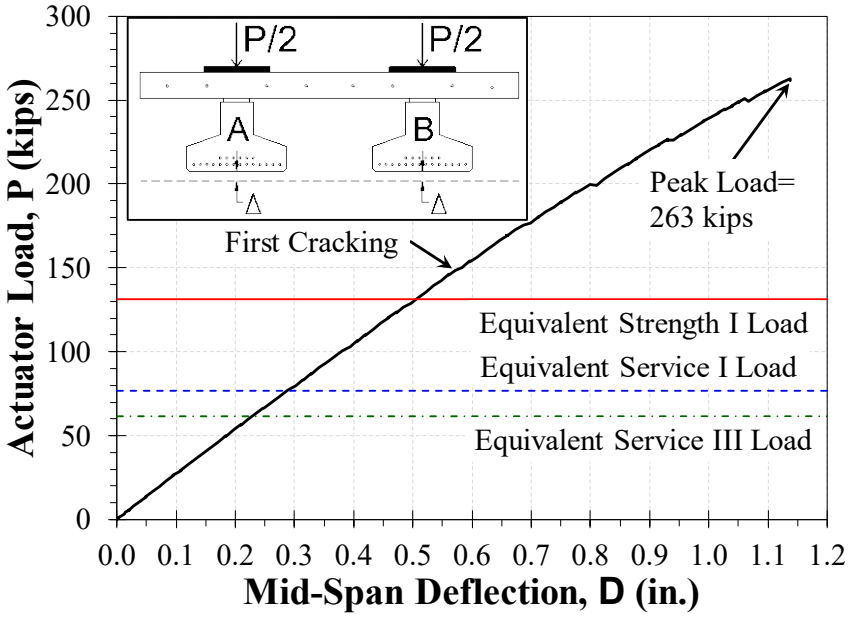

Figure 4.36 Measured Mid-span Force-Deformation Relationship Under Strength Testing of the Precast Bridge Specimen

Force-Displacement Relationship

Figure 4.36 shows the force-displacement relationship for the bridge at the mid-span during the strength testing. The figure also shows the equivalent loads for different limit states. The mid-span net girder deflection at the Service I limit state load of 76.7 kips was 0.29 in., which was only 39% of the AASHTO allowable deflection at this limit state (0.74 in.) for this bridge. The girder deflection at the peak applied load of 263 kips was 1.14 in. The test was stopped at 263 kips because of the setup limitation. Furthermore, Fig. 4.36 shows that the first girder cracking occurred at a higher load than that of the Strength I limit state, indicating that the bridge design was sufficient (since the superstructure should remain capacity protected). No yielding of the prestressing tendons was observed during the ultimate test. The calculated tendon yield force based on a moment-curvature analysis was 362 kips. Overall, the bridge showed satisfactory performance in terms of displacement and force capacities.

Four load cells were installed under the south end girders to continuously measure the girder reactions. Reactions at applied loads corresponding to the Service I limit state, the Strength I limit state, first cracking, and the ultimate load are shown in Fig. 4.37. It can be seen that approximately 49% of the applied load was resisted by Girder A, and the remaining load was resisted by Girder B. The total south end reaction was 24.9 kips under the equivalent Service I limit state load, 58.8 kips under the equivalent Strength I limit state load, 67.0 kips under the first cracking load, and 119.1 kips under the peak load. It was noticed that the south end measured reactions were always 10% lower than the calculated reactions from statics. The cause was probably a slight offset in the actual location of the applied load or a minor tilt in the bridge deck.

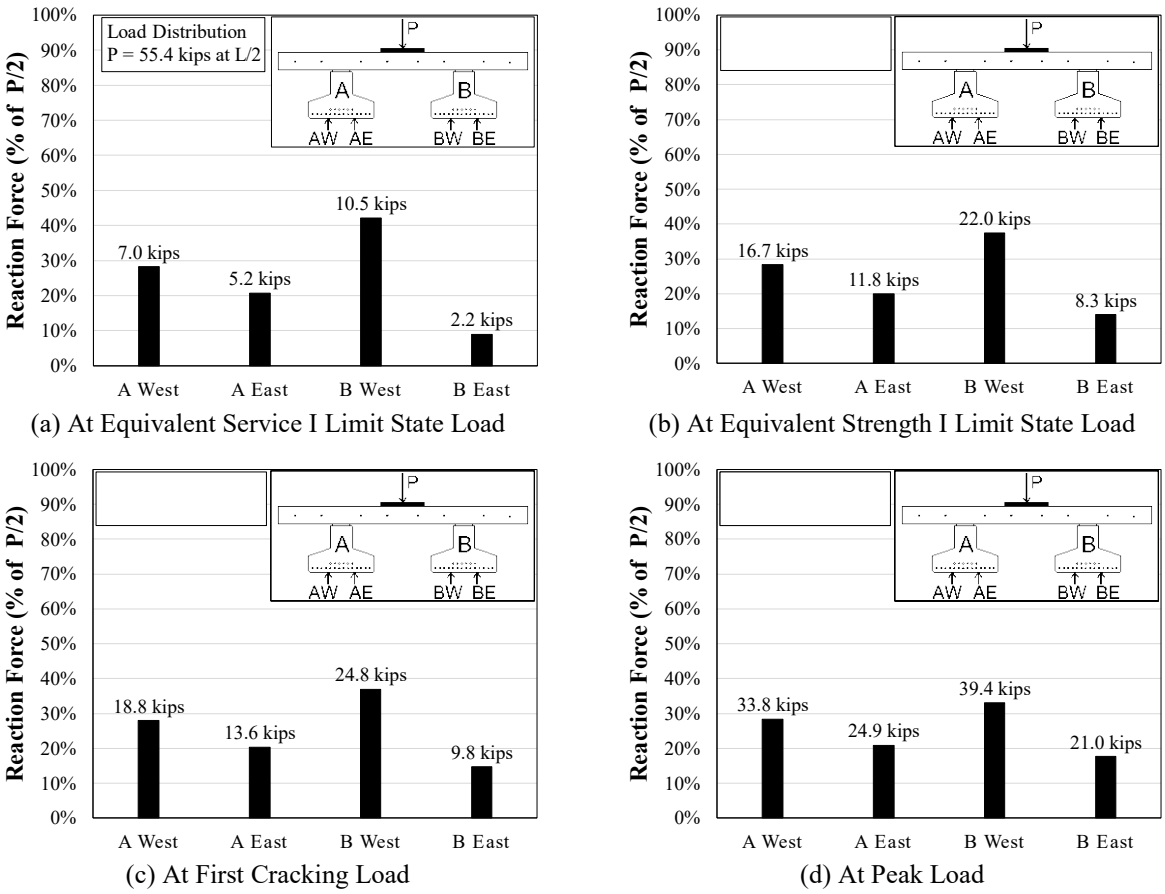

Figure 4.37 Measured Girder End Reactions Under Strength Testing of the Precast Bridge Specimen

Measured Strains

Strain gauges were installed on prestressing strands and reinforcing steel bars. The measured strain data during the strength test is discussed.

Tendon and Reinforcement Strains. Figure 4.38 shows the measured strain of prestressing strands during the strength testing. The initial strains of the strands were determined using strain gauge data collected during stressing. Note that the strands' initial strains account for short-term losses, such as elastic shortening, but no long-term losses, such as relaxation, creep, and shrinkage. It can be seen that the tendons did not yield up to 263 kips where the test was stopped. The yield strain of the tendons was 8,772 microstrain. Figure 4.39 shows the measured strains for the longitudinal deck mild steel and the embedded concrete strain gauges during ultimate loading. The measured data for the embedded concrete strain gauges (EM-1 & 2) also include the initial strains recorded during cutting of the prestressing strands. It can be seen that the longitudinal deck mild steel did not yield up to 263 kips. The embedded concrete strain gauges were located 1.6 in. below the theoretical composite girder section neutral axis. The measured concrete strains agree with calculated strains from statics.

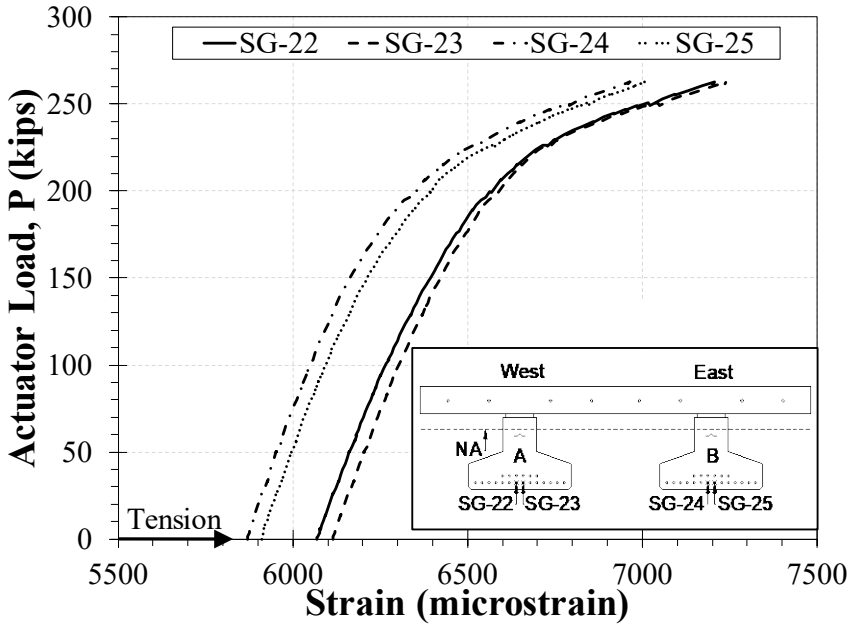

Figure 4.38 Measured Prestressing Strand Strains During Strength Testing of the Precast Bridge Specimen

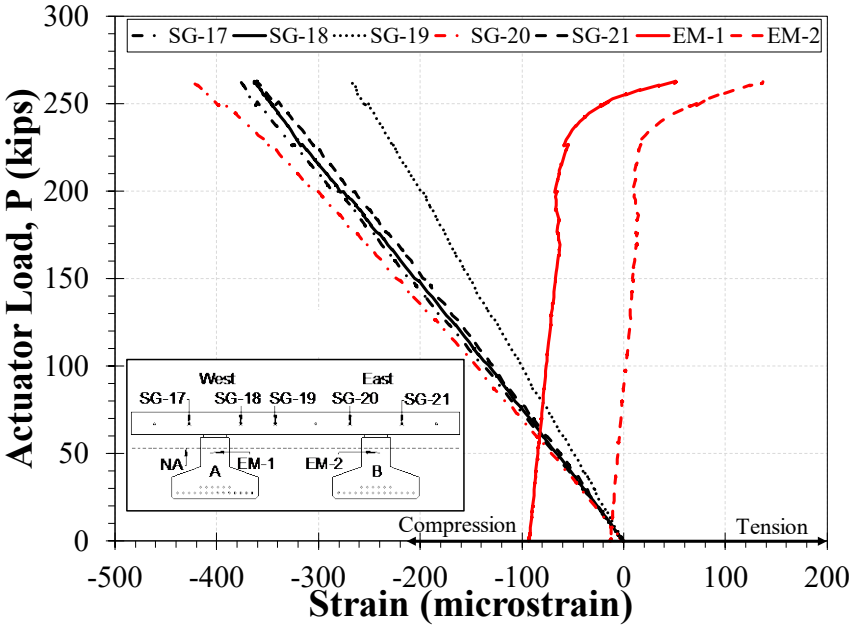

Figure 4.39 Measured Longitudinal Deck Steel Strain and Girder Concrete Strain During Strength Testing of the Precast Bridge Specimen

Shear Stud Strains and Stresses. The actuator load versus measured strain for the double-headed shear studs is shown in Fig. 4.40. It can be seen that the double-headed studs did not yield in any direction. Since the strain gauges were installed in a rosette type layout in each pocket (one in the axial direction of the stud, and two at ±45 degrees with respect to the stud's longitudinal axis), the maximum principal stresses (Fig. 4.41) could be estimated for the studs in each pocket. It can be seen that the maximum

principal stress of the double-headed studs was 19.4 ksi, well below the yield stress (69.9 ksi), indicating sufficient design.

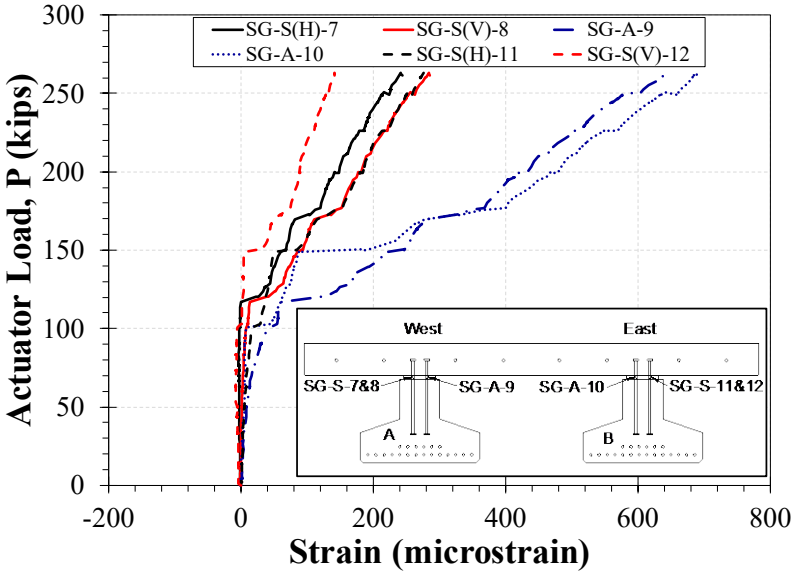

Figure 4.40 Measured Strain for No. 5 Double Headed Studs During Strength Testing of the Precast Bridge Specimen

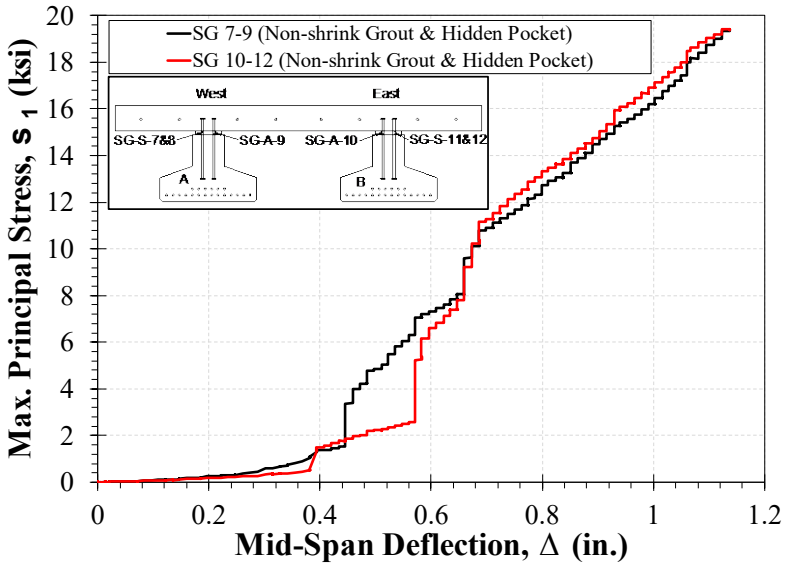

Figure 4.41 Maximum Principal Stresses for No. 5 Double Headed Studs vs. Mid-Span Deflection During Strength Testing of the Precast Bridge Specimen

The load required to cause horizontal shear cracks in the girder haunch can be determined using the stud strain or stress data where strains or stresses suddenly change (Fig. 4.41). The deflection associated with the sudden change of strains in studs was identified then converted to the actuator load using the force-displacement relationship. The first haunch cracks, based on the measured data (Fig. 4.41) of the headed studs in the hidden pockets filled with non-shrink grout, occurred at an actuator load of 100.6 kips, which is larger than the Service I limit state load of 76.7 kips.

The actuator load versus measured strain for the inverted U-shape shear studs is shown in Fig. 4.42. It can be seen that these studs did not yield in any direction. The maximum principal stresses (Fig. 4.43) were estimated in each pocket similarly to what was done for the double-headed studs. It can be seen that the maximum principal stress for the inverted U-shape shear studs was 23.9 ksi for the pocket filled with LMC and 27.6 ksi for the pocket filled with non-shrink grout. Therefore, the principal stresses were well below the stud yield stress, indicating sufficient design.

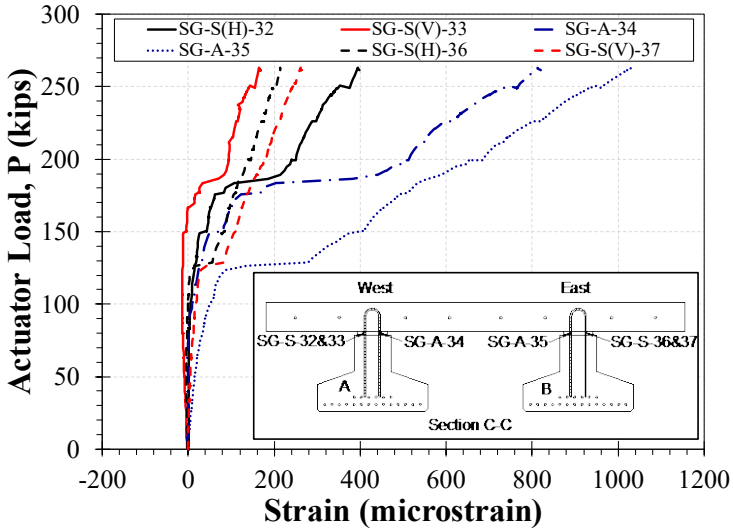

Figure 4.42 Measured Strain for No. 4 Inverted U-shape Studs During Strength Testing of the Precast Bridge Specimen

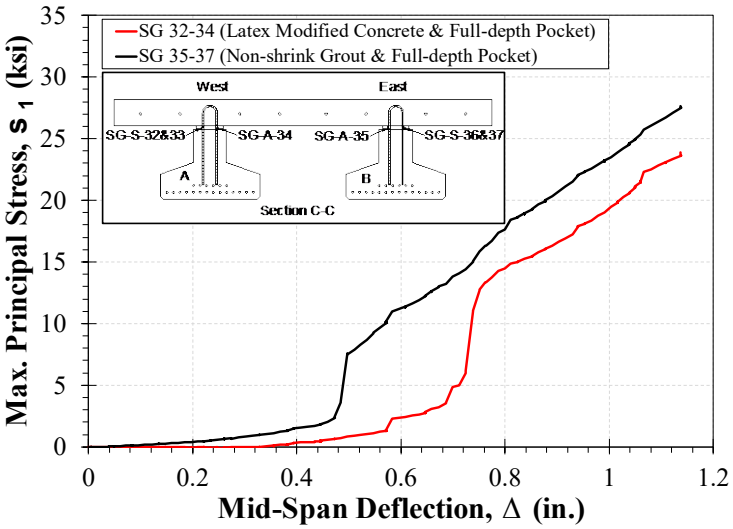

Figure 4.43 Maximum Principal Stresses for No. 4 Inverted U-shape Studs vs. Mid-Span Deflection During Strength Testing of the Precast Bridge Specimen

The load required to cause horizontal shear cracks in the girder haunch was also determined. The first haunch cracks based on the measured strain data (Fig. 4.43) for the inverted U-shape shear studs in the full-depth pockets filled with non-shrink grout occurred at an actuator load of 124 kips, and at a load of

149 kips for the full-depth pockets filled with LMC. Both loads are larger than the Service I limit state load of 76.7 kips, confirming that the shear pocket detailing was sufficient.

Transverse Joint Reinforcement Strains. Figure 4.44 shows the measured strains of the transverse bars in the transverse joints during the strength testing. Strain gauge SG-A-15 failed at 170 kips (marked with * in the figure). It can be seen that none of the strains exceeded 50 microstrain and were negligible.

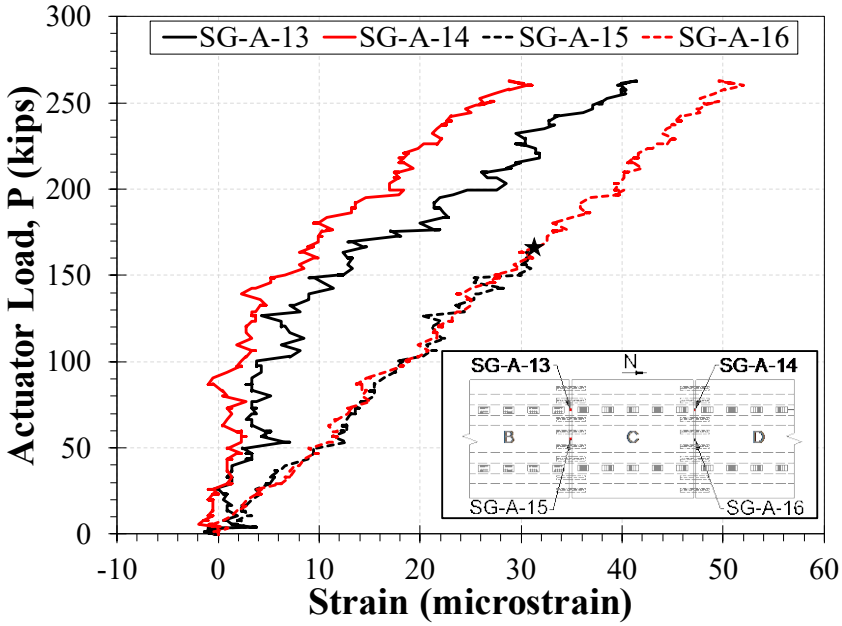

Figure 4.44 Measured Strains of No. 6 Transverse Bars in Transverse Joints During Strength Testing of the Precast Bridge Specimen

Two No. 6 dowel bars installed in the transverse joints had strain gauges in a rosette layout to estimate the maximum principal stresses (Fig. 4.45) transferred between the two adjacent decks. It can be seen that the maximum principal stress for the reinforcement in the joints filled with either non-shrink grout or LMC was well below the yield strength, indicating sufficient design.

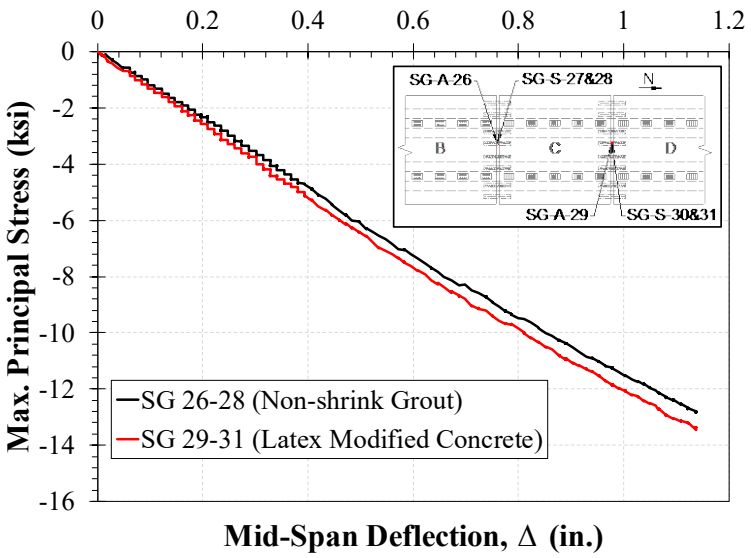

Figure 4.45 Maximum Principal Stresses for No. 6 Lap-Spliced Bars vs. Mid-Span Deflection During Strength Testing of the Precast Bridge Specimen

Performance of Joints

The mid-panel joints' relative deflections and rotations during strength testing are shown in Fig. 4.46. The joint filled with non-shrink grout had a relative deflection of 0.0014 in. at 263 kips. The joint filled with latex modified concrete had a relative deflection of 0.0015 in. at 263 kips. Both deflections were negligible. Furthermore, the joint filled with non-shrink grout had a rotation of 0.009 degrees at 263 kips. The joint filled with latex modified concrete had a rotation of 0.01 degrees at 263 kips. Both joint rotations were negligible.

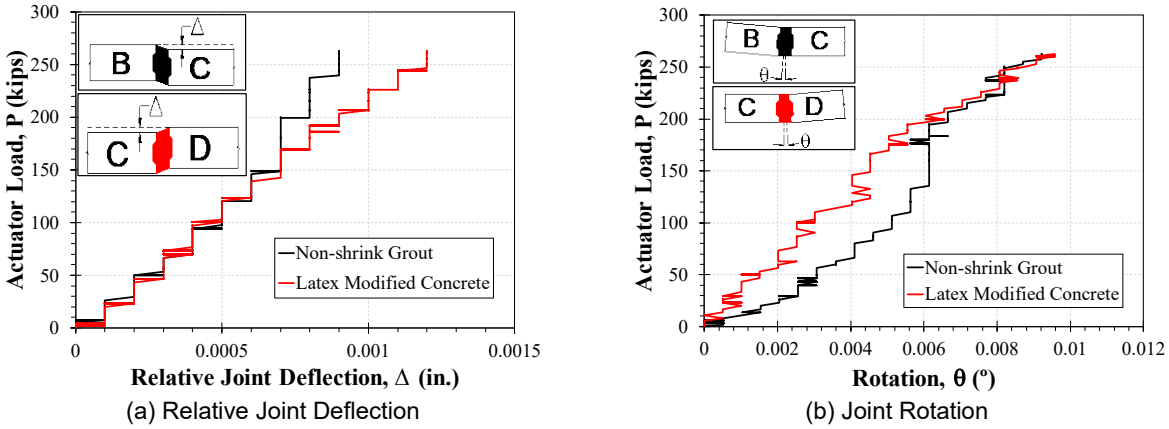

(a) Relative Joint Deflection (b) Joint Rotation

Figure 4.46 Measured Relative Deflections and Joint Rotations During Strength Testing of the Precast Bridge Specimen

The relative displacement between the bottom of the deck and the top of the girder (deck-to-girder slippage) was measured in three locations. Figure 4.47 shows the deck-to-girder slippage during the strength testing. A plateau can be seen at a girder load of approximately 60 kips, which can be attributed to the cracking of the haunch region (e.g., Fig. 4.34), and the relatively small shear deformations of the haunch region.

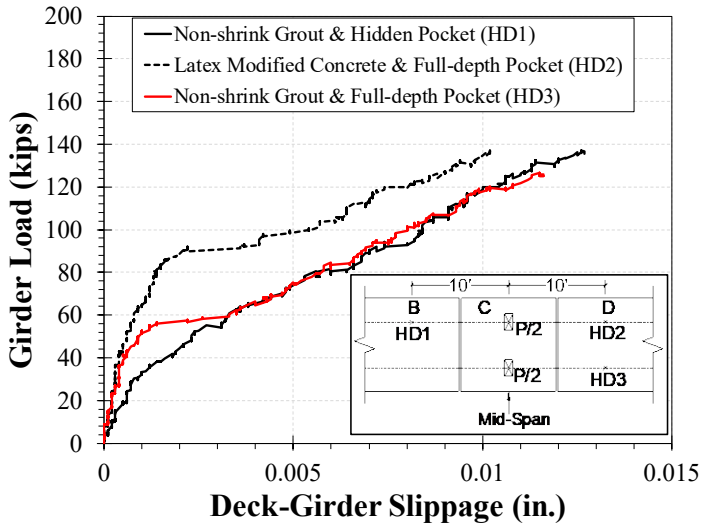

Figure 4.47 Measured Deck-to-Girder Slippage During Strength Testing of the Precast Bridge Specimen

4.3 Glulam Timber Girder Bridge Specimen

Two types of glulam timber bridges (Fig. 3.17) were introduced in the previous section: (1) bridges built with transverse glulam decks supported on glulam stringers (hereafter referred to as "girder bridges"), and (2) longitudinal glulam deck bridges (hereafter referred to as "slab bridges"). The structural performance of a glulam girder bridge was evaluated through full-scale experiment. This section includes a summary of the design, construction, instrumentation, test setup, loading protocols, and test results for the full-scale girder bridge test specimen.

4.3.1 Glulam Timber Girder Bridge Test Specimen

4.3.1.1 Design of Test Specimen

The prototype glulam girder bridge was assumed to be 50-ft long and 34.5-ft wide (Fig. 4.48a). A full-scale bridge model was selected for testing, but with a width approximately equal to the width of one-lane of traffic. The bridge test specimen (Fig. 4.48b) consisted of the following: (1) three 50-ft long girders with a 30.25-in. depth and a 8.5 in. width; (2) 13 deck panels each 48-in. long (in the longitudinal direction of the bridge), 110.75-in. wide (in the transverse direction of the bridge), and 5.5-in. thick (this is the actual thickness, the nominal thickness was 6 in.), and (3) 10 rectangular glulam cross braces, each with a dimension of 5 in. by 10 in. to improve the bridge stability.

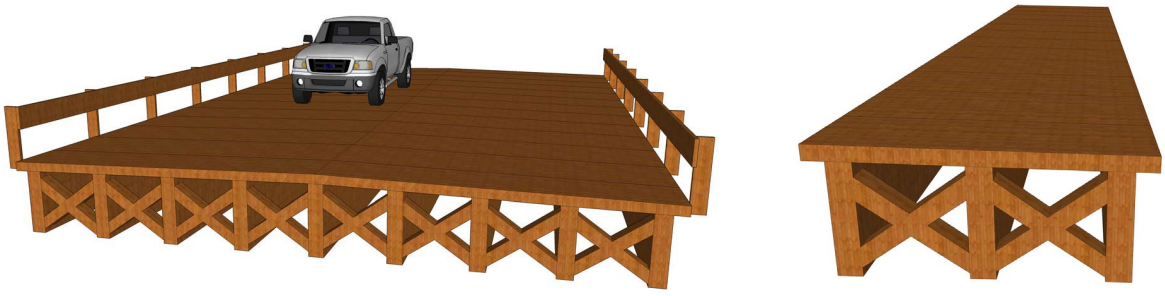

(a) Prototype Bridge (b) Test Model

Figure 4.48 Glulam Girder Bridge Test Model

AASHTO (2013) was used for the design of the bridge components. This bridge was designed for the HL-93 loading, which consists of a design truck or tandem accompanied by the design lane load.

Design of Glulam Deck Panels

The deck panels were analyzed and designed according to AASHTO (2013). A structural analysis was performed using the Strength I limit state loads with the assumptions that the deck panels are continuous beams and the girders are simply supported at the ends. According to the structural analysis, the deck could be less than 6 in. However, the depth of the deck was controlled by the minimum nominal thickness of 6 in. required by AASHTO. The width of the deck panels was determined to be 4 ft for the ease of fabrication and installation.

Design of Glulam Girders (Stingers)

The girders were also designed according to AASHTO (2013). Live load distribution factors were used to calculate the moment demand for an interior girder, since the girders used in the test bridge simulate interior girders of the prototype bridge model.

The girders were assumed to be partially composite with the deck, and were designed based on the mechanical properties for 26F-1.9E Southern Yellow Pine. The design girder was 30.25-in. deep and 8.5-in. wide. To provide sufficient bearing area for girders at the ends and to have a 50-ft clear span, the girder length was increased from 50 to 52 ft.

To further aid bridge designers, a spreadsheet was developed for the design of glulam girders, checking the capacity to demand ratio for all design parameters as well as the girder deflection.

Design of Cross Braces

The cross braces were designed to resist lateral loads according to AASHTO (2013), Section 8.11. Even though solid diaphragms and steel cross braces are recommended by AASHTO, the use of glulam cross braces was proposed and investigated in this project due to the ease of construction. The final glulam rectangular cross braces were 6.875-in. wide and 8-in. deep.

Design of Deck-to-Stringer Connection

As discussed in the previous section, there are three main types of deck-to-stringer connections: (1) lag bolt connection, (2) aluminum bracket connection, and (3) epoxy connection. The use of epoxy to

connect the deck to the stringers was proposed in the present study, and the connection performance was evaluated experimentally. This connection type is expected to be better than the other types due to minimal drilling from the top of the deck. The deck panels were attached to the girders using a layer of epoxy (Fig. 4.49b). Note that some screws were utilized to compress the deck to the girder to activate the epoxy.

(a) Installation of Cross Braces

(b) Placement of Epoxy between Girder and Deck

(c) Drilling GRK Screws

(d) Placing Epoxy in Deck-to-Deck Connection

(e) Placement of Second Panel

(f) Interlocking Deck Panels

Figure 4.49 Assembly of Glulam Timber Girder Bridge Test Specimen

4.3.1.2 Fabrication and Assembly of Glulam Timber Girder Bridge Test Specimen

The entire test bridge was fabricated by a manufacturer then shipped as one piece to the Lohr Structures Laboratory. The following sections discuss the fabrication, assembly, and transportation of the test specimen.

Fabrication of Deck Panels

The glulam deck panels were built from M-29 Southern Yellow Pine. Thirty-five 1.375-in. thick laminations were glued together to form the 48-in. deck panels. Each panel was clamped to apply pressure and to activate the epoxy between the laminations. This type of epoxy does not activate until a minimum pressure of 150 psi is applied. The panels were stored in the construction facility with ambient room temperature to allow the epoxy to dry and harden. After epoxy hardening, the panel edges were grooved and routed to form a male-female connection.

Fabrication of Girders

The girders were specified to be built using 26F-1.9E Southern Yellow Pine. However, the ultimate testing showed that a wrong type of wood (24F-2.0E) was used in the fabrication process by mistake. This issue will be discussed later under the testing results. Twenty-two 1.375-in. thick laminations were glued together to form the girders. Each girder was clamped to apply pressure and to activate the glue after placing the epoxy between the laminations. The girders were placed in the construction area with an ambient room temperature to allow the epoxy to dry and harden.

Fabrication of Cross Braces

The cross braces were specified to be built with 26F-1.9E Southern Yellow Pine. However, they were also built with 24F-2.0E by mistake. The cross braces were cut and prepared with high precision to easily fit between the stringers.

Assembly of Bridge Test Specimen

The test specimen was completely assembled at the manufacturing site then shipped to the Lohr Structures Laboratory for testing. First the girders were placed beside one another (Fig. 4.49a); then the cross braces were installed between them. Epoxy was placed between the cross braces and the girders were installed. After completion of the diaphragms, the first deck panel was placed at the south end of the specimen. The panel was held upright by a forklift while the epoxy was placed on the top of the girders (Fig. 4.49b). Long screws were then installed to hold the panel in place and to allow the epoxy to cure (Fig. 4.49c). The next panel was installed with the same method, but was placed with care to ensure that the panel-to-panel connection was adequate. A bead of epoxy was placed along the male connection before the second panel was in place (Fig. 4.49d to 6.49f). This process continued until the deck system was completed.

Transportation of Test Specimen

The test specimen was transported from the manufacturer site in Tea, SD, to the Lohr Structures Laboratory in one piece. The bridge was loaded onto a truck using two forklifts. Upon arrival at the lab, the truck backed as far into the lab as possible. Two straps were placed approximately 20 ft apart. Wooden blocks were installed at these points to keep the straps in place and to avoid stressing the deck during lifting. The straps were hooked to a chain, which was connected to a 15-ton crane. The test specimen was then lifted, and the truck drove away. Finally, the abutments (reaction blocks) were placed and the test specimen was slowly dropped in place.

4.3.1.3 Test Setup for Glulam Timber Girder Bridge

The girder bridge specimen was tested under two different loading scenarios: (1) fatigue loading and (2) ultimate (strength) loading. The test setups for the two test procedures were slightly different, and are discussed.

Fatigue Test Setup

The bridge was supported on three reaction blocks at each end (Fig. 4.50). The reaction blocks at the north end were 28.5-in. tall while the reaction blocks at the south end were 4.5-in. shorter (24-in. tall) to allow for placement of load cells. Rectangular neoprene bearing pads, each with a dimension of 6-in. by 12-in., were placed under each girder. The length of the pad was based on the AASHTO requirements. Two 22-kip actuators were used to apply the load at the mid-span at 6.6 in. from the inside edge of the exterior girders. The location of the point loads was selected to produce equal reactions in the three girders. The load frame used to support the actuators had a height of 20 ft and a clear spacing of 10 ft between the columns.

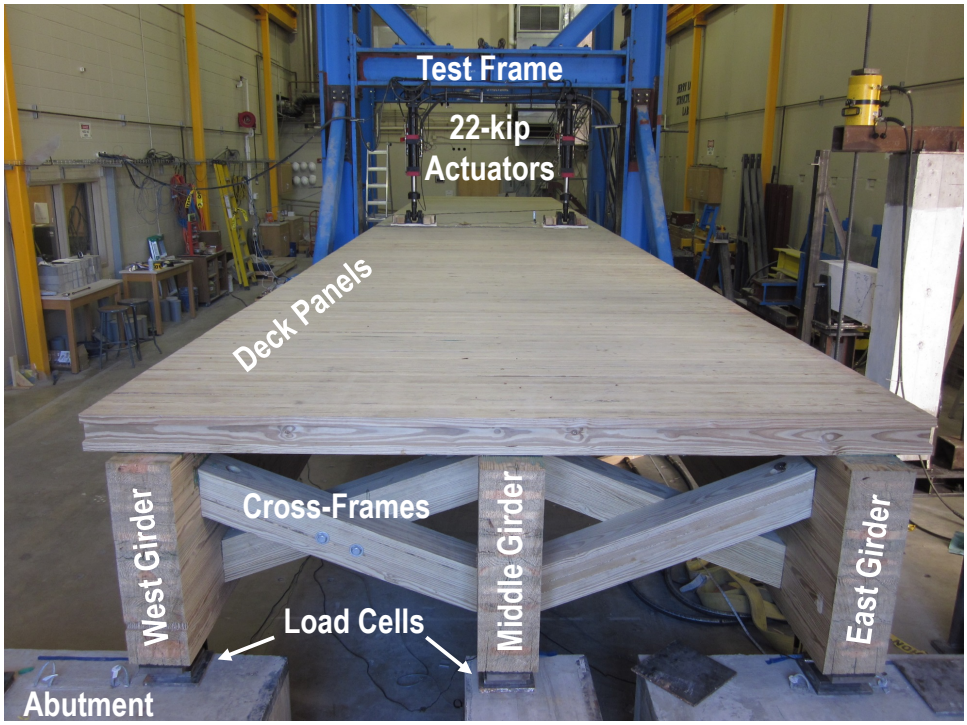

Figure 4.50 Fatigue Test Setup for Timber Girder Bridge

Ultimate (Strength) Test Setup

For the ultimate test, a 328-kip actuator was used to monotonically apply the load at the mid-span of the bridge. The load was distributed directly to the three girders using a spreader beam (Fig. 4.51).

Figure 4.51 Ultimate Test Setup

4.3.1.4 Instrumentation Plan for Glulam Timber Girder Bridge

The bridge test specimen was instrumented with strain gauges, linear variable differential transformers (LVDTs), load cells, and string potentiometers (string pots) to measure the response of the bridge at different load levels. Note that actuators also provide load and displacement data at the location of the applied load. This section presents the bridge instrumentation detailing.

Strain Gauges

Figure 4.52 shows the strain gauge plan for the test bridge. Strain gauges were installed only at the mid-span where the bending moment was at maximum. Three strain gauges were installed on the interior girder, and two gauges were placed on the exterior girders. Sixteen strain gauges were installed on the top of the deck to investigate the effective width of the deck for composite action. Wood strain gauges (PFL-30-11-5L), each with a length of 30 mm (1.18 in), were used in this project.

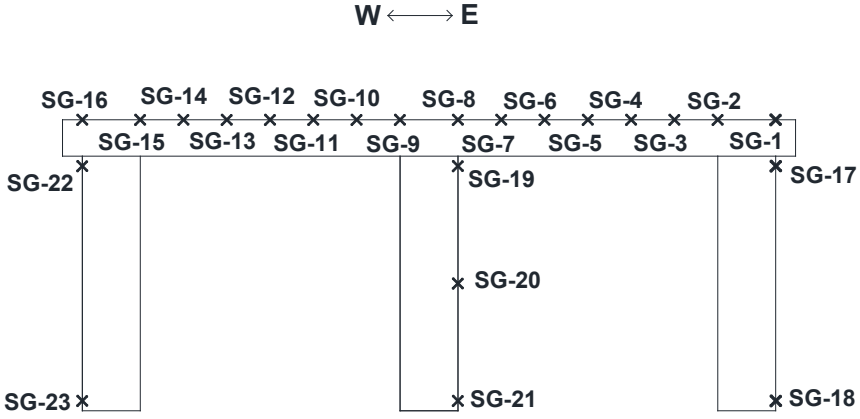

Figure 4.52 Strain Gauge Plan for Timber Girder Bridge

Linear Variable Differential Transformers (LVDTs)

Fourteen LVDTs were used to record displacements and rotations at various locations on the bridge (Fig. 4.53). Since the girders were placed on bearing pads, which compress under applied load, vertical LVDTs were installed at the end of each girder to measure the deformation of the pads and to calculate the net mid-span deflection. Three additional vertical LVDTs were installed at the mid-span to measure the girder deflections. Six horizontal LVDTs were used to measure either the relative displacements of the joints or the rotations.

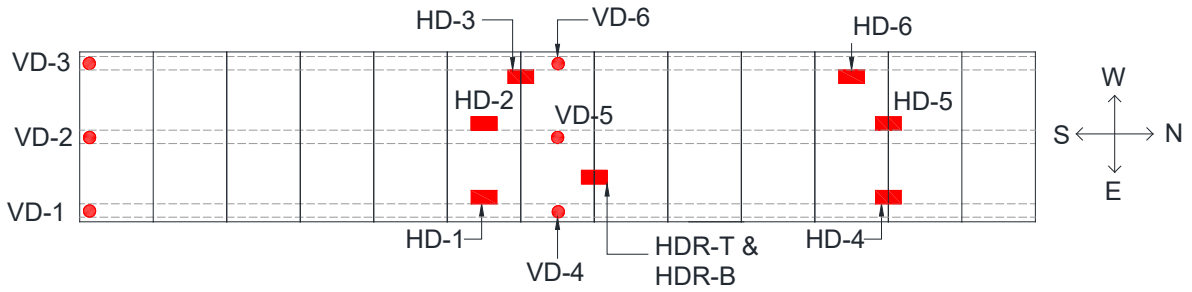

Figure 4.53 LVDT Installation Plan for Fatigue Testing of Glulam Timber Girder Bridge

For the ultimate testing, the LVDT installation plan was slightly modified. Since large displacements were expected under the ultimate load, the LVDTs at the mid-span of the bridge were removed (due to a small measuring range) and placed in other locations. VD-4 was removed and placed as HD-7 to measure the opening of the joint at the bottom of the bridge (2 joints south of HD-6). Note that VD-5 and VD-6 were removed at 1.25-in. displacement to avoid damage to the device.

String Potentiometers (String POTs)

Since string pots usually have a larger measuring range than LVDTs, they were used at the mid-span of the bridge during the ultimate test to measure deflections. The string pots were installed at the centerline of the girders at their bottom face.

Load Cells

Load cells were placed under each of the three girders at the south end to measure the support reactions. It was assumed that the reactions at both ends of the girders were equal because the load was applied at the mid-span.

Data Acquisition System

All of the instrumentation was connected to a 128-channel data acquisition system. A scan rate of 10 readings per second was used for the monotonic loading, and a scan rate of 100 readings per second was used for the cyclic loading.

4.3.1.5 Test Procedure for Glulam Timber Girder Bridge

The bridge specimen was tested under two loading scenarios: fatigue and ultimate. Fatigue testing was performed to investigate the performance of the bridge under 75 years of service life, and the ultimate testing was carried out to determine the capacities of the bridge. The test procedures are described in detail herein.

Fatigue Testing

Phase I of the bridge testing consisted of fatigue testing. Two 16-kip point loads were cyclically applied at the mid-span of the bridge (Fig. 4.50). The fatigue loading protocol was determined using AASHTO (2013) Fatigue II Limit State specifications. The number of the fatigue loading cycles was determined to be 410,625 cycles based on an average daily truck traffic (ADTT) of 15 for the 75 years of the design life. The total load cycle was increased to 500,000 to account for unexpected higher traffic. Force-based controlled cyclic loads were applied at a frequency of 0.7 Hz. The lower bound of the applied load during the fatigue testing was 300 lbs. to prevent the actuator from uplifting. Stiffness tests were performed at an interval of 50,000-load cycles, including an initial stiffness test. The stiffness load amplitude was 30 kips. The load was applied under a displacement-based control condition at a displacement rate of 0.007 in/sec.

Ultimate Testing

After completion of the fatigue testing, an ultimate test was carried out to determine the capacity of the timber girder bridge and to investigate the failure mode. A point load was applied at the mid-span of the bridge. The specimen was loaded under a monotonic displacement-controlled protocol to failure with a displacement rate of 0.007 in/sec. The data was recorded after completion of each displacement step. The displacement step was 0.05 in. up to a displacement of 1.30 in. then the displacement step was increased to 0.1 in. to the end of the testing.

4.3.2 Material Properties for Timber Girder Bridge

Table 4.6 presents mechanical properties of the timber that was used in the as-built test specimen (24F-2.0E), the timber that was specified to be used in the bridge (26F-1.9E), and M-29 glulam, which was used to construct the deck panels.

Table 4.6 Mechanical Properties of Glulam Timber Used in Girder Bridge

Properties	Notation	Unit	26F-1.9E	24F-2.0E	M-29
Tension Zone Stressed in Tension	F_{bxo}^{+}	ksi	2.6	2.4	1.55
Compression Zone Stressed in Tension	F_{bxo}^{-}	ksi	1.95	1.45	1.55
Shear Parallel to Grain	F_{vxo}	ksi	0.265	0.265	0.175
Modulus of Elasticity	E_{xo}	ksi	1900	2000	1700

The girders were specified to be built using 26F-1.9E Southern Yellow Pine. However, the ultimate testing showed that the wrong type of wood (24F-2.0E) was used in the fabrication process by mistake.

4.3.3 Test Results for Timber Girder Bridge

The girder bridge specimen was first tested under 500,000 cycles of the AASHTO (2013) Fatigue II loading using two 22-kip actuators at the mid-span. Then it was loaded monotonically to failure using a 328-kip actuator applying point loads at the mid-span. Results of both tests are presented.

4.3.3.1 Fatigue Testing of Glulam Timber Girder Bridge

Observed Damage

No damage to any components of the bridge was observed up to 250,000 load cycles, which was approximately equivalent to 46 years of service. However, deck-to-deck connections cracked at the 250,000 load cycle, and then the crack extended and widened at higher load cycles. Figure 4.54 shows

the damage to some of the joints before and after loading. There was no other apparent damage in any other components during the fatigue testing.

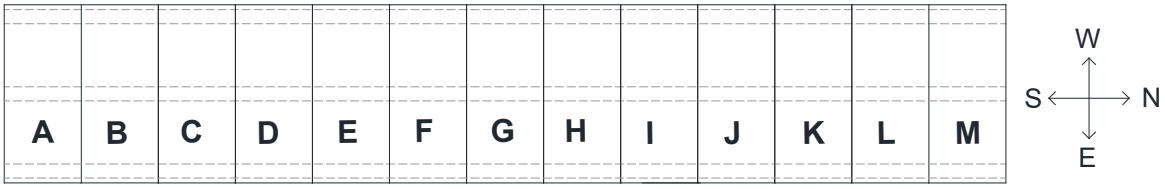

(a) Plan View of Bridge Deck

(b) Panel I-to-J Connection (East Side) at 0 Cycles

(c) Panel I-to-J Connection at 250,000 Cycles

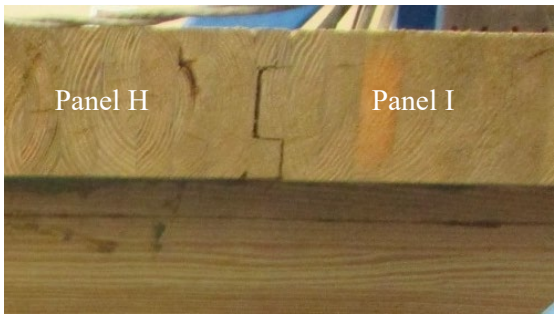

(d) Panel H-to-I Connection (West Side) at 0 Cycles

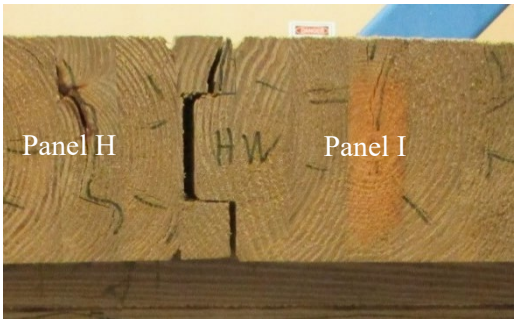

(e) Panel H-to-I Connection after 250,000 Cycles

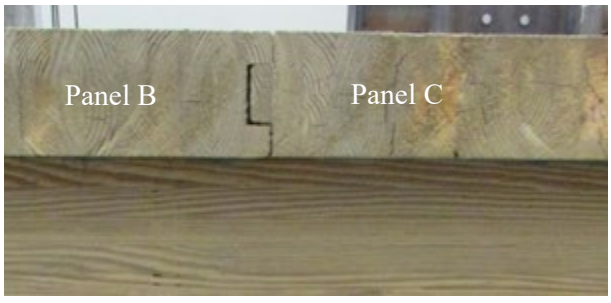

(f) Panel B-to-C Connection (West Side) at 0 Cycles

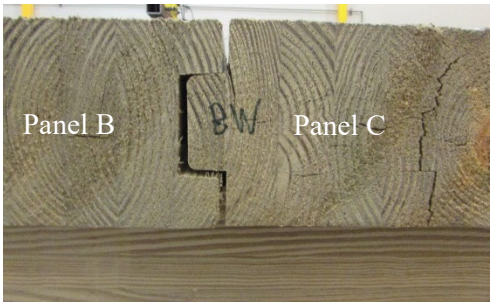

(g) Panel B-to-C Connection after 250,000 Cycles

Figure 4.54 Cracking of Deck-to-Deck Panel Connections for Glulam Timber Girder Bridge

Stiffness Degradation and Joint Integrity

Figure 4.55 shows the measured force-displacement relationship during the stiffness tests, which were performed every 50,000 load cycles. It can be seen that the bridge essentially remained linear-elastic during the fatigue testing with no stiffness degradation. Note that the stiffness is the ratio of the actuator load to the average net mid-span deflection of the girders.

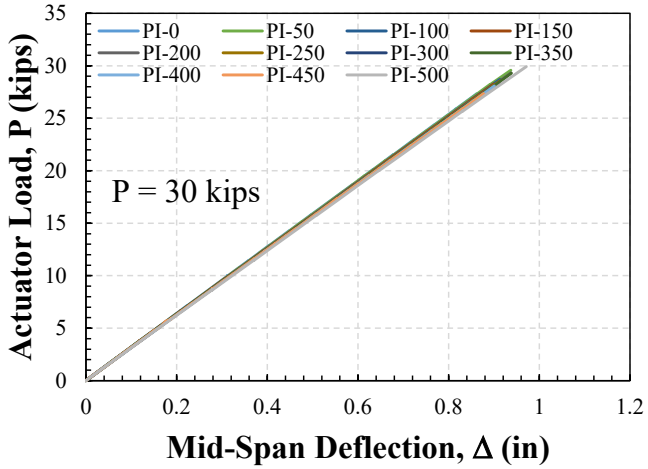

Figure 4.55 Measured Stiffness During Fatigue II Testing of the Glulam Timber Girder Bridge Specimen

Figure 4.56 shows the measured effective stiffness (EI) versus the number of load cycles. It can be seen that the overall bridge stiffness remained constant throughout the fatigue testing, confirming that the proposed glulam girder bridge detailing is structurally viable for 75 years of service.

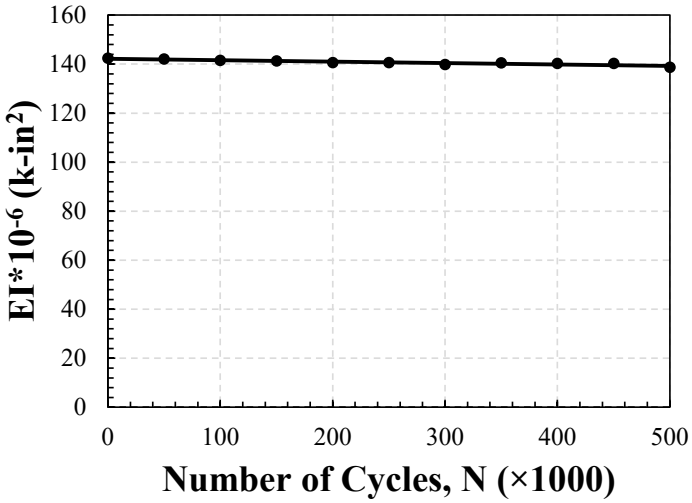

Figure 4.56 Stiffness Degradation during Fatigue II Testing of the Glulam Timber Girder Bridge Specimen

Measured Strains

The strain profiles of the timber bridge girders are shown in Fig. 4.57. It can be seen that the strain profiles remained approximately the same through all 500,000 load cycles of the fatigue testing. "PI-X" in the graph refers to the stiffness test at X-thousands of load cycles. Although there was some partial composite action, the graphs clearly show that the deck-to-girder connection did not act compositely since the strains of the deck were not compatible with the girder strains. Note that a partial composite action was considered during the design of the bridge. This assumption proved to be un-conservative since the composite action was minimal during the test. Therefore, the glulam girders should be designed as fully non-composite members.

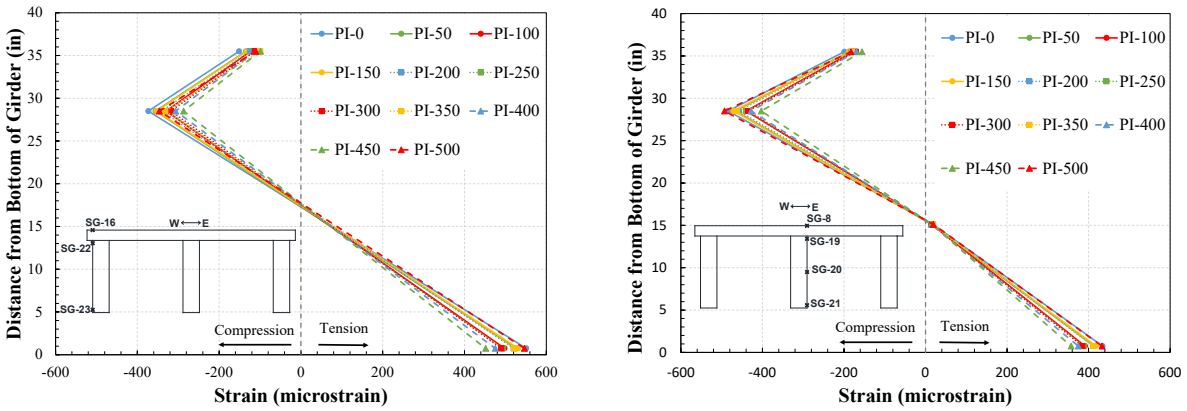

(a) West Girder (b) Interior Girder

Figure 4.57 Strain Profiles for Stingers of the Glulam Timber Girder Bridge Specimen

The strain profile of the deck is shown in Fig. 4.58. Sixteen strain gauges were installed on the deck surface to determine the effective width of the deck in a composite behavior. However, the full composite behavior was not achieved using the proposed deck detailing.

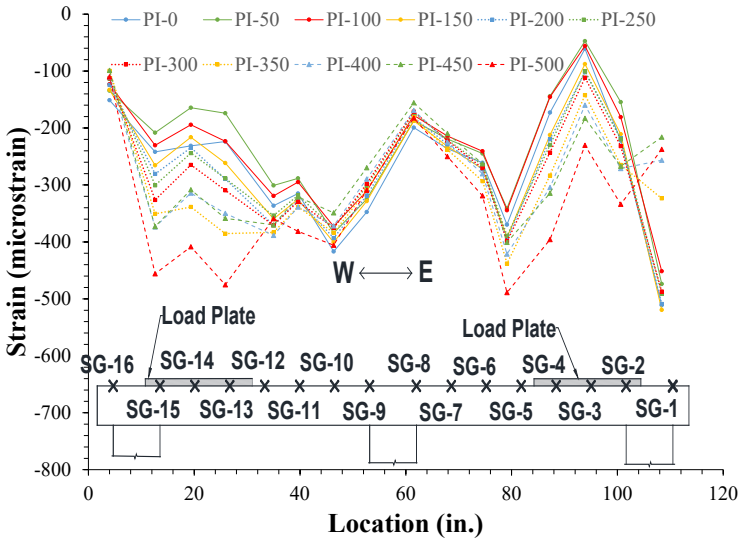

Figure 4.58 Deck Strain Profiles for the Glulam Timber Girder Bridge Specimen

Joint Rotations and Relative Displacements

The measured joint rotations versus the number of load cycles for one of the transverse joints are shown in Fig. 4.59. The joint rotations were negligible throughout the fatigue testing. The increase in the joint rotations at the cycle of 250,000 was due to the damage of the tongue-and-groove deck connections discussed in Sec. 4.2.3.1. Before the failure, the rotation was restrained by the panels while there was no such restrain after the failure of the connection; thus, the rotations increased afterward.

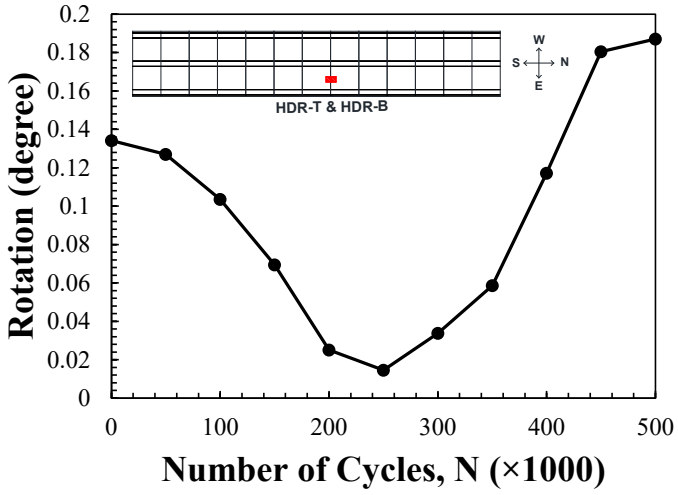

Figure 4.59 Transverse Joint Rotation During Fatigue Testing of the Glulam Timber Girder Bridge Specimen

The relative horizontal displacements between the girder and the deck (deck-to-girder slippage) were measured at different locations using six LVDTs during each stiffness test (Fig. 4.60). It can be seen that the relative displacements were negligible throughout the fatigue testing, indicating that the epoxy was able to hold the deck in place and prevent relative movement. Therefore, the proposed deck-to-girder connection using epoxy was adequate and may be used in the construction of new glulam girder bridges.

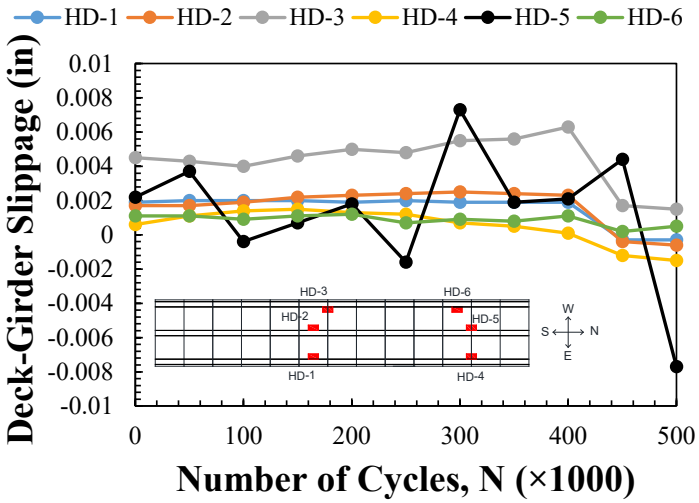

Figure 4.60 Deck-to-Girder Slippage During Fatigue Testing of the Glulam Timber Girder Bridge Specimen

Girder Load Distribution in Timber Girder Bridge

The load cell data was used to comment on the girder load distribution. The test setup was designed to produce the same loads in the three girders. Figure 4.61 shows the percentage of the load in each girder with respect to the total load during fatigue testing. It can be seen that the girder loads were 3% to 12% different from the target load (33% for each girder), and the overall distribution remained the same throughout the fatigue testing. The differences were attributed to the load cell accuracy.

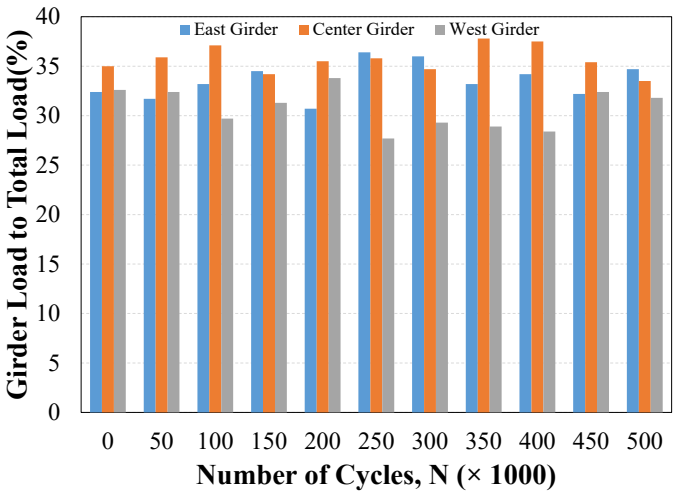

Figure 4.61 Girder Load Distribution During Fatigue Testing of the Glulam Timber Girder Bridge Specimen

4.3.3.2 Strength Testing of Timber Girder Bridge

The actuator load was equally spread to the three girders at the mid-span of the bridge. The bridge was loaded monotonically using a displacement-controlled loading to failure.

Observed Damage

The first crack in the form of delamination was observed in the west girder of the bridge (6 ft away from the bridge mid-span, underneath Panel I shown in Fig. 4.54a) at 101 kips (Fig. 4.62), followed by delamination of the center girder (at the mid-span) at 113 kips. When the specimen displaced farther downward, the bridge deck significantly tilted. The specimen failed by simultaneous failure of the west and the interior girders at a peak load of 123 kips (Fig. 4.63). There was no apparent damage in the east girder throughout the strength testing.

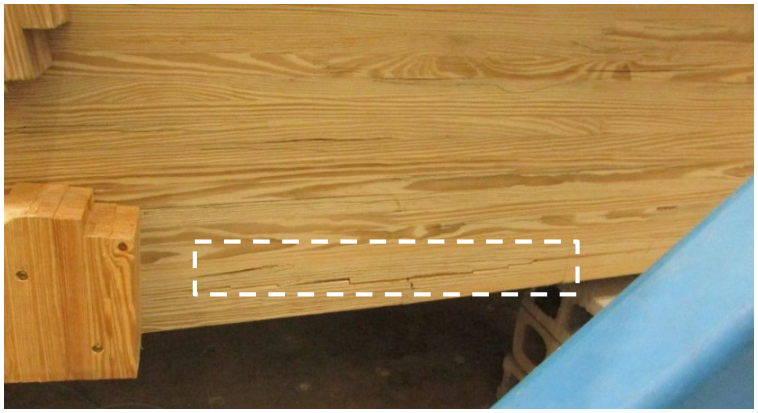

Figure 4.62 First Crack During Strength Testing in the West Girder

(a) Failure of West Girder

(b) Failure of West Girder

(c) Failure of Interior Girder

(d) Failure of Interior Girder

(e) Condition of East Girder at Mid-span

(f) Condition of East Girder at Mid-span

Figure 4.63 Glulam Girder Bridge Specimen Failure

Force-Displacement Relationship

Figure 4.64 shows the measured force-displacement relationship for the glulam girder bridge. The equivalent load level for each of the limit states is also shown in the figure with dashed lines. It can be seen that the bridge remained linear up to the first cracking, which occurred in the west girder. Load carrying capacity was significantly reduced when the interior girder cracked. The bridge failed at 123 kips.

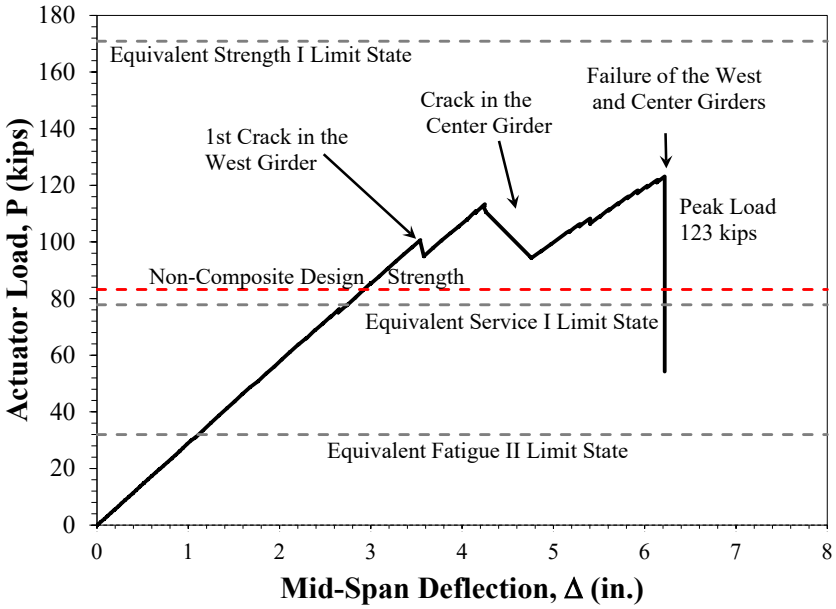

Figure 4.64 Force-Displacement Relationship During Strength Testing of the Glulam Timber Girder Bridge Specimen

Figure 4.64 clearly shows that the bridge did not meet the AASHTO strength limit state requirements because (1) the as-built girder constituent material was weaker than the specified material due to construction error, and (2) the bridge girders were designed assuming composite action. Review of the material datasheet provided by the manufacturer revealed that the girders were built with 24F-2.0E, while the design was based on 26F-1.9E. Furthermore, the strain profiles discussed in the previous section showed that the composite action was not achieved in this type of deck system.

Based on these findings, the bridge was redesigned with the as-built material properties and fully non-composite behavior, and the capacity was shown in Fig. 4.64 with a dashed red line. It can be seen that the AASHTO specification requirements can be achieved using the proper design assumptions. Therefore, the AASHTO method for design of timber bridges is applicable for the proposed glulam girder bridges.

Measured Strains

Figure 4.65 shows the bridge girder strains during the strength testing. Tensile and compressive strains were identified in the graph. It can be seen that the strain distribution was linear for glulam girders up to the failure. The flexural strain capacity of the girder on the tension side was 1900 microstrain, which was 58% higher than the design strain capacity (F_b / E=1200 microstrain) for 24F-2.0E.

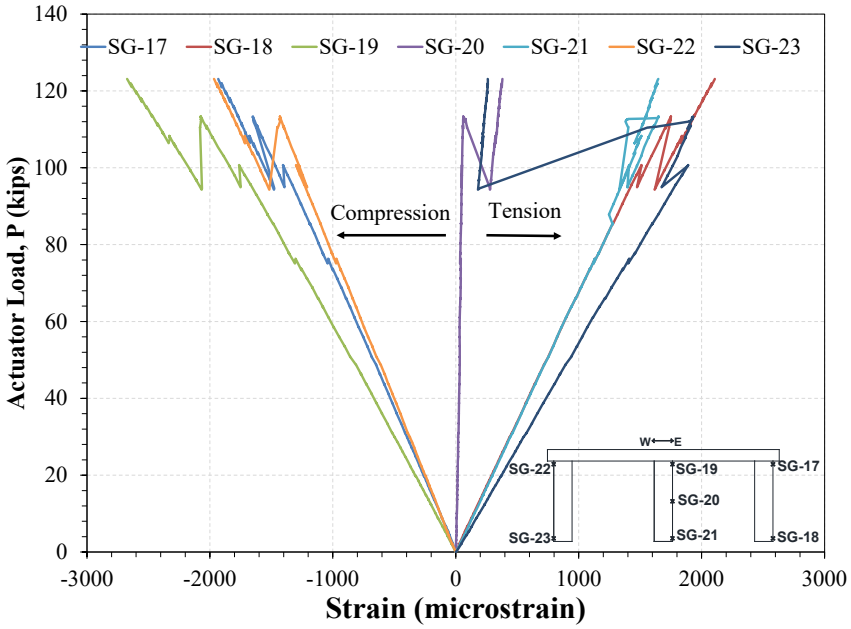

Figure 4.65 Measured Girder Strains During Strength Testing of the Glulam Timber Girder Bridge Specimen

Figure 4.66 shows the strain profile for the east girder of the bridge under the strength loading at various load levels. The glulam girder-deck sections were not composite since the strains were not linear over the depth of the section. However, the assumption of "plane section remains plane" was valid only for the glulam girders.

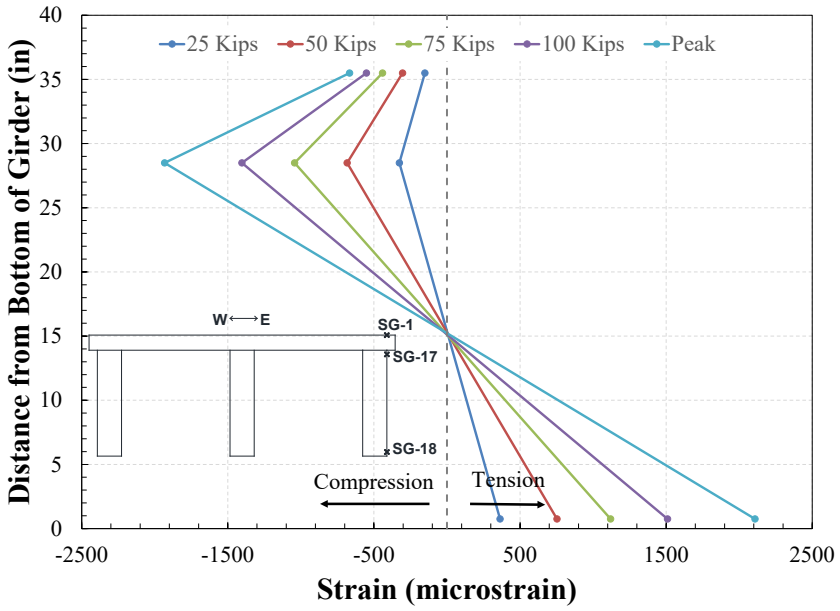

Figure 4.66 East Girder Strain Profile During Strength Testing of the Glulam Timber Girder Bridge Specimen

Figure 4.67 shows the deck strain profile during the ultimate testing at different load levels. Since the maximum strain was lower than the design strain capacities of the deck, the deck thickness was sufficient in the proposed bridge system.

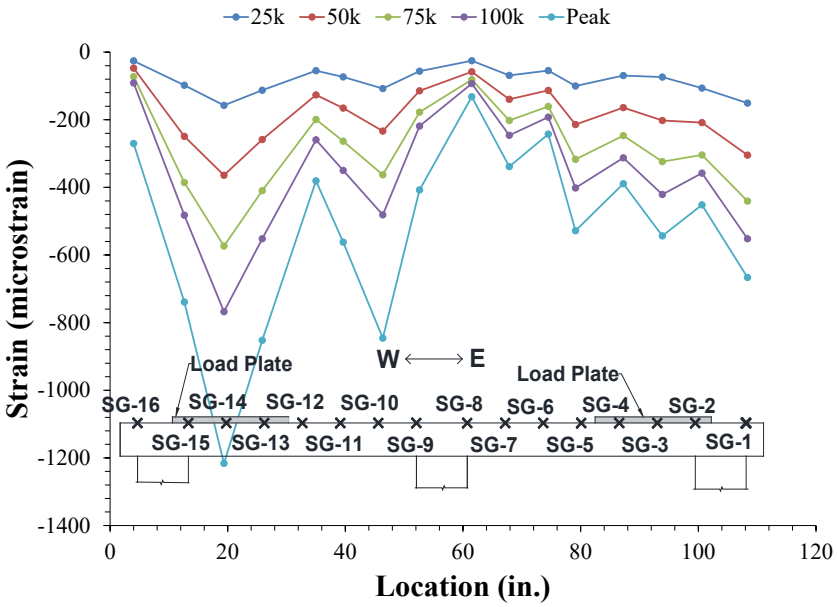

Figure 4.67 Deck Strain Profile During Strength Testing of the Glulam Timber Girder Bridge Specimen

Joint Rotations and Relative Displacements

LVDTs were placed at the top and the bottom of the bridge deck on the transverse joint closest to the mid-span to measure the joint rotation. Figure 4.68 shows the rotation during the ultimate testing. It shows that the joint rotated monolithically, and rotation increased linearly under the applied load. The maximum rotation was negligible, however.

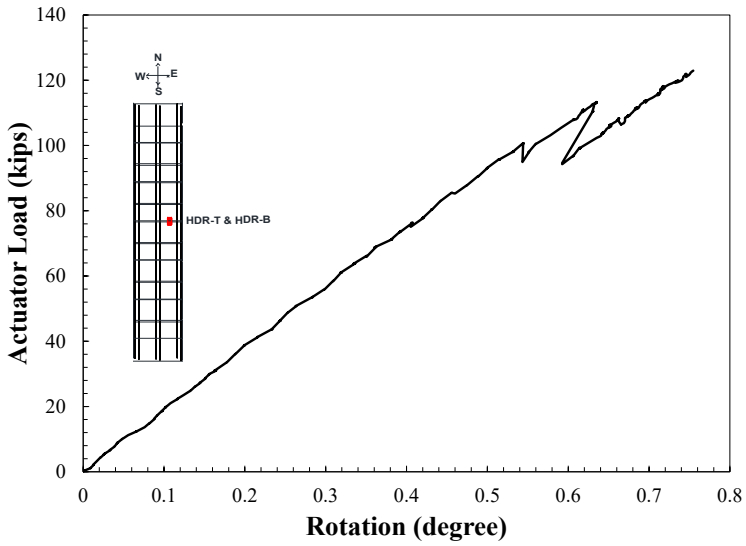

Figure 4.68 Transverse Joint Rotation During Strength Testing of the Glulam Timber Girder Bridge Specimen

The deck-to-girder slippage for six different locations (HD-1 to HD-6) (Fig. 4.69) indicates that all of the relative displacements were negligible. For the ultimate test, HD-7 was added to measure the opening of the deck transverse joint at the bottom of the deck. The deck-to-deck opening was higher for HD-7 compared with HD-1 through HD-6 measurements, and the girder failed beneath joint HD-7.

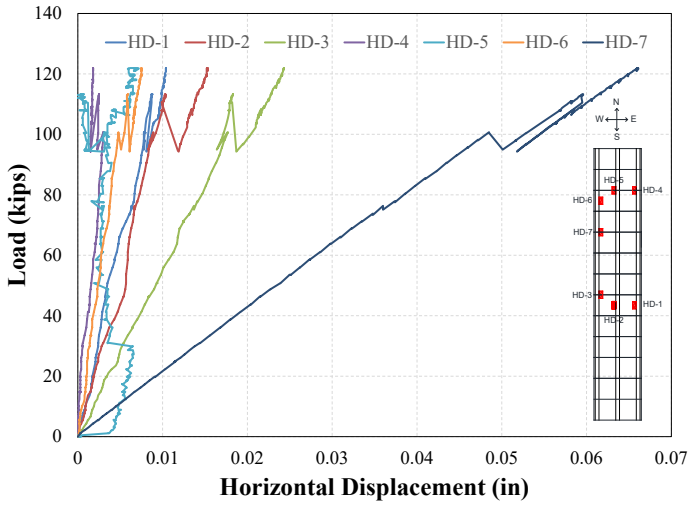

Figure 4.69 Deck-to-Girder Slippage During Strength Testing of the Glulam Timber Girder Bridge Specimen

4.4 Glulam Slab Bridge Specimen

Two types of glulam timber bridges (Fig. 3.17) were introduced in the previous section: (1) bridges built with transverse glulam decks supported on glulam stringers (referred to as the "girder bridges"), and (2) longitudinal glulam deck bridges (referred to as "slab bridges"). The structural performance of a glulam slab bridge was evaluated through full-scale experimentation. This section includes a summary of the design, construction, instrumentation, test setup, loading protocols, and test results for the full-scale timber slab bridge test specimen.

4.4.1 Glulam Timber Slab Bridge Test Specimen

4.4.1.1 Design of Test Specimen

Slab bridges can span up to 30 ft and cover several lanes of traffic. The prototype glulam timber slab bridge selected in the present study was assumed to be 16.5-ft long and 34.5-ft wide (Fig. 4.70a). The length was selected based on the manufacturer's limitations in producing deeper slabs, and the width is typical for two lanes of traffic sufficient for local roads. A full-scale bridge model was selected for testing, but with a width approximately equal to the width of one lane of traffic. The bridge test specimen (Fig. 4.70b) consisted of (1) two 20-ft long longitudinal deck panels with a depth of 10.75 in. and a width of 48.125 in., and (2) three stiffeners each 7.5-ft long (in the transverse direction of the bridge), 5-in. wide (in the longitudinal direction of the bridge), and 5.5-in. thick. The panels were connected to the stiffeners using two 0.75-in. diameter lag bolts per panel.

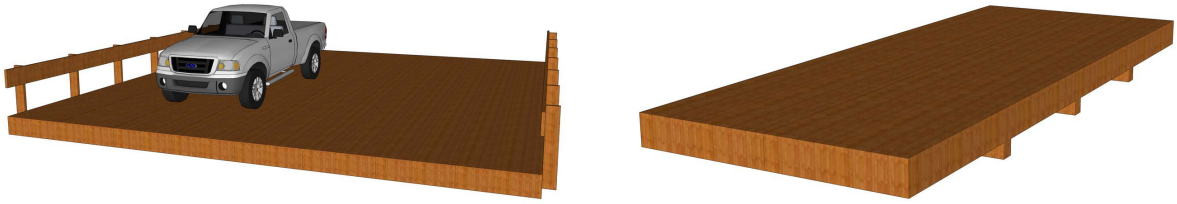

(a) Prototype Bridge (b) Test Model

Figure 4.70 Glulam Timber Slab Bridge

AASHTO (2013) standards and specifications were used in the design of the bridge components. The bridge was designed for HL-93 loading, which consists of a design truck or tandem accompanied by the design lane load.

Design of Deck Panels

The deck panels were analyzed and designed according to AASHTO (2013). Wheel load fractions were used to calculate the moment demand for each deck panel. The deck panels were designed using mechanical properties for 24F-2.0E Southern Yellow Pine. The final design resulted in 10.75-in. deep, 48.125-in. wide, and 16.5-ft long panels.

To further aid the designers, a spreadsheet was developed to find the capacity to demand ratio of the slab bridge in flexure, shear, compression, and tension. The spreadsheet allows checking the deflection of the bridge for different scenarios.

Design of Transverse Stiffeners

The transverse stiffeners were also designed according to AASHTO (2013). One stiffener must be placed at the mid-span, and the spacing of the stiffeners cannot exceed 8 feet. According to AASHTO specifications, the strength of a stiffener based on the adjusted modulus of elasticity (*E'*) times the moment of inertia (*I*) must be greater than 80,000 kip-in^2. The stiffeners were designed using 24F-2.0E Southern Yellow Pine. The final design resulted in 5.5-in. deep, 5-in. wide, and 7.5-ft long stiffeners.

Design of Deck-to-Stiffener Connections

The deck panels were attached to the stiffeners using 0.75-in. diameter lag bolts, each 12-in. long. Two bolts were used per panel. Initially, epoxy was considered to be used along the length of the stiffener in addition to the bolts, but the epoxy was deemed unnecessary for this connection since the bolt was connected from the bridge underneath with minimal durability issues.

4.4.1.2 Fabrication and Assembly of Glulam Timber Slab Bridge Test Specimen

The entire test bridge was fabricated in Tea, SD, then shipped as one piece to the Lohr Structures Laboratory. The following sections discuss the fabrication, assembly, and transportation of the test specimen.

Fabrication of Deck Panels

The glulam deck panels were built from 24F-2.0E Southern Yellow Pine. Thirty-five 1.375-in. thick laminations were glued together to form one 48-in. deck panel. The laminations were clamped together to apply pressure and to activate the epoxy between the laminations. This type of epoxy does not activate until a minimum pressure of 150 psi is applied. The panels were stored in the construction facility with ambient room temperature to allow the epoxy to dry and harden.

Fabrication of Stiffeners

The stiffeners were also made from 24F-2.0E Southern Yellow Pine. Four 1.375-in. thick laminations were glued together to form each stiffener. After the epoxy was placed between the laminations, the panel was clamped to apply pressure. The stiffeners were then stored in ambient room temperature until the epoxy dried and hardened.

Transportation of Test Specimen

The test specimen was transported from the manufacture site in Tea, SD, to the Lohr Structures Laboratory on a trailer pulled by a pickup truck. In Tea, the deck panels were loaded onto the trailer using a forklift, and the stiffeners were placed in the truck bed. Upon arrival at the lab, the trailer backed as far into the lab as possible. Two straps were placed around the panels to lift them. The straps were hooked to a 15-ton crane. The panels were then lifted and placed on the reaction blocks.

Assembly of Test Specimen

The test specimen was assembled in the Lohr Structures Laboratory. First, the deck panels were placed beside one another on the reaction blocks and then were shimmed up to have continuous support. Subsequently, the stiffeners were installed from the underside of the deck. The center stiffener was installed first; then the other two were bolted to the deck. A pilot hole was initially drilled in the stiffener, and then the lag bolts were screwed 6.5 in. into the underside of the deck.

4.4.1.3 Test Setup for Glulam Timber Slab Bridge

The slab bridge test specimen was tested under two different loading scenarios: fatigue loading, and ultimate (strength) loading. The test setup for the two test procedures were slightly different, and are discussed.

Fatigue Test Setup

The bridge test specimen was continuously supported on two reaction blocks at each end (Fig. 4.71). A continuous neoprene bearing pad was used at each end, between the panel and the abutment, to allow the specimen to rotate freely. Two 22-kip actuators were used to apply the load at the center of the panel at the mid-span.

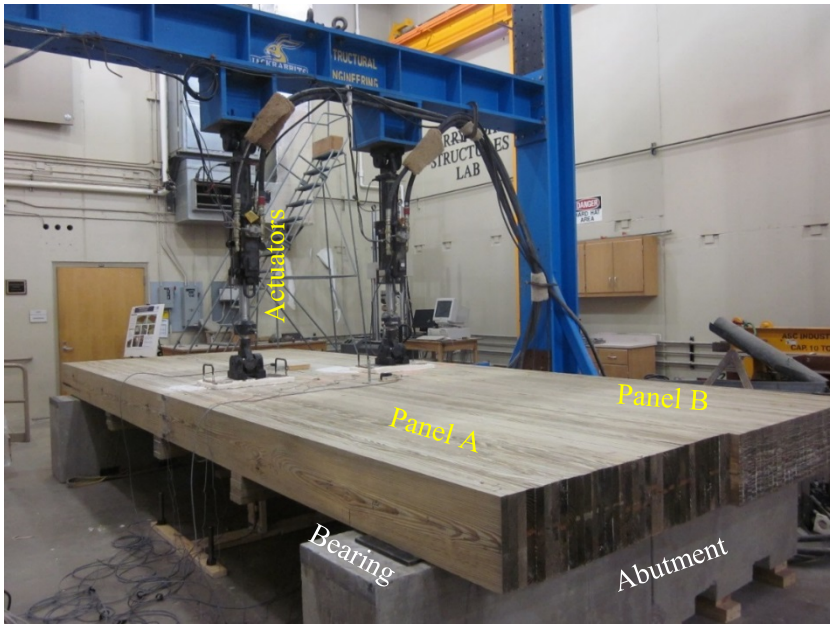

Figure 4.71 Fatigue Test Setup for Glulam Timber Slab Bridge

Ultimate (Strength) Test Setup

For the ultimate test, a 328-kip actuator was used to monotonically apply the load at the mid-span of the bridge. The load was equally distributed to the two panels using a spreader beam (Fig. 4.72).

Figure 4.72 Strength Test Setup for Glulam Timber Slab Bridge

4.4.1.4 Instrumentation Plan for the Glulam Timber Slab Bridge Specimen

The glulam timber slab bridge test specimen was instrumented with strain gauges, LVDTs, load cells, and string potentiometers (string pots) to measure the response of the bridge at different load levels. This section presents the bridge instrumentation detailing.

Strain Gauges

Each panel was instrumented with three strain gauges on the side surface to measure the strains at different depths of the panel (Fig. 4.73). Two additional strain gauges were installed on the top and bottom of the deck 6 in. away from the bridge longitudinal centerline. All deck panel strain gauges were offset 6 in. from the bridge transverse centerline to avoid interfering with the stiffener. The center stiffener was instrumented with five strain gauges measuring the strain in the transverse direction (Fig. 4.73c). Wood strain gauges (PFL-30-11-5L), each with a length of 30 mm (1.18 in.), were used in this project.

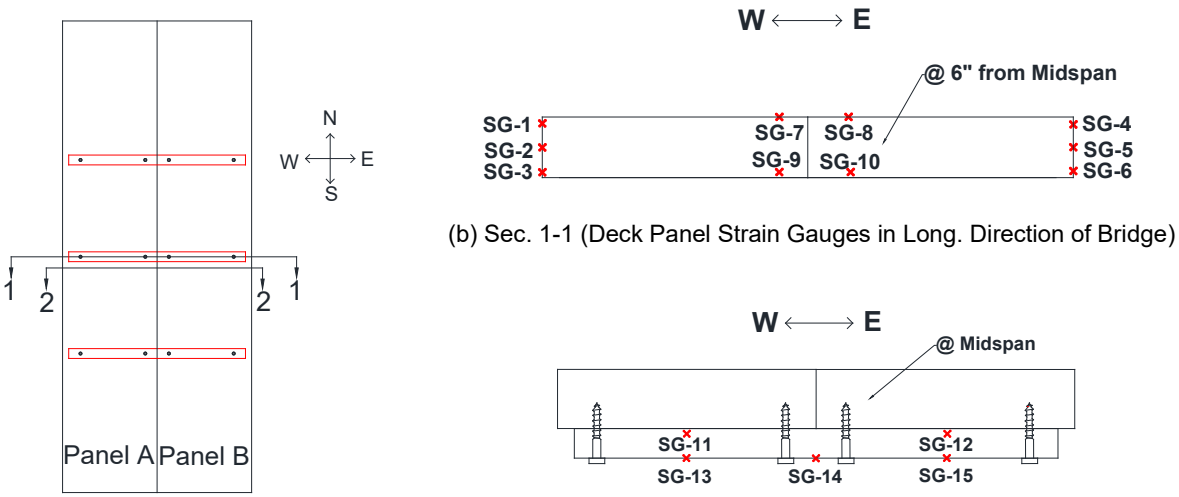

(a) Bridge Plan View

(b) Sec. 1-1 (Deck Panel Strain Gauges in Long. Direction of Bridge)

(c) Sec. 2-2 (Stiffener Strain Gauges in Trans. Direction of Bridge)

Figure 4.73 Strain Gauge Plan for the Glulam Timber Slab Bridge Specimen

Linear Variable Differential Transformers

Fourteen LVDTs were used to record displacements and rotations at various locations of the glulam timber slab bridge specimen (Fig. 4.74). Since the panels were placed on bearing pads that compress under applied load, vertical LVDTs were installed at the end of each panel to measure the deformation of the pads and to calculate the net mid-span deflection. Two additional vertical LVDTs were placed at the mid-span under the stiffener to measure deflection. Two more vertical LVDTs were placed 4.5 in. away from the mid-span on the deck panels. Six horizontal LVDTs were used to measure the slippage, relative displacements, and rotations. The HD-1 was installed to measure the slippage between the deck panels in the longitudinal direction. The HD-2 was used to measure the relative transverse displacement of the deck panels. The HD-3 was installed to measure the slippage between the deck panels and the stiffener. Two rotational LVDTs were installed above and below the longitudinal joint to measure the joint rotation.

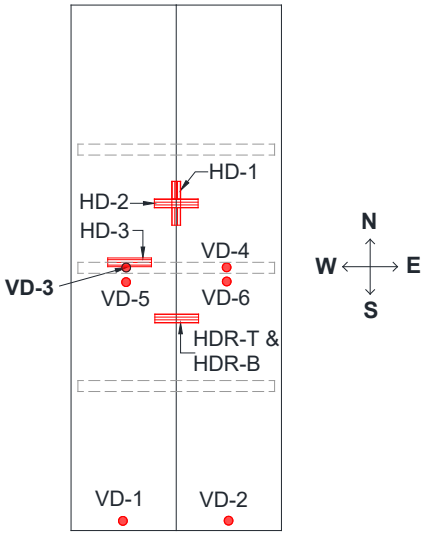

Figure 4.74 LVDT Installation Plan for the Glulam Timber Slab Bridge Specimen

String Potentiometers (String POTs)

Since string pots usually have a larger measuring range than LVDTs, they were used at the mid-span of the bridge during the ultimate test to measure deflections. The string pots were installed at the centerline of the girders at their bottom face.

Data Acquisition System

All of the instrumentation was connected to a 128-channel data acquisition system. A scan rate of 10 readings per second was used for the monotonic loading, and a scan rate of 100 readings per second was used for cyclic loading.

4.4.1.5 Test Procedure for the Glulam Timber Slab Bridge Specimen

The bridge specimen was tested under two loading scenarios: fatigue and ultimate. Fatigue testing was performed to investigate the performance of the bridge under 50 years of service, and the ultimate testing was carried out to determine the capacities of the bridge. The test procedures are described in detail.

Fatigue Testing

Phase I of slab bridge testing was fatigue loading. Two 11-kip point loads were cyclically applied at the mid-span of the bridge (Fig. 4.71). The fatigue loading protocol was determined using the AASHTO (2013) Fatigue II Limit State specifications. Since the slab bridge specimen is shorter than 40 ft, every truck passing the bridge applies two load cycles. This is because there are two 32-kip axles per truck; each has a significant contribution to the maximum moment. Therefore, applying two load cycles on the test bridge was equivalent to one truck load in field. The fatigue test was performed with 550,000 cycles of loading, which is equivalent to 50.2 years of service life based on the expected average daily truck traffic of 15. The load was applied at a frequency of 1.3 Hz and a magnitude of 22 kips. Stiffness tests were performed at an interval of 50,000 load cycles, including an initial stiffness test. The stiffness load amplitude was 30 kips. The load was applied under a displacement-based control condition at a displacement rate of 0.007 in/sec.

Ultimate Testing

After completion of the fatigue testing, an ultimate test was carried out to determine the capacity of the bridge and to investigate the failure mode. A point load was applied at the mid-span of the bridge. The specimen was loaded under a monotonic displacement-controlled protocol to failure with a displacement rate of 0.007 in/sec. The data was recorded after completion of each displacement step, which was 0.02 in.

4.4.2 Material Properties for the Glulam Timber Slab Bridge Specimen

Grade 24F-2.0E glulam was used for the construction of the test specimen. Table 4.7 presents the mechanical properties of the material. Correction factors were applied to these values for the design.

Table 4.7 Mechanical Properties of Glulam Timber Used in Slab Bridge

Properties	Notation	Unit	24F-2.0E
Tension Zone Stressed in Tension	F_{bxo}^{+}	ksi	2.4
Compression Zone Stressed in Tension	F_{bxo}^{-}	ksi	1.45
Shear Parallel to Grain	F_{vxo}	ksi	0.265
Modulus of Elasticity	E_{xo}	ksi	2000

4.4.3 Test Results of Timber Slab Bridge Specimen

The slab bridge specimen was first tested under 550,000 cycles of the AASHTO (2013) Fatigue II loading using two 22-kip actuators at the mid-span. Then it was loaded monotonically to failure using a 328-kip actuator applying point loads at the mid-span. Results of each testing are presented.

4.4.3.1 Fatigue Testing of the Glulam Timber Slab Bridge Specimen

Observed Damage

The only apparent damage during the fatigue test was the widening and extending of existing natural or manufacturing cracks at higher load cycles (Fig. 4.75). For example, the crack between the two laminations at the south end of the bridge was increased from 0.06 in. to 0.0625 in. before and after 550,000 load cycles. In field applications, the bridge deck will be flooded with epoxy; thus, the damage observed during testing should not occur. No other damage was observed in the fatigue testing of the slab bridge.

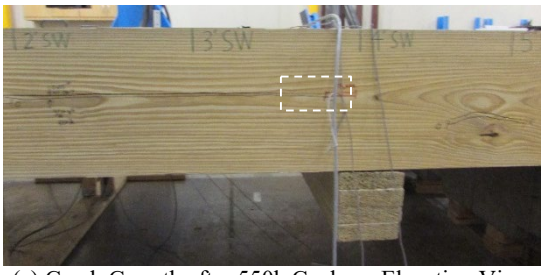

(a) Crack Growth after 550k Cycles – Elevation View

(b) Crack Growth after 550k Cycles – Slab at North Support

(c) Separation of Lamination after 550k Cycles at Southwest Support

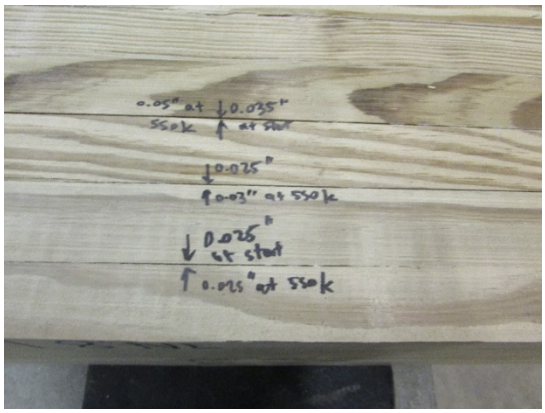

(d) Separation of Lamination after 550k Cycles at Southeast Support

Figure 4.75 Observed Damage During Fatigue II Testing of the Glulam Timber Slab Bridge Specimen

Stiffness Degradation

Figure 4.76 shows the measured force-displacement relationships for the glulam slab bridge during the stiffness tests that were performed after every 50,000 load cycles. It can be seen that the bridge essentially remained linear-elastic during the fatigue testing with no stiffness degradation. The stiffness is the ratio of the actuator load to the average net mid-span deflection of the deck panels.

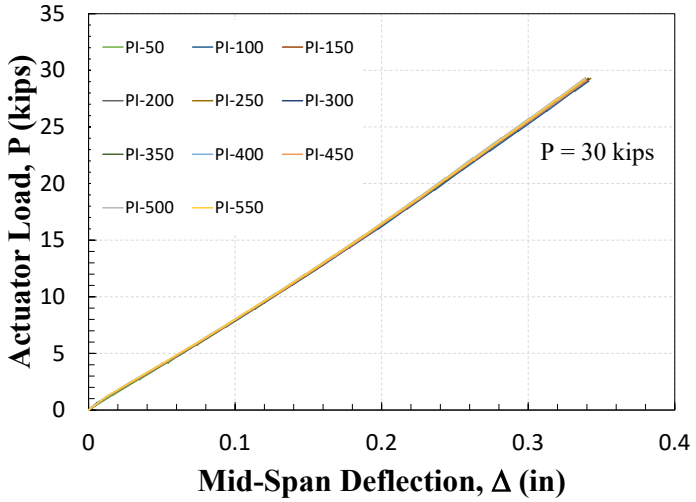

Figure 4.76 Measured Stiffness During Fatigue II Testing of the Glulam Timber Slab Bridge Specimen

Figure 4.77 shows the measured effective stiffness (*EI*) versus the number of load cycles. The overall bridge stiffness remained constant throughout the fatigue testing, confirming that the proposed glulam slab bridge detailing is structurally viable for the design service life.

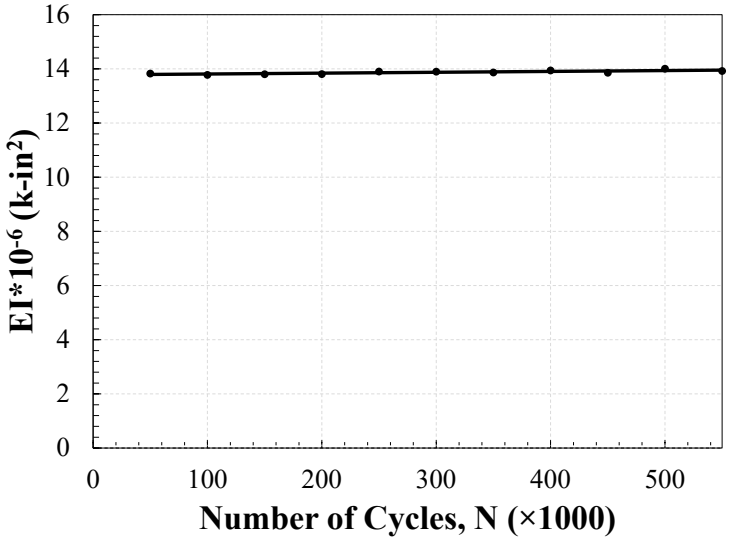

Figure 4.77 Stiffness Degradation During Fatigue II Testing of the Glulam Timber Slab Bridge Specimen

Measured Strain

Strain profiles of the deck panels throughout fatigue testing did not change (Fig. 4.78), indicating minimal damage and degradation of the bridge. The strain distribution was almost linear, showing that the "plane section remains plane" assumption is valid for the design of timber slab bridges. The strain profile might not be completely linear due to a slight misalignment of the strain gauges.

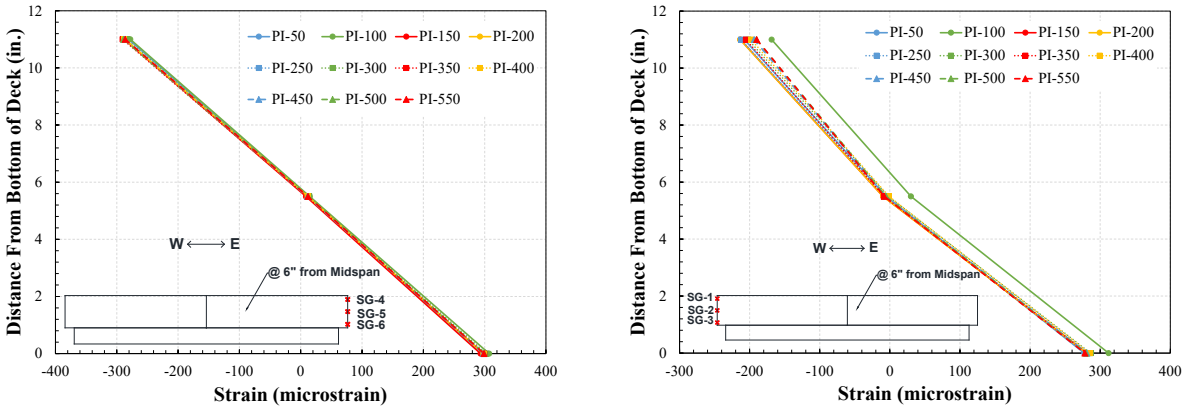

(a) East Face of Deck Panel

(a) West Face of Deck Panel

Figure 4.78 Deck Panel Strain Profiles under Fatigue II Testing of the Glulam Timber Slab Bridge Specimen

Joint Rotations and Relative Displacements

The measured joint rotations in the transverse direction of the bridge versus the number of load cycles for one of the transverse joints indicates that joint rotations were very small and remained relatively constant through all 550,000 load cycles of Fatigue II testing (Fig. 4.79).

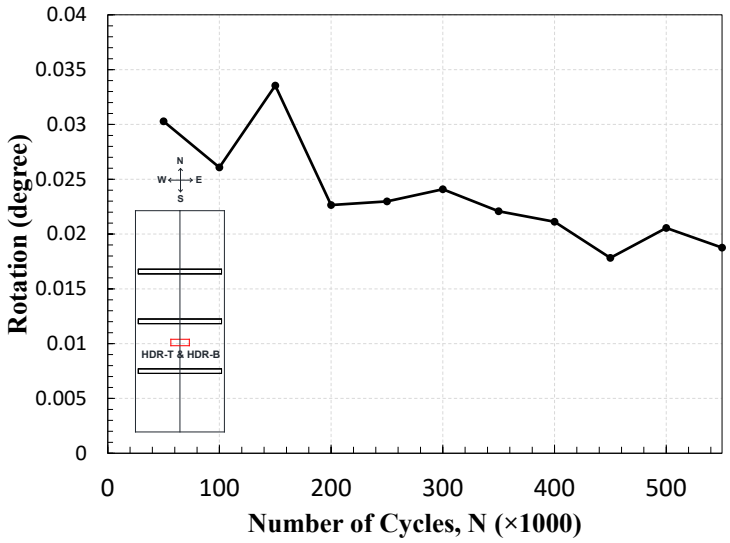

Figure 4.79 Joint Transverse Rotation During Fatigue II Testing of the Glulam Timber Slab Bridge Specimen

Shown in Fig. 4.80 are the (1) slippage between the two slabs (LVDT HD-1) in the longitudinal direction of the bridge, (2) opening of the joint at the bottom of the specimen (LVDT HD-2) in the transverse direction of the bridge, and (3) slippage between the deck and the stiffener (LVDT HD-3) in the transverse direction of the bridge during each stiffness test. All of these values were negligible, indicating adequate performance.

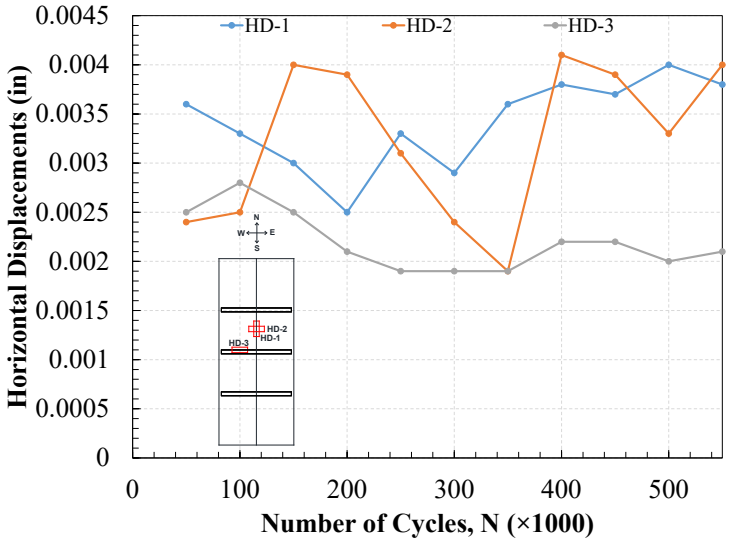

Figure 4.80 Horizontal Joint Displacements During Fatigue II Testing of the Glulam Timber Slab Bridge Specimen

4.4.3.2 Ultimate (Strength) Testing of the Glulam Timber Slab Bridge Specimen

The actuator load was equally spread to the two panels at the mid-span of the bridge at the centerline of each panel. The deck panels were loaded monotonically under a displacement controlled loading protocol until 270 kips, when the test was stopped due to setup limitations.

Observed Damage

There was no major damage throughout the entire strength testing of the glulam timber slab bridge specimen (Fig. 4.81). The only apparent damage was the widening and extending of the existing wood cracks and minor separation of the stiffeners from the deck panels (Fig. 4.81b). This problem could easily be fixed by retightening the bolts, if needed.

(a) Crack Growth at South Support after Testing

(b) Separation of Deck Panel and Stiffener

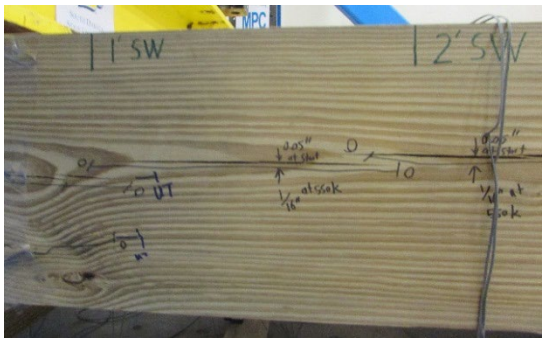

(c) Crack Growth Near Mid-span after Ultimate Test

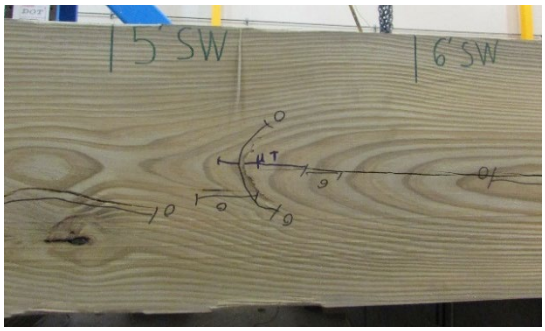

(d) Crack Growth Near South Support after Testing

Figure 4.81 Damage of Glulam Slab Timber Bridge Specimen under Ultimate Loading

Force-Displacement Relationship

Figure 4.82 shows the measured force-displacement relationship of the timber slab bridge during strength testing. The equivalent loads for each of the AASHTO (2013) limit states are also shown in Fig. 4.82 with dashed lines. The test was stopped at a peak load of 270 kips due to the setup limitations. Based on AASHTO (2013) specifications, the allowable displacement for the service limit state is 0.466 in. for this bridge. The measured service level displacement was 0.29 in., which is lower than the AASHTO (2013) requirement, indicating that the design was adequate. Note these limit state values are not the same for different bridges due to their geometry. Overall, since there was no significant damage, and the bridge surpassed all the AASHTO (2013) limit states, it can be concluded that this bridge is a viable short-span option for local roads.

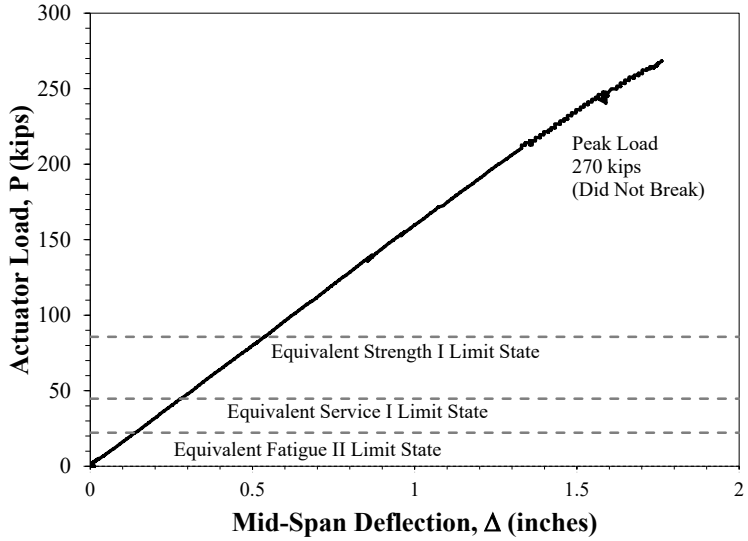

Figure 4.82 Force-Displacement Relationship During Strength Testing of the Glulam Timber Slab Bridge Specimen

Measured Strains

Figure 4.83 shows the strains in the deck in the longitudinal direction of the bridge during the strength testing. Negative numbers correspond to compression, and positive numbers correspond to tension. It can be seen that the strain distribution is linear for the panels. The lower bound flexural strain capacity of the panels on the tension side was 4,000 micro-strain, which was 3.33 times higher than the design strain capacity (F_b / E=1200 micro-strain) for 24F-2.0E glulam timber. Strain data from SG-5 was not reliable; thus, it was not shown in the figure.

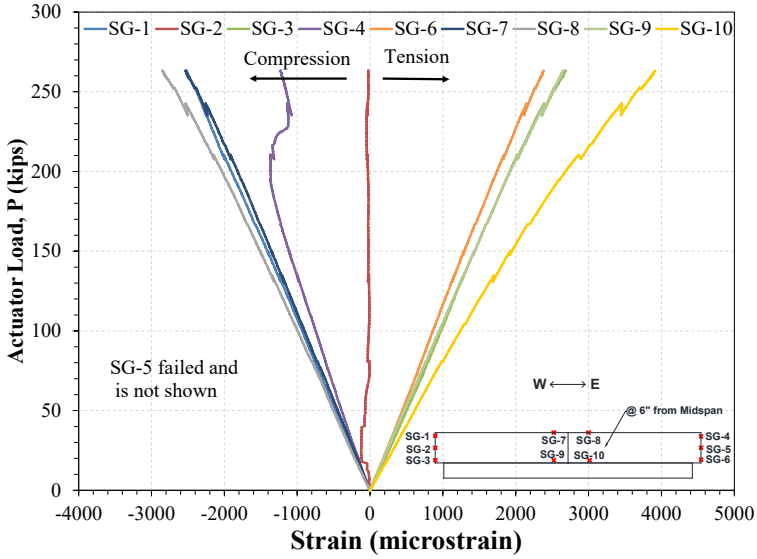

Figure 4.83 Measured Deck Strains During Strength Testing of the Glulam Timber Slab Bridge Specimen

Figure 4.84 shows the strains in the middle stiffener in the transverse direction of the bridge during strength testing. The strains were not completely linear since there was some slight slippage between the

deck panels and the stiffeners, changing the load transfer between the members. Overall, it can be concluded that the stiffeners were engaged at different load levels; thus, they should be utilized in the design and construction of this type of bridge to unify the deck system.

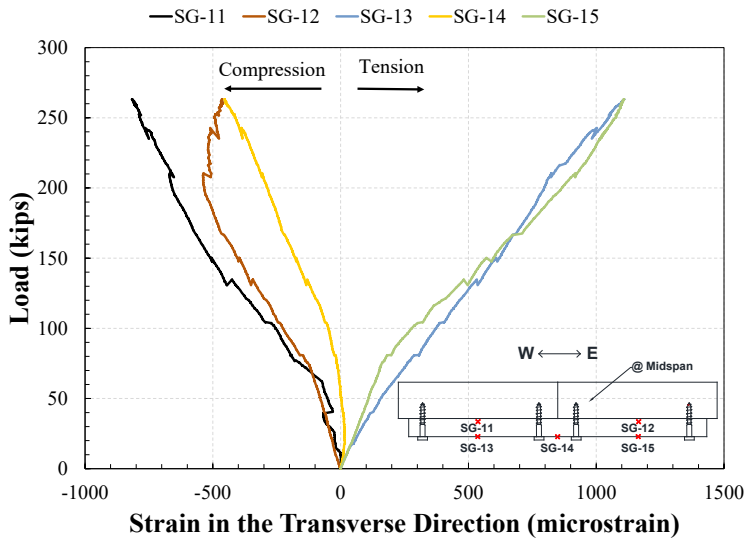

Figure 4.84 Measured Stiffener Strains During Strength Testing of the Glulam Timber Slab Bridge Specimen

Joint Rotations and Relative Displacements

LVDTs were installed at the top and bottom of the specimen on the longitudinal joint in the bridge transverse direction to measure the joint rotations. During the ultimate testing, joint rotations increased approximately linearly under the applied increasing load (Fig. 4.85). However, the maximum rotation was negligible.

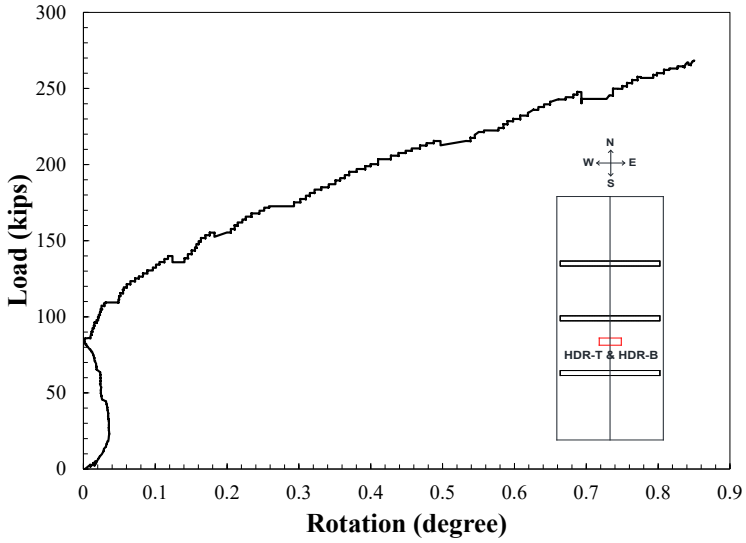

Figure 4.85 Joint Transverse Rotation During Strength Testing of the Glulam Timber Slab Bridge Specimen

During ultimate testing, Fig. 4.86 shows (1) slippage between the two panels (using LVDT HD-1) in the longitudinal direction of the bridge, (2) opening of the joint at the bottom of the specimen (HD-2) in the transverse direction of the bridge, and (3) slippage between the deck and the stiffener (HD-3) in the transverse direction of the bridge. It can be seen that the deck panel's relative movement was negligible in the longitudinal direction of the bridge. All relative displacements were negligible at the AASHTO (2013) service limit state (less than 0.01 in.), as well as the AASHTO strength limit state (approximately 0.015 in.). However, the longitudinal joint opened in the transverse direction of the bridge, and the stiffener slipped with respect to the panels at higher loads.

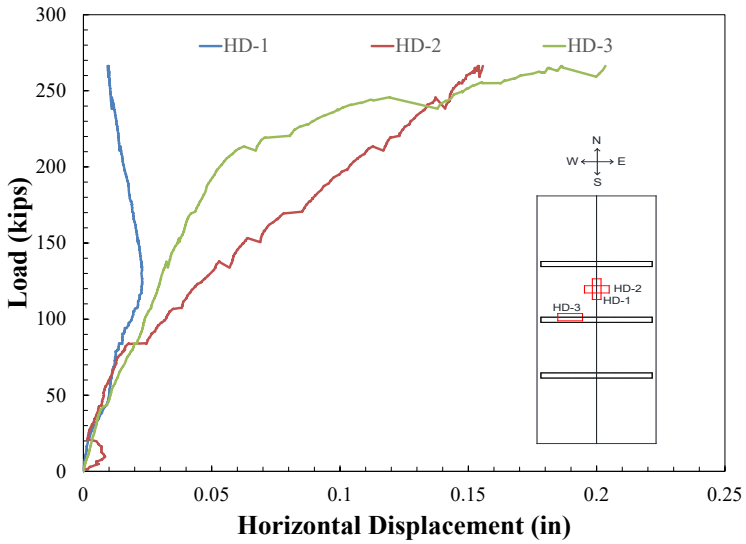

Figure 4.86 Relative Horizontal Joint Displacements During Strength Testing of the Glulam Timber Slab Bridge Specimen

5. EVALUATION OF PROPOSED BRIDGE SYSTEMS

This section presents an evaluation of the three proposed bridge systems, including (1) structural performance, (2) comparison with the modified double-tee bridges (for the precast bridge only), (3) constructability, and (4) superstructure costs.

5.1 Full-Depth Deck Panels Supported on Inverted Tee Girders

5.1.1 Performance under Service, Fatigue II, and Strength Limit States

The number of trucks passing the prototype bridge over a 75-year design life is 411,000, based on the average daily truck traffic (ADTT) of 15 for local roads in South Dakota. The full-scale, single-lane test bridge was subjected to 500,000 load cycles at the mid-span and an additional 150,000 load cycles adjacent to the mid-span panel transverse joints to maximize the shear transfer. The load at the mid-span corresponded to the moment experienced by the interior girders of the prototype bridge, based on the Fatigue II limit state loading specified by AASHTO (2013).

The test bridge stiffness did not degrade, and the joints remained watertight through 650,000 fatigue load cycles (Fig. 5.1). The 650,000 fatigue load cycles are equivalent to 119 years of service for this bridge on South Dakota local roads. The stiffness change during the entire fatigue test was less than 3% with respect to the bridge's initial stiffness. Narrow or shallow shrinkage cracks were observed in the haunch region and the deck full-depth pockets, as well as the transverse joints filled with either conventional grout or latex modified concrete. However, no crack was observed on the hidden pockets. No other significant damage was observed during the entire fatigue testing for decks, joints, and girders.

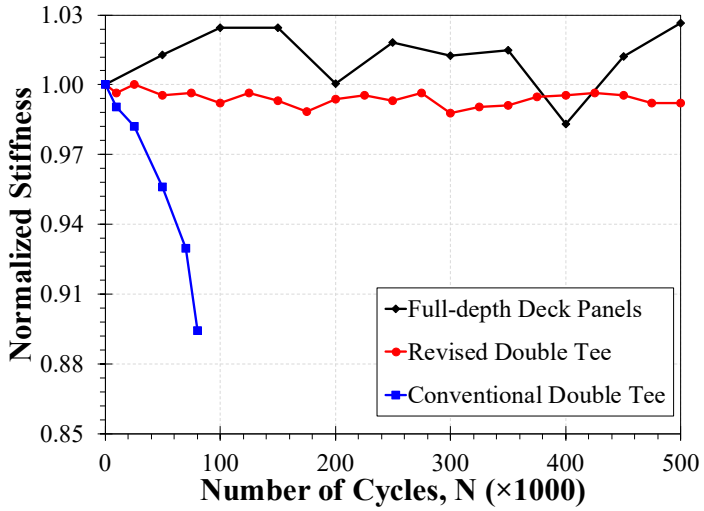

Figure 5.1 Comparison of Stiffness Degradation for Precast Bridges

Double-tee bridges consist of precast prestressed girders commonly used for superstructure bridges on SD local roads. A previous experimental study by Wehbe et al. (2016) was performed to revise the longitudinal joint detail to improve serviceability and strength performance of double-tee bridges. They showed that the stiffness of the revised double-tee girders did not deteriorate under 500,000 fatigue load cycles, while original double-tee girders were not structurally sufficient for long-term performance (Fig. 5.1). The present experimental study confirmed that the stiffness of the full-depth deck panels supported on inverted tee girders can be expected to remain essentially the same for 75 years of service.

The equivalent AASHTO (2013) Service I limit state load was 76.7 kips, and the Strength I limit state load was 131.4 kips for the proposed precast bridge. The test bridge girders did not crack at these limit states. The test bridge girder's first flexural crack occurred at a load of 149 kips, which indicates that the bridge has adequate capacity (Fig. 5.2). More cracks formed on the girders at higher loads. The test was stopped at 263 kips due to setup limitations. The load corresponding to the flexural failure of the test bridge was 402 kips, based on a moment-curvature analysis. No significant damage was observed in the deck panels, joints, and haunch region under the entire ultimate testing.

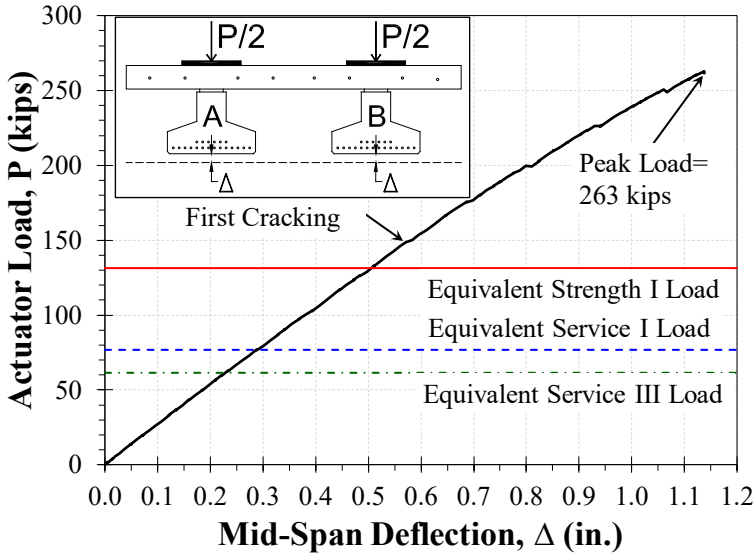

Figure 5.2 Measured Force-Displacement Relationship for Proposed Precast Bridge

5.1.2 Constructability

The constructability of the main components of the precast full-depth deck panels supported on inverted tee girders is evaluated.

5.1.2.1 Precast Inverted Tee Girders

The precast inverted tee girders were cast using partial-depth I-girder forms. Overall, the proposed girder design and construction are similar to current practice.

An actual bridge on a local road will typically consist of seven inverted tee girders; whereas, local road bridges built with double-tee girders consist of nine girders. Onsite construction is expected to be rapid for each system, but more involved for the proposed inverted tee girder bridges since there are more joints to be filled.

5.1.2.2 Full-Depth Deck Panels

The formwork for full-depth deck panels were made of 2-in. by 4-in. lumber and 1-in. plywood. Overall, current practice can be applied for the design and construction of the proposed deck panels.

The full-depth deck panels were quickly installed in the laboratory. In terms of onsite activities, special care should be taken on the adjustment of the panel grades, which can be easily done by adjusting the leveling bolts. Double-tee bridges will be easier to install onsite since the deck is integrated with the webs.

5.1.2.3 Shear Pockets

The hidden pocket detail was formed using plywood for the pocket and PVC pipes for the grout and vent ports. Fabrication of the hidden shear pockets was relatively easy and efficient. Pockets should be cleaned before installation of the panel.

5.1.2.4 Horizontal Shear Studs

Both the double headed and inverted U-shape shear studs were found to be viable options for use in inverted tee girders. The studs are installed prior to girder casting.

5.1.2.5 Transverse Joints

The transverse joint female-to-female shear key geometry was formed with plywood. The hollow structural steel (HSS) sections were secured to the transverse joint formwork using threaded rods, nuts, and steel plates inside the HSS. Transverse joints can be easily prepared, sealed, and filled with grout from the top of the bridge during onsite construction.

5.1.2.6 Leveling Bolts

A leveling bolt device was formed using a threaded rod welded to a steel plate at the bottom and a nut at the top, a vertical steel pipe embedded in concrete to encase the rod, and a 2-in. by 4-in. lumber piece for the blockout at the top of the deck (Fig. 5.3).

Figure 5.3 Leveling Bolt Construction Detail

5.1.2.7 Grouted Haunch

It is expected that forming and sealing the grouted haunch of the proposed system from the top of the bridge will be the most challenging onsite activity. In the laboratory, the grouted haunch was formed by securing 2 in. by 4 in. lumber between the girders to hold ¾-in. thick plywood against the girder sides (Fig. 5.4). Placing the forms inside the girders was easier than placing forms outside the girders, which required clamping reaction lumber to the bridge deck to secure 2-in. by 4-in. struts and to hold the plywood.

Figure 5.4 Grouted Haunch Region Formwork Installed between Girders

5.1.3 Precast Bridge Cost Estimate

Table 5.1 presents a comparison of superstructure materials and fabrication cost for the proposed precast bridge system and the modified double-tee (new detailing based on Wehbe et al., 2016) systems for a 50-ft long by 34.5-ft wide bridge. Materials and fabrication cost for 46-in. wide by 23-in. deep precast double-tee girders is approximately $247 per linear foot, based on data provided by SDDOT. The nine double-tee girders used in a 50-ft long by 34.5-ft wide bridge would cost approximately $111,000 for the superstructure materials and fabrication.

Table 5.1 Proposed Precast Bridge and Modified Double Tee Superstructure Material and Fabrication Cost Comparison

Bridge System	Precast Full-Depth Deck Panels on Inverted Tee Girders	Modified Double-Tee Girders
Materials/Fabrication ($)	123,000	111,000
Materials/Fabrication ($/sq. ft.)	71	64

The 21-in. deep precast inverted tee girders were estimated to cost $130 per linear foot, and the precast 8-in. thick full-depth deck panels were estimated to cost $45 per square ft. The 50-ft long by 34.5-ft wide actual bridge materials and fabrication cost estimate in Table 4.1 was calculated based on seven 50-ft long by 21-in. deep precast inverted tee girders with a total cost of $45,500, and five 34.5-ft wide by 10-ft long by 8-in. deep precast full-depth deck panels with a total cost of $77,625. The total materials and fabrication cost estimated by the manufacturer for precast full-depth deck panels supported on inverted tee girders is approximately $123,000 for the actual bridge. Therefore, the material and fabrication cost of this type of bridge is approximately 11% more than that for double-tee bridges.

Note that other costs, such as mobilization, onsite activities, and substructure fabrication, and construction, are not included in Table 5.1. The total superstructure cost, including mobilization and onsite activities for the proposed precast bridge, is estimated to be from $99 to $108 per square foot. These data were not available for double-tee bridges at the time of this writing.

Overall, the cost of the proposed bridge system is slightly more than the double-tee bridge system, which is the most common type of bridge on SD local roads. It is expected that the proposed precast bridge system will be more competitive with the double-tee bridges when spans are more than 40 ft.

5.2 Glulam Timber Girder Bridges

5.2.1 Performance under Service, Fatigue II and Strength I Limit States

Based on the ADTT of 15 for local roads in South Dakota, approximately 411,000 trucks will cross a bridge in 75 years. The full-scale 50-ft long test bridge was subjected to 500,000 load cycles at the mid-span to simulate the traffic loading for 75 years. The load at the mid-span corresponded to the maximum moment experienced by the interior girders of the prototype bridge based on the Fatigue II limit state loading specified in AASHTO (2013).

The bridge specimen's stiffness did not degrade throughout the 500,000 cycles (Fig. 5.5). The change in the stiffness throughout the fatigue test was less than 3%, compared with the initial bridge stiffness. The only damage observed during the fatigue testing was at the deck-to-deck connections in which the tongue-and-groove connection cracked. This type of connection shall be avoided in field applications. One possible solution is to place the two deck panel faces directly against one another and to fill the joint with wood adhesive epoxy.

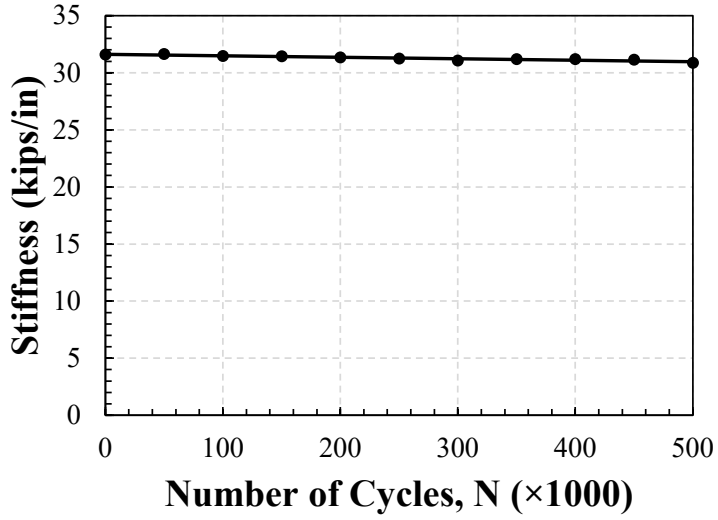

Figure 5.5 Stiffness of Glulam Timber Girder Bridge under Fatigue II Loading

Figure 5.6 shows the measured load-deflection for the glulam timber girder bridge specimen. Shown in the figure are the equivalent AASHTO (2013) service I limit state load (77.8 kips) and the Strength I Limit State load (170.9 kips). The first crack in the glulam timber bridge girders occurred at a load of 101 kips, 30% higher than the Service I Limit State load. However, the specimen's load carrying capacity of 123 kips was lower than estimated and the girders failed before reaching the Strength I Limit State load. Overestimation of the specimen's load carrying capacity was due to (1) a construction error, which resulted from using weaker than specified wood grade, and (2) the incorrect design assumption that composite action would develop between the girders and the deck panels. The design capacity of a non-composite timber girder bridge with the same geometry and materials as those used in the bridge test specimen would be 83.21 kips, which is less than the measured load carrying capacity of 123 kips. Thus, glulam girder bridge design should be conservatively based on a non-composite section. No significant damage was observed on the deck panels throughout the ultimate testing.

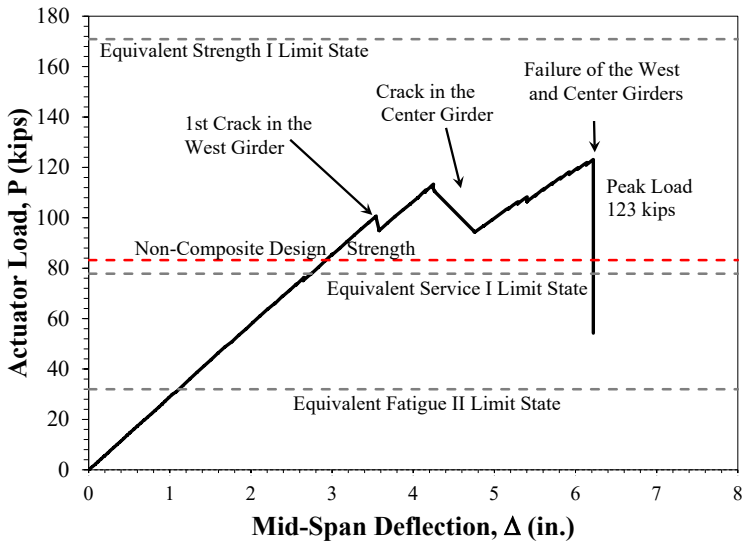

Figure 5.6 Force-Displacement Relationship During Strength Testing of the Glulam Timber Girder Bridge Specimen

Overall, the AASHTO (2013) method of design for glulam girder bridges was found to be adequate assuming non-composite behavior.

5.2.2 Constructability

The constructability of the main components of a glulam timber girder bridge is evaluated. The construction of this bridge system is generally fast and does not require skilled labor.

5.2.2.1 Glulam Girders

The glulam girders will be prefabricated in a controlled environment at the manufacturer's plant. A 34.5-ft wide bridge will consist of nine glulam girders. Onsite activities regarding the girders would be minimal since they would be prefabricated and ready to be installed on site.

The construction of a glulam timber girder bridge can be further accelerated if the bridge is prefabricated. The timber bridge construction can be in line with the accelerated bridge construction (ABC) paradigm if the bridge is prefabricated in one or more segments and shipped to the bridge site. This is especially favorable since wood is a relatively lightweight material.

5.2.2.2 Glulam Deck Panels

The glulam deck panels will be prefabricated in a controlled environment at the manufacturer's plant. Field installation of the deck panels can be relatively fast and requires minimal training and skills. The construction workers will place adhesive epoxy between the girders and the deck to complete the deck-to-girder connections. The amount and placement of epoxy and surface preparation should follow the epoxy manufacturer's requirements. As discussed in the previous section, a fully prefabricated bridge in line with the ABC paradigm does not need this step.

5.2.2.3 Glulam Cross Braces

The glulam cross braces will be prefabricated in a controlled environment at the manufacturer's plant. The field installation of glulam diaphragms is more involved than the other members, since diaphragms have to be placed perfectly between the girders. After alignment, the workers will drill lag bolts through the diaphragms into the girders. If the system is prefabricated, this process will be eliminated in the field.

5.2.3 Costs of Glulam Timber Girder Bridges

Table 5.2 presents material and fabrication costs for the superstructures of a 50-ft span, two-lane, glulam timber girder bridge and a modified double-tee bridge (new detailing based on Wehbe et al., 2016). The materials and fabrication cost for 46-in. wide by 23-in. deep precast double-tee girders is approximately $247 per linear foot, based on data provided by SDDOT. Nine double-tee girders are used in a 34.5-ft wide bridge. Therefore, the total superstructure material and fabrication cost for this bridge is approximately $111,000.

Table 5.2 Material and Fabrication Cost for Glulam Timber Girder Bridge and Modified Double-Tee Bridge Superstructures

Bridge System	Glulam Timber Girder Bridge	Modified Double-Tee Bridge
Materials/Fabrication ($)	78,000	111,000
Materials/Fabrication ($/sq. ft.)	45	64

The total material and fabrication cost estimated by the manufacturer for a 50-ft long and 34.5-ft wide glulam timber girder bridge is approximately $78,000. Therefore, the material and fabrication cost of this type of bridge is approximately 30% less than that for double-tee bridges. The transportation cost for glulam girder bridges is $2.65 per mile at the time of this writing. Additional costs, such as assembly, onsite activities, life cycle costs, and substructure fabrication and construction, should be added to the total bridge cost. Including the additional costs, glulam timber girder bridges are estimated to be 15% to 20% less costly to construct and install than the modified double-tee bridges.

5.3 Glulam Timber Slab Bridge Prototype

5.3.1 Performance under Service, Fatigue II and Strength I Limit States

Based on the ADTT of 15 for SD local roads, approximately 411,000 trucks will cross a bridge in 75 years. Since these types of bridges are very short span, each truck will count as two load cycles (the maximum moment will occur when each of the rear axles crosses the mid-span). The full-scale 16.5-ft long test bridge was subjected to 550,000 load cycles at the mid-span, which is equivalent to 50 years of traffic loading. The fatigue test was stopped at this load cycle since there was no damage to the bridge, and the stiffness did not degrade. The load at the mid-span corresponds to the maximum moment experienced by an interior deck panel of the prototype bridge based on the Fatigue II limit state loading specified in AASHTO (2013).

The test bridge stiffness remained constant throughout the 550,000 fatigue II loading (Fig. 5.7). The change in stiffness throughout the fatigue test was less than 1% with respect to the initial bridge stiffness. There was no apparent damage from the fatigue testing. Therefore, it can be concluded that this bridge system is adequate for the entire service life.

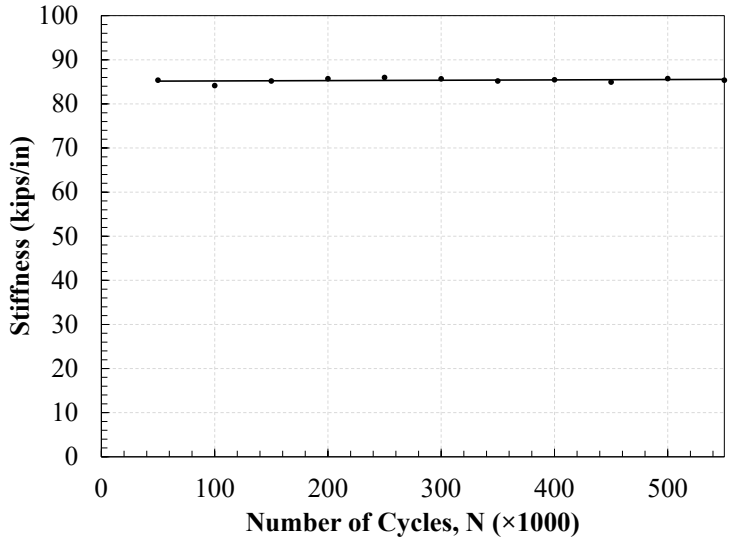

Figure 5.7 Stiffness of GlulamTimber Slab Bridge under Fatigue II Loading

The equivalent AASHTO (2013) service I limit state load was 44.8 kips and the strength I limit state load was 85.7 kips (Fig. 5.8). Note these limit state values are not the same for different bridges due to their geometry. The test bridge did not crack up to 270 kips, where the test was stopped due to setup limitations. This indicates that the bridge design was adequate. No significant damage was observed in the deck panels and stiffeners under the ultimate loading. The glulam slab timber bridge was found to be a viable option for short spans on local roads.

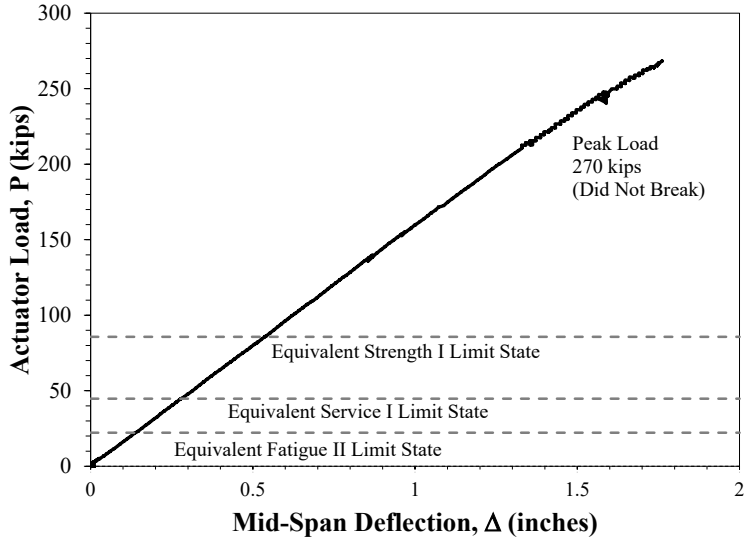

Figure 5.8 Measured Force-Displacement Relationship – Strength Testing of Glulam Timber Slab Bridge

5.3.2 Constructability

The constructability of the main components of a glulam timber slab bridge was evaluated. The construction of this bridge system is relatively fast and does not require highly skilled labor.

5.3.2.1 Glulam Deck Panels

The glulam deck panels will be prefabricated in a controlled environment at the manufacturer's plant. A two-lane bridge with shoulders on both sides will consist of eight glulam deck panels. Onsite construction will be minimal since the only onsite work will be to place the panels and to anchor them at the ends. The construction can be further accelerated if the entire bridge is prefabricated.

5.3.2.2 Glulam Stiffeners

The glulam stiffeners will also be constructed in a controlled environment at the manufacturer's plant. Glulam stiffeners can be installed very rapidly in the field. The construction workers need to clamp the stiffeners to the deck panels, and then install stiffener-to-deck lag bolts from the underside of the bridge. The onsite installation of stiffeners can be eliminated if the bridge is prefabricated in line with the ABC paradigm.

5.3.3 Costs of Glulam Timber Slab Bridges

Table 5.3 presents a comparison of superstructure materials and fabrication costs for a timber slab bridge to a modified double-tee bridge with a 16.5-ft length and a 34.5-ft width. The materials and fabrication cost for double-tee girder bridges is approximately $64 per square foot. Note that the estimated cost of the double-tee bridge was the cost per square foot for a bridge with a 50-ft length and a 34.5-ft width.

Table 5.3 Material and Fabrication Cost for Glulam Timber Slab Bridge and Modified Double-Tee Bridge Superstructures

Bridge System	Glulam Timber Slab Bridge	Modified Double-Tee Girders Bridge
Materials/Fabrication ($)	17,000 (for 16.5-ft long 34.5-ft wide bridge)	111,000 (for 50-ft long 34.5-ft wide bridge)
Materials/Fabrication ($/sq. ft.)	30	64

The total material and fabrication cost estimated by the manufacturer for a 16.5-ft long by 34.5-ft wide glulam timber slab bridge is approximately $17,000. Therefore, the material and fabrication cost of a glulam timber slab bridge superstructure is approximately half that of modified double-tee girder bridge superstructure.

The transportation cost for glulam timber slab bridges is $2.65 per mile at the time of this writing. Additional costs, such as assembly, onsite activities, and substructure fabrication and construction, should be included in the total bridge cost. In summary, the cost of glulam slab bridges is expected to be 50% of that of double-tee bridges. However, direction comparison could not be made due to span length differences.

5.4 Application of Proposed Bridge Systems

The three proposed bridge systems can span a wide range of terrains. Figure 5.9 shows the recommended span length for each tested system based on the structural performance of the bridge test models, material availability in South Dakota, and the constructability. The depth of each system should be calculated based on the load combinations and span length. The overall precast bridge depth is comparable to current double-tee bridge depths. The overall depth of glulam timber girder bridges will be 50% more than that for current double-tee bridges. The overall depth of glulam timber slab bridges is less than that for double-tee bridges.

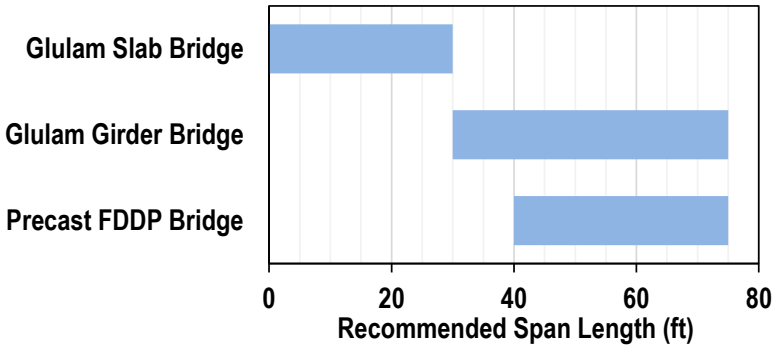

Figure 5.9 Recommended Span Length for Three Proposed Bridge Systems

Table 5.4 presents a summary of the cost estimate for the three bridges. It can be concluded that the proposed timber bridges are the most cost-effective options compared with double-tee bridges.

Table 5.4 Material and Fabrication Costs for Three Proposed Bridge Systems

Bridge System	Glulam Timber Slab Bridge	Modified Double-Tee Girders Bridge
Precast FDDP Bridge	$74 / sq. ft	$64 / sq. ft
Glulam Girder Bridge	$45 / sq. ft	
Glulam Slab Bridge	$30 / sq. ft	

6. RECOMMENDATIONS AND BENEFITS

6.1 Recommendations

Based on the findings of this study, the research team offers the following recommendations.

6.1.1 Recommendation 1: Precast Full-Depth Deck Panel Bridges

The guidelines, as detailed in Section A.1 of Appendix A, should be adopted for the construction of "precast full-depth deck panel bridges." A span length of 40 ft to 70 ft is recommended for this bridge type.

Precast full-depth deck panel bridges generally consist of precast inverted tee girders and precast full-depth deck panels. The test results of a full-scale 50-ft long precast full-depth deck panel bridge showed that this bridge type is a viable alternative to double-tee girder bridges, which are common in South Dakota. To minimize durability issues due to cold joints, (1) only hidden pocket detailing was allowed, (2) all bridge deck reinforcement was recommended to be epoxy coated, and (3) hollow structural steel sections, which are used to reduce the splice length, were recommended to be galvanized. These precast bridges with the recommended span lengths are constructible in South Dakota and may cost slightly more than double-tee bridges.

6.1.2 Recommendation 2: Glulam Timber Girder Bridges

The guidelines, as detailed in Section A.2 of Appendix A, should be adopted for the construction of "glulam timber girder bridges." A span length of 30 ft to 70 ft is recommended for this bridge type.

Glulam timber girder bridges generally consist of glulam girders, glulam deck panels, and diaphragms. The test results of a full-scale 50-ft long glulam girder bridge showed that this bridge type is a viable alternative to double-tee girder bridges. Glulam timber bridges with the recommended span lengths can be fabricated in South Dakota and will be more cost-effective than double-tee bridges.

6.1.3 Recommendation 3: Glulam Timber Slab Bridges

The guidelines, as detailed in Section A.3 of Appendix A, should be adopted for the construction of "glulam timber slab bridges." A span length of 30 ft or less is recommended for this bridge type.

Glulam timber slab bridges generally consist of glulam deck panels and glulam stiffeners. The test results of a full-scale 16.5-ft long glulam slab bridge showed that this bridge type is a viable alternative to double-tee girder bridges. Currently, glulam slab bridges with a span length of 20 ft can be fabricated in South Dakota and will be more cost-effective than double-tee or glulam timber bridges.

6.2 Research Benefits

Numerous bridges in South Dakota need replacement due to deterioration. The expected design life of these existing bridges was 75 years, but some built less than 40 years ago already need replacement. The double-tee precast girder bridge is the standard bridge system used on SD local roads. The most common problem in double-tee bridges is that longitudinal joints deteriorate over time, most likely due to inadequate shear transfer between girders, allowing water and debris to enter the joints. It is only a matter of time before the joint begins to spall, creating a path for moisture to reach the prestressing steel, initiate corrosion, and degrade the structural capacity of the bridge.

Facing limited budgets, local governments in the state need a durable and inexpensive bridge system that is easy to construct and will last for at least 75 years. Three new bridge systems were proposed and tested through full-scale experiments. Those systems included a fully precast bridge, a glulam timber girder bridge, and a glulam timber slab bridge. It was found that all three bridge systems are viable alternatives to the currently used double-tee bridges.

Each proposed system is suitable for a certain range of span length, as discussed under Sec. 5.4. The cost of the three new bridge systems is comparable to or lower than the cost of double-tee bridges, as discussed under Sec. 5.4. However, the proposed timber bridges offer the highest cost saving compared with double-tee and the precast bridges. The overall precast bridge depth is comparable to current double-tee bridge depths, especially for long spans (e.g., more than 50 feet). The overall depth of glulam timber girder bridges will be 50% more than that for current double-tee bridges. However, the overall depth of glulam timber slab bridges is less than that for double-tee bridges.

Local governments will now have four options (three proposed systems in the present study and the modified double-tee girder bridge proposed by Wehbe et al., 2016) when planning to construct a new bridge or to replace an old one on local roads in South Dakota.

7. CONCLUSIONS

Based on design, construction, full-scale testing, and cost estimation for the three proposed bridge systems, the following conclusions can be drawn.

7.1 Fully Precast Full-Depth Deck Panel Bridge

- The proposed construction process does not require advanced technology and was relatively simple.
- The proposed bridge system did not exhibit any sign of deterioration or water leakage through 500,000 Fatigue II load cycles (91 service years assuming ADTT = 15) and an additional 150,000 Fatigue II load cycles adjacent to the interior panel transverse joints (27 service years). The bridge's overall stiffness essentially remained the same throughout the fatigue testing.
- Shrinkage cracks were observed in almost all full-depth shear pockets, all transverse joints, and grouted haunch regions at 125,000 load cycles. Shrinkage cracks in the haunch can be minimized by using two longitudinal reinforcing steel bars placed in the haunch region.
- The first horizontal shear cracks in the grouted haunch region were observed at an actuator load of 200 kips, which was higher than the equivalent AASHTO (2013) Strength I limit state load of 131.4 kips.
- Both inverted U-shape shear studs and double headed shear studs performed adequately throughout the entire fatigue testing, as well as the ultimate testing.
- The hidden pocket detail was found to be a better alternative than the full-depth pockets since they provide better durability. Shrinkage cracks were observed in almost all full-depth pockets, but none for hidden pockets.
- The test bridge girders did not crack until the applied load exceeded the equivalent Strength I limit state load, indicating adequate design and performance.
- No significant damage in addition to the shrinkage cracks was observed throughout the entire fatigue testing, and the overall bridge stiffness remained the same.
- The superstructure material and fabrication cost of the proposed system for a 50-ft long by 34.5-ft wide bridge is 11% higher than that for a double-tee bridge with the same bridge geometry.

Overall, it can be concluded that the proposed bridge system, full-depth deck panels supported on inverted tee girders, is a viable alternative to the precast double-tee girder bridges.

7.2 Glulam Girder Bridge

- Construction of a glulam girder bridge is fast and does not require advanced technology or skilled labor.
- The girder bridge did not exhibit any signs of deterioration throughout the 500,000 AASHTO (2013) Fatigue II load cycles (equivalent to 91 years of service life) and the bridge's overall stiffness essentially remained constant throughout the fatigue testing.
- Damage of tongue-and-groove deck-to-deck connections was observed at 250,000 load cycles (equivalent to 45 years of service life). The damage can be eliminated by connecting flat deck panels with epoxy instead of using a tongue-and-groove connection.
- Although there was partial composite action, it was not sufficient to warrant composite design. The girders should be designed fully non-composite.
- The epoxy connection for the deck-to-girder connection in the girder bridge performed adequately throughout all testing phases.
- The girder bridge did not meet the AASHTO (2013) service and strength limit state requirements under strength testing because a wrong grade of wood was used in the fabrication by mistake.

- A calculation of the bridge capacity assuming non-composite behavior and as-built material properties and bridge geometry led to accurate estimation of the bridge test model's capacities. Therefore, the current AASHTO (2013) design method for this type of bridge is valid.
- The superstructure cost for a 50-ft long by 34.5-ft wide glulam girder bridge is 70% of that for a double-tee bridge with the same bridge geometry.

Overall, it can be concluded that glulam girder bridges are viable alternatives to the precast double-tee girder bridges, the type most commonly used in South Dakota.

7.3 Glulam Slab Bridge

- Construction of a glulam slab bridge is fast and does not require advanced technology or skilled labor.
- The glulam slab bridge stiffness did not degrade through the 550,000 AASHTO (2013) Fatigue II load cycles (equivalent to 50 years of service life).
- No damage was observed at an actuator load of 270 kips, which was three times higher than the AASHTO (2013) Strength I limit state load of 85.7 kips. The test was stopped due to setup limitations.
- The superstructure cost per square foot for a 16.5-ft long by 34.5-ft wide glulam slab bridge is only 50% of that for a typical double-tee bridge with the same geometry.

Overall, it can be concluded that glulam slab bridges are viable alternative to the precast double-tee girder bridge, the type most commonly used in South Dakota.

8. REFERENCES

Aaleti, S., and Sritharan, S. (2014). "Design of Ultrahigh-Performance Concrete Waffle Deck for Accelerated Bridge Construction." *Transportation Research Record: Journal of the Transportation Research Board, No. 2406*. Transportation Research Board of the National Academies, Washington, D.C., pp. 12-22, DOI: 10.3141/2406-02.

Aktan, H., and Attanayake, U. (2013). "Improving Bridges with Prefabricated Precast Concrete Systems." Report No. RC-1602. Western Michigan University. , Kalamazoo, MI. Retrieved from *https://www.michigan.gov/documents/mdot/RC-1602_Part_1_444145_7.pdf.*

AASHTO (2013). "AASHTO-LRFD Bridge Design Specifications, Sixth Edition." American Association of State Highway and Transportation Officials, Washington, DC.

ASTM A370 (2011). "Standard Test Methods and Definitions for Mechanical Testing of Steel Products." American Society for Testing Materials, West Conshohocken, PA.

ASTM C39 (2010). "Standard Test Method for Compressive Strength of Cylindrical Concrete Specimens." American Society for Testing Materials, West Conshohocken, PA.

ASTM C109 (2010). "Standard Test Method for Compressive Strength of Hydraulic Cement Mortars (Using 2-in. Cube Specimens)." American Society for Testing Materials, West Conshohocken, PA.

ASTM C143 (2010). "Standard Test Method for Slump of Hydraulic-Cement Concrete." American Society for Testing Materials, West Conshohocken, PA.

ASTM C231 (2010). "Standard Test Method for Air Content of Freshly Mixed Concrete by the Pressure Method." American Society for Testing Materials, West Conshohocken, PA.

Badie, S., Baishya, M., and Tadros, M. (1998). "NUDECK – An Efficient and Economical Precast Prestressed Bridge Deck System." *PCI Journal*, *43*(5), pp. 56-74. DOI: 10.15554/pcij.09011998.56.74.

Badie, S., Tadros, M, and Girgis, A. (2006). "Full-Depth, Precast-concrete Bridge Deck Panel Systems." NCHRP Report No. 12-65, TRB. National Research Council, Washington, D.C. Retrieved from *www.trb.org/notesdocs/nchrp12-65_fr.pdf.*

Badie, S., and Tadros, M. (2008). "Full-Depth Precast Concrete Bridge Deck Panel Systems." NCHRP Report No. 584, TRB. National Research Council, Washington, D.C., Retrieved from *https://www.scribd.com/document/220593817/nchrp-rpt-584.*

Badie, S., and Tadros, M. (2008). "Full-Depth Precast Concrete Bridge Deck Panel Systems." NCHRP Report No. 584 Appendix, TRB. National Research Council, Washington, D.C., Retrieved from *https://www.scribd.com/document/220593817/nchrp-rpt-584.*

Baer, C. (2013). "Investigation of Longitudinal Joints between Precast Prestressed Deck Bulb Tee Girders Using Latex Modified Concrete." M.S. Thesis. Columbia, SC: University of South Carolina. Retrieved from http://scholarcommons.sc.edu/etd/2452.

BASF Corporation (2011). "Placement of Latex Modified Concrete." Charlotte, NC: BASF Corporation.

Brashaw, B., Wacker, J., and Jalinoos, F. (2013). "Field Performance of Timber Bridges: A National Study." International Conference on Timber Bridges, Las Vegas, NV. pp. 1-12. Retrieved from http://www.woodcenter.org/docs/ICTB2013/technical/papers/ID_132_BRASHAW.pdf

California Department of Transportation (2012). "Bridge Design Manual." Sacramento, CA: Caltrans.

Carnahan, Z.C. (2017). "Glulam Timber Bridges for Local Roads," MS Thesis, South Dakota State University, 182 pp., Available at: https://openprairie.sdstate.edu/etd/1173/.

Computers and Structures, Inc. (2016). "CSi Bridge, Version 18." Berkeley, CA.

Computers and Structures, Inc. (2016). "SAP2000, Version 18." Berkeley, CA.

Chandra, V. and Kim, J. (2012). "World's First Recycled Plastic Bridges." *Proc., Integrating Sustainable Practices in the Construction Industry*, Kansas City, MO, pp. 585-593. Retrieved from *ascelibrary.org/doi/abs/10.1061/41204%28426%2972.*

Ekholm, K. (2013). "Performance of Stress-Laminated-Timber Bridge Decks." Chalmers University of Technology, Gothenburg, Sweden. Retrieved from *publications.lib.chalmers.se/records/fulltext/183986/183986.pdf.*

Erie Canal Bridge. (2014). Retrieved from http://laminatedconcepts.com/.

Erikkson Technologies, Inc. (2011), "PSBEAM, Version 4.27." Temple Terrace, FL.

Federal Highway Administration. (2012a). "Bridge Inspector's Reference Manual." Retrieved from https://www.fhwa.dot.gov/bridge/nbis/pubs/nhi12049.pdf.

Federal Highway Administration. (2012b). "Deficient Bridges by State and Highway System." Retrieved from https://www.fhwa.dot.gov/bridge/nbi/no10/defbr12.cfm.

Franke, S., Franke, B., and Harte, A. (2015). "Failure Modes and Reinforcement Techniques for Timber Beams - State of the Art." *Construction and Building Materials,* Vol. 97, pp. 2-13. Retrieved from https://doi.org/10.1016/j.conbuildmat.2015.06.021.

Grace, N., Enomoto, T., Baah, P., Bebawy, M. (2012). "Innovative CFCC Prestressed Decked Bulb T Beam Bridge System." *Proc., Innovative Infrastructures- Toward Human Urbanism*, IABSE, Seoul, Korea, pp. 1-8, DOI: 10.2749/222137912805110394.

Graybeal, B. (2010). "Behavior of Field-Cast Ultra-High Performance Concrete Bridge Deck Connections under Cyclic and Static Structural Loading." Report No. FHWA-HRT-11-023, Federal Highway Administration, McLean, VA. Retrieved from *https://ntl.bts.gov/lib/35000/35400/35413/FHWA-HRT-11-023.pdf.*

Hoadley, R.B. (1980). *Understanding Wood: A Craftsman's Guide to Wood Technology.* Newton, CT.: Taunton Press.

Hosteng, T. (2013). "Advances in Timber Bridge Design." 2013 Annual Conference, National Association of County Engineers, Des Moines, IA.

Idaho Transportation Department (IDT) (2015). "Idaho Manual for Bridge Evaluation." ITD, Boise, ID Retrieved from *apps.itd.idaho.gov/apps/bridge/manual/IMBE2016.pdf.*

Ji, H.S., Son, B.J., and Chang, S.Y. (2007). "Field testing and capacity-ratings of advanced composite materials short-span bridge superstructures." *Composite Structures*, 78(2), pp. 299-307, Retrieved from https://doi.org/10.1016/j.compstruct.2005.10.014.

Jones, A., and Oppong, K. (2015). "Structure Alternatives for Local Roads." Report No. SD2013-06, South Dakota State University, Brookings, SD.

Joyce, P. (2014). "Development of Improved Connection Details for Voided Slab Bridges." MS thesis, Civil Engineering. Virginia Polytechnic Institute and State University, Blacksburg, VA. Retrieved from https://vtechworks.lib.vt.edu/bitstream/handle/10919/49108/Joyce_PC_T_2014.pdf?sequence=1.

Konrad, M. (2014). "Precast Bridge Girder Details for Improved Performance." M.Sc. Thesis, South Dakota State University, Brookings, SD.

Mingo, M.J. (2016), "Precast Full-Depth Deck Panels Supported on Inverted Bulb-Tee Bridge Girders," MS Thesis, South Dakota State University, 208 pp., Available at: https://openprairie.sdstate.edu/etd/1093/.

Pirayeh Gar, S., Head, M., Hurlebaus, S., and Mander, J. (2013). "Comparative Experimental Performance of Bridge Deck Slabs with AFRP and Steel Precast Panels." *Journal of Composite Construction*, 17(6), 04013014. Retrieved from https://doi.org/10.1061/(ASCE)CC.1943-5614.0000380#sthash.w7ngAdsc.dpuf.

Ritter, M.A. (1990). "Timber Bridges: Design, Construction, Inspection, and Maintenance." Washington, D.C., 944 p. Retrieved from *https://www.fpl.fs.fed.us/documnts/misc/em7700_8--entire-publication.pdf.*

Ritter, M.A., Faller, R.K., Lee, P.D.H., Rosson, B.T., and Duwadi, S.R. (1995). "Plans for Crash-Tested Bridge Railings for Longitudinal Wood Decks." United State Department of Agriculture, Forest Service, General Technical Report FPL-GTR-87, http://www.woodcenter.org/docs/fplgtr87.pdf.

Ritter, M.A., Faller, R.K., Lee, P.D.H., Rosson, B.T., and Duwadi, S.R. (1998). "Plans for Crash-Tested Wood Bridge Railings for Concrete Decks." United State Department of Agriculture, Forest Service, General Technical Report FPL-GTR-108, http://www.woodcenter.org/toolkit/guardrails/documents/FPL%20Files/fplgtr108.pdf.

Smith, M. (2014). "Timber Bridge Blog." *Laminated Concepts Inc*. retrieved from *laminatedconcepts.com/timber-bridge-blog/.*

Scholz, D., Wallenfelsz, J., Lijeron, C., and Roberts-Wollmann, C. (2007). "Recommendations for the Connection between Full-Depth Precast Bridge Deck Panel Systems and Precast I-Beams." Report No. FHWA/VTRC 07-CR17, Virginia Polytechnic Institute & State University, Charlottesville, Virginia. Retrieved from *www.virginiadot.org/vtrc/main/online_reports/pdf/07-cr17.pdf.*

Stenko, M.S. and Chawalwala, A.J. (2001). "Thin Polysulfide Epoxy Bridge Deck Overlays." *Transportation Research Record 1749*. 01(0154), pp. 64-67, Retrieved from https://doi.org/10.3141/1749-10.

Virginia Department of Transportation. (2005). "Prestressed Concrete Voided Slabs Preliminary Design Tables." Volume 5, Part 2, File 12.05-3. Retrieved from http://www.virginiadot.org/business/resources/pc-voidedslabs-12.pdf.

Wacker, J.P. and Smith, M.S. (2001). "Standard Plans for Timber Bridge Superstructures." U.S. Department of Agriculture, Forest Service, and Forest Products Laboratory, General Technical Report No. FPL-GTR-125, Madison, WI, 53 pp. Retrieved from *https://www.fpl.fs.fed.us/documnts/fplgtr/fplgtr125.pdf.*

Wehbe, N., Konrad, M., and Breyfogle, A. (2016). "Joint Detailing Between Double Tee Bridge Girders for Improved Serviceability and Strength." *Transportation Research Record: Journal of the Transportation Research Board, No. 2592,* Transportation Research Board of the National Academies, Washington, D.C. Retrieved from https://trid.trb.org/view.aspx?id=1393072.

Wenzlick, J.D. (May 2006). "Evaluation of Very High Early Strength Latex Modified Concrete Overlays." Organizational Results Research Report. Report No. OR06-004, Missouri Department of Transportation, Jefferson City, MO. Retrieved from *https://library.modot.mo.gov/RDT/reports/Ri04005/or06004.pdf.*

APPENDIX A: DESIGN AND CONSTRUCTION GUIDELINES

Based on the findings, the research team proposes the following design and construction guidelines for each of the three proposed bridge systems: fully precast full-depth panel bridge, glulam timber girder bridge, and glulam timber slab bridge.

A.1 Precast Full-Depth Deck Panel Bridges

The proposed design recommendations are based on the experimental data of the full-scale bridge test model with the proposed detailing. The construction recommendations are based on a literature review, fabricating and assembling of the test girders, and engineering judgment.

A.1.1 Inverted Tee Girders

Inverted tee girders should be designed and constructed using current codes and practices (e.g., AASHTO, 2013).

Note that the installation of shear studs in the inverted tee girders require tight construction tolerances to allow for proper embedment into the shear stud pockets in the deck.

A.1.2 Full-Depth Deck Panels

Full-depth deck panels should have a minimum thickness of 7 in. according to AASHTO (2013). The width of the full-depth deck panels is recommended to be the same as the bridge width (in the transverse direction), resulting in a single-grade for the bridge deck (Fig. A.1). Single-grade decks do not need longitudinal joints to connect precast panels, resulting in lower cost, faster construction, and improved durability. The length of each full-depth precast panel (in the longitudinal direction of the bridge) should not exceed 12 ft.

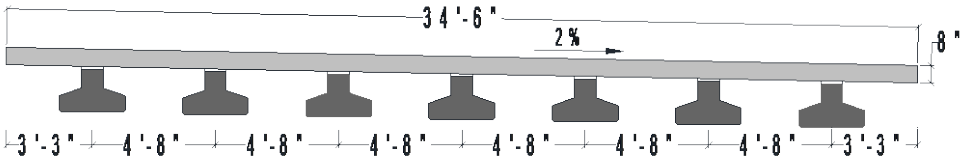

Figure A.1 Cross-Section of Precast Bridge System with Single-Unit Panel

If a crown along the longitudinal centerline is desired (deck with two grades), the precast panels should be connected with a longitudinal joint along the center of the bridge (Fig. A.2). Previous studies developed detailing for longitudinal joints (e.g., Baer, 2013; Aaleti and Sritharan, 2014). One of the proof tested longitudinal joint details is shown in Fig. A.3, which uses U-shape bars extending from two adjacent panels into the longitudinal joint to transfer shear and moment, and headed bars in the longitudinal direction of the bridge, to aid in developing the U-shape reinforcing steel bars.

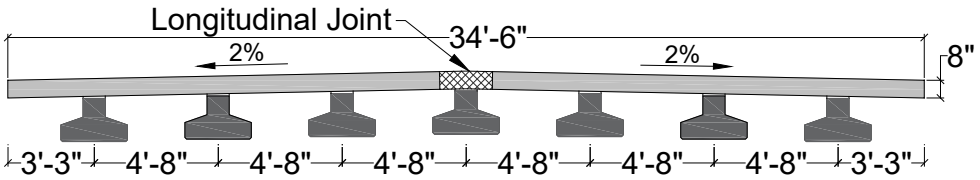

Figure A.2 Cross-Section of Fully Precast Bridge with Two-Unit Panels

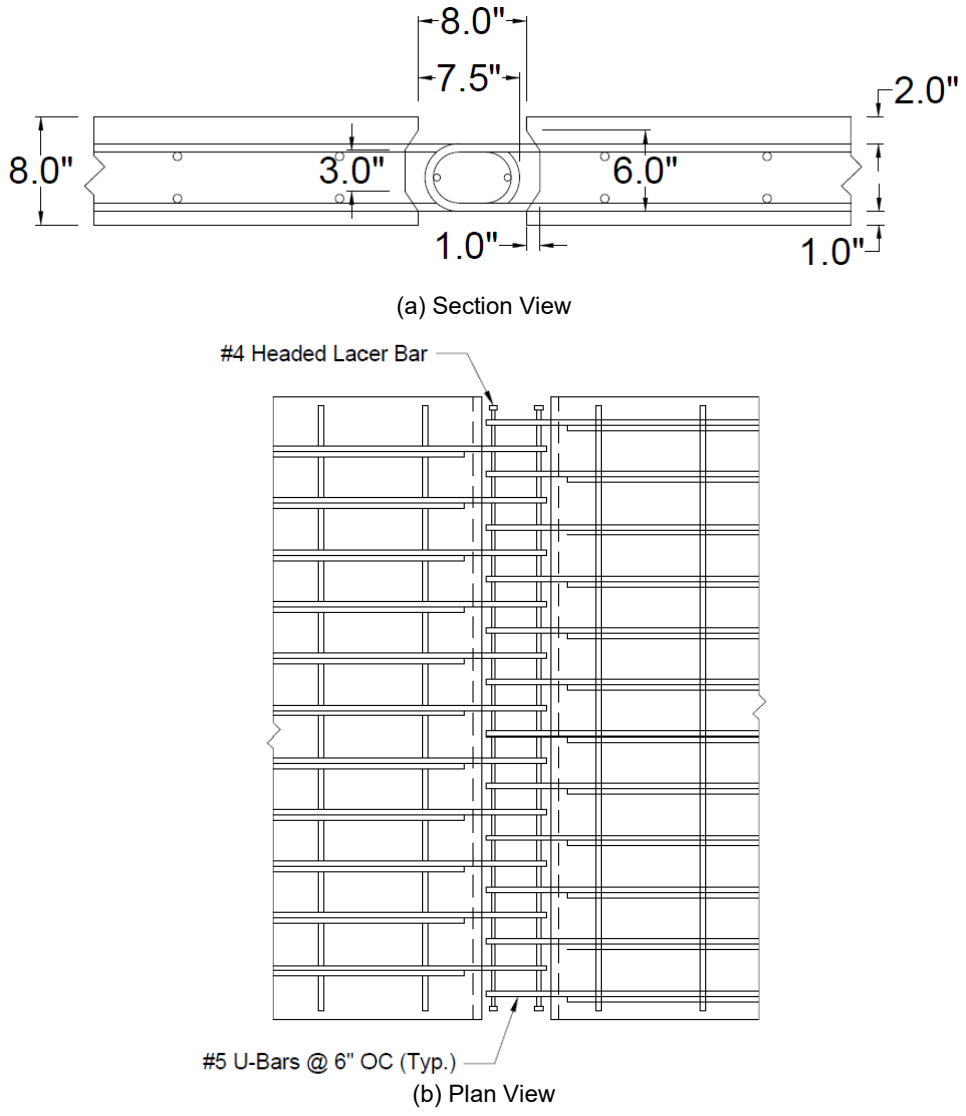

Figure A.3 Longitudinal Deck-to-Deck Joint Detailing in Fully Precast Bridge (after Baer, 2013)

The deck reinforcement should be designed according to a current code such as AASHTO (2013). All deck reinforcing steel bars should be epoxy coated to increase the durability of the deck against shrinkage cracks that may develop in the pockets, grouted haunch, and at the transverse joints.

A.1.2.1 Shear Pockets

The center-to-center spacing of the shear pockets should not exceed 24 in. according to Article 5.8.4.2 of AASHTO (2013). Only hidden pockets shall be used (Fig. A.4) since they provide better durability. Furthermore, the shear pockets should be designed to allow a minimum of 0.75-in. clear spacing between the shear studs and all side surfaces of the shear pockets. The hidden-pocket grout port diameter should be at least 2 in. to allow grout to be easily poured. Two 0.75-in. diameter vent ports should be provided on the opposite sides of the grout ports to avoid air pockets. The shear studs should be designed according to Section 5.8.4 of AASHTO (2013). The embedment length of shear studs into the pocket should not be less than six times the stud diameter ($6d_b$). AASHTO (2013) minimum concrete cover requirements should be followed for the studs in hidden pockets. Two types of shear studs, double-headed and inverted U-shape bars, are allowed to be inserted in hidden pockets (Fig. A.4). Full-depth pockets shall not be used since shrinkage cracks may develop at the edge of these pocket. The hidden pocket can be filled with conventional non-shrink grout. All pockets should be free of debris, oil, or any other foreign materials to ensure good bond.

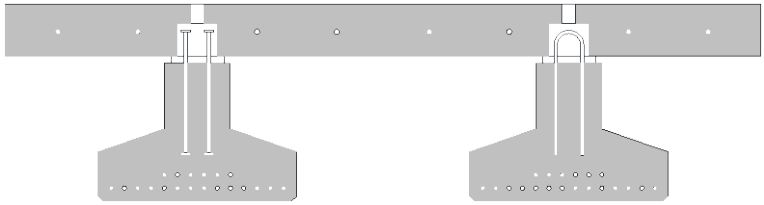

(a) Hidden Pockets – Transverse Section View

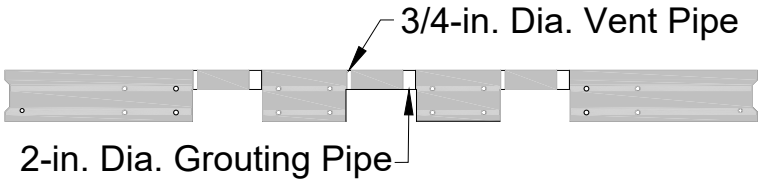

(b) Hidden Pockets – Longitudinal Section View

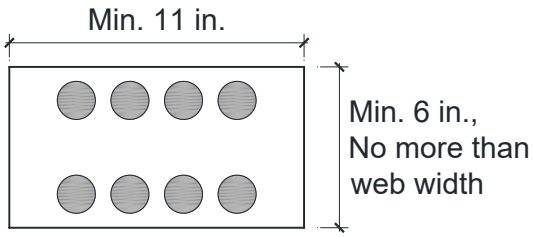

(c) Double Headed Studs Footprint

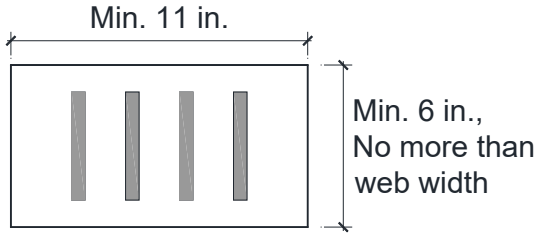

(d) Inverted U-Shape Bar Studs Footprint

Figure A.4 Proposed Detailing for Studs and Shear Pockets

A.1.2.2 Transverse Joints

Figure A.5 shows proposed female-to-female transverse joint detailing. A minimum gap of 2.75 in. in the longitudinal direction of the bridge should be provided between the precast panels. A reinforcing steel bar with the same type, grade, and size as those of the largest deck transverse reinforcement should be placed in the transverse joints. Steel dowels with the same type, grade, and size as those of the deck's largest longitudinal reinforcement should be spliced with the deck reinforcement (Fig. A.6). Hollow structural steel sections, which are used to reduce the splice length, should be galvanized to avoid

corrosion and to increase the bridge's overall durability. All transverse joints should be clean and free of debris or any foreign contaminant to ensure a good bond.

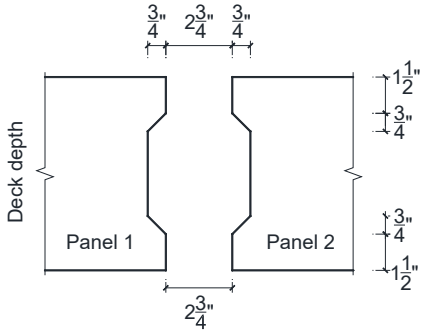

Figure A.5 Female-to-female Transverse Joint Detailing for Fully Precast Bridge

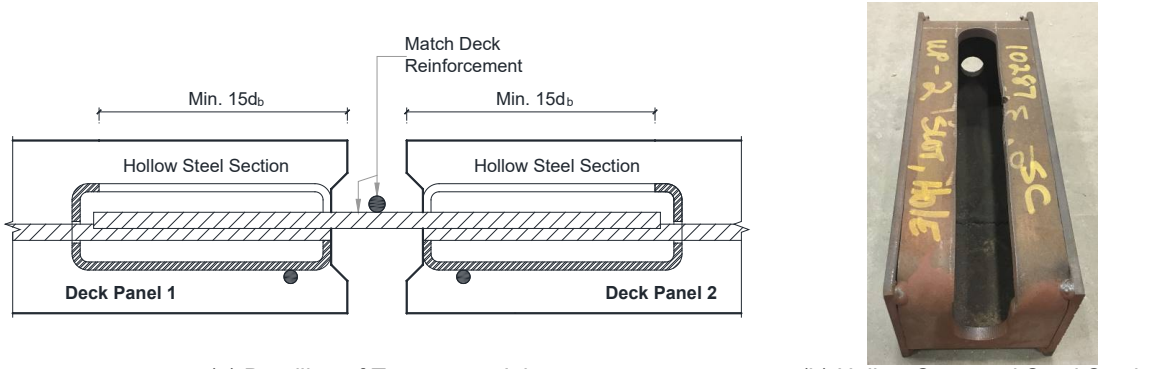

(a) Detailing of Transverse Joint (b) Hollow Structural Steel Section

Figure A.6 Transverse Joint Detailing for Fully Precast Bridge

A.1.2.3 Leveling Bolts

A minimum of four leveling bolts should be incorporated into each precast full-depth deck panel to adjust the grades (Fig. A.7). The bolts should be located above the centerline of the supporting girders. Each bolt should be designed to carry at least 25% of the weight of the precast panel. The use of long bolts in lieu of threaded rods with welded nuts is recommended.

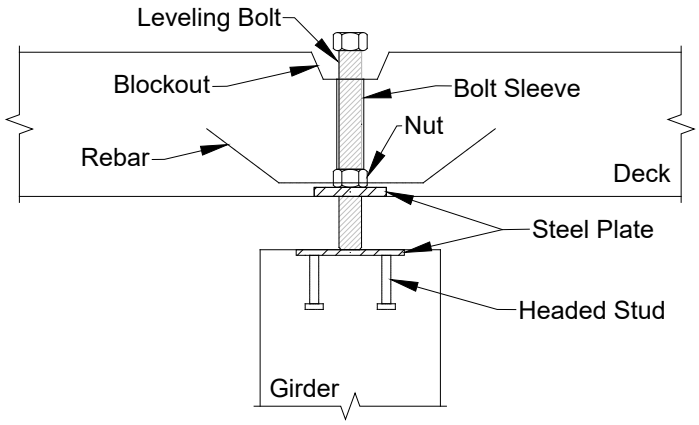

Figure A.7 Leveling Bolt Detailing for Fully Precast Bridge

A.1.3 Grouted Haunch

The haunch depth at the bridge mid-span should not be less than 0.75 in. to allow the grout to easily flow through the haunch and to avoid air pockets (Fig. A.8). A minimum of two longitudinal reinforcing steel bars should be placed in the haunch region and sized according to AASHTO Section 5.10.8 (2013) to eliminate shrinkage cracking (Fig. A.8).

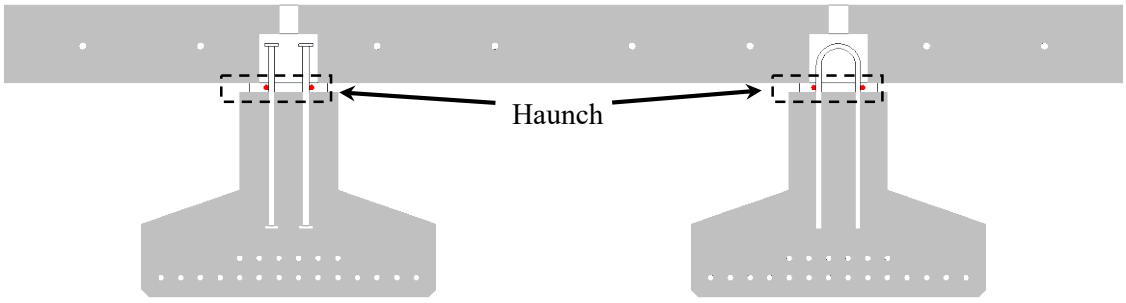

(a) Haunch Longitudinal Reinforcing Steel Bars Detailing

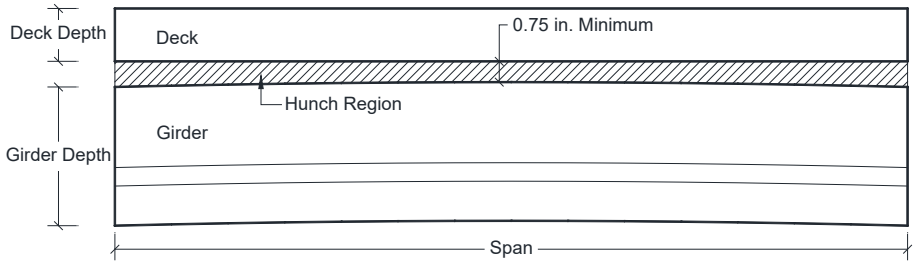

(b) Girder Elevation View

Figure A.8 Haunch Detailing for Precast Bridge

Several methods can be used to form the haunch from the top of the bridge. One example is shown in Fig. A.9, in which the form was made using threaded rods and anchorage plates to clamp plywood to the girder top flange. Compressible foam was glued to the top of the plywood to seal the haunch area after the panel placement.

Figure A.9 Grouted Haunch Formwork (Aktan and Attanayake, 2013)

A.2 Glulam Timber Girder Bridges

Design and construction guidelines are proposed for different components of glulam timber girder bridges (Fig. A.10) including: (1) glulam girders, (2) glulam deck panels, (3) diaphragms, (4) wearing surface, (5) railing system, and (6) abutments. Those components and inspection and maintenance recommendations are discussed herein.

Figure A.10 Typical Glulam Timber Girder Bridge

A.2.1 Glulam Girders

Glulam girders shall be designed fully non-composite meeting the requirements of current AASHTO (2013) bridge design standards. The base material type and properties shall be according to AASHTO (2013). The AASHTO does not specify the spacing between glulam girders. Nevertheless, a girder spacing of 3 to 6 ft generally results in the most cost effective design.

The type, rating, treatment, and geometry of the wood shall be verified and approved by the designer before fabrication of the girders. The girders shall be precision milled to allow the deck panels to form the crown and to meet the minimum camber required by AASHTO (2013).

A.2.2 Glulam Deck Panels

Glulam deck panels shall be at least 6 in. deep as required by AASHTO (2013). The width of the deck panels can cover either the full width of the bridge with one cross slope, or can cover one-half of the bridge width with two cross slopes (Fig. A.11).

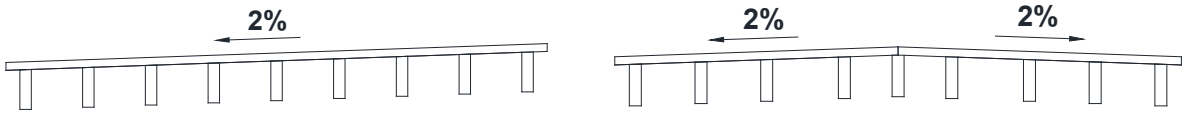

(a) Glulam Timber Girder Bridge with Single Cross Slope

(b) Glulam Timber Girder Bridge with Two Cross Slopes

Figure A.11 Cross-Section of Glulam Timber Girder Bridges

There would be a longitudinal joint directly above the middle girder when installing the bridge with two grades. The panel edges should be cut and prepared to minimize the gap at the joint. The gap should be filled with wood adhesive epoxy.

Compared with the wood used for glulam girders that is often Southern Pine, a weaker wood is often used for deck panels to minimize costs. The edge of each deck panel shall be straight then covered with epoxy to complete deck-to-deck connections in the longitudinal direction of the bridge, as shown in Fig. A.12.

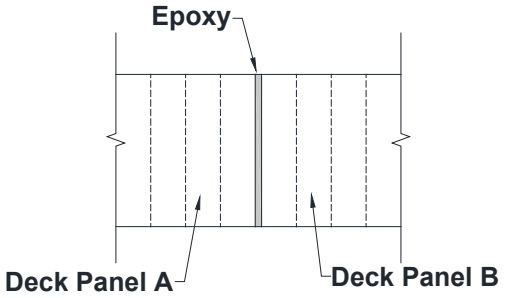

Figure A.12 Recommended Deck-to-Deck Connections for Glulam Girder Bridges

The deck panels can be connected to the girders using adhesive epoxy at the interface. Two rows of screws spaced no more than 18-in. apart along the length of the girder shall be incorporated to hold the panels and to activate the epoxy (Fig. A.13).

Figure A.13 Deck-to-Girder Connections for Glulam Timber Girder Bridges

A.2.3 Diaphragms

AASHTO (2013) allows the use of two types of diaphragms to be installed between the girders to improve the stability of the bridge: (1) solid glulam diaphragms (Fig. A.14a) and (2) steel cross braces (Fig. A.14b). Another type of diaphragm, glulam cross braces (Fig. A.14c), was used in the full-scale bridge test model of the present study and was found to be a viable alternative. All three options are recommended for field applications.

(a) Solid Glulam Diaphragm, (after Hosteng, 2013)

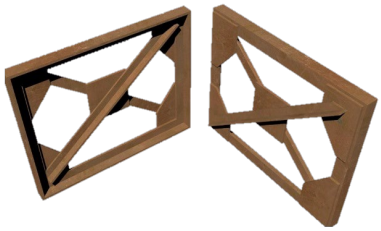

(b) Steel Cross Braces, (after etraxx.com)

(c) Glulam Cross Braces

Figure A.14 Three Types of Diaphragms for Glulam Timber Girder Bridges

A.2.4 Wearing Surface

The use of four types of wearing surfaces shall be allowed for glulam timber bridges: (1) asphalt overlay, (2) asphalt chip seal, (3) aggregate overlay, or (4) epoxy with embedded grit. Figure A.15 shows an example of each wearing type. Option (4) may be preferred to other methods since the wood natural cracks and joints will be filled with adhesive epoxy, which is compatible with glulam. Long term performance of the first three options confirmed that they are adequate, as long as they are well maintained.

(a) Asphalt Overlay

(b) Asphalt Chip Seal (after Gruen-Wald 2011)

(c) Aggregate Overlay

(d) Epoxy with Embedded Grit

Figure A.15 Different Types of Wearing Surfaces for Glulam Girder Bridges

A.2.5 Railing System

According to AASHTO (2013), a bridge railing system must be positioned to safely contain an impacting vehicle without allowing it to pass over, under, or through the rail elements. Furthermore, a proper railing system must be free of features that may catch on the vehicle or cause it to overturn or decelerate rapidly.

Any crash-tested railing configuration (details can be found in Ritter et al., 1995; and Ritter et al., 1998) or those designed according to AASHTO (2013) Section 13.7 can be used for timber bridges. Timber bridge components connected to rails shall be designed to resist the railing design loads. The rail material can be timber, metal, or concrete. Timber railings (Fig. A.16) are recommended for aesthetic reasons.

Figure A.16 Timber Railing for Timber Bridges

A.2.6 Abutments

Timber bridge abutments are typically constructed using either timber or concrete, as shown in Figure A.17. The connections should be designed to resist appropriate design loads (AASHTO, 2013). It is recommended that the existing abutments, if any, be modified for reuse to potentially save time and money. Bearing pads designed according to AASHTO (2013) shall be used to allow the girder to freely rotate.

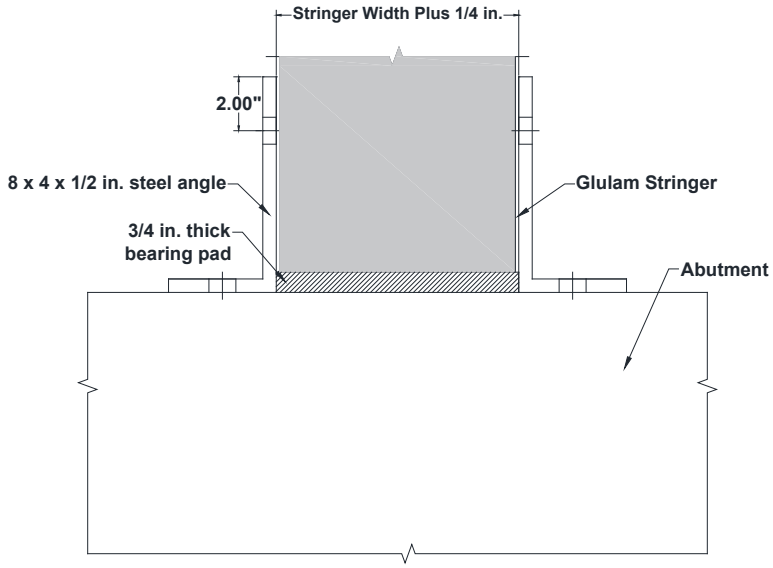

Figure A.17 Glulam Timber Bridge Girder-to-Abutment Sample Connection

A.2.7 Inspection and Maintenance

It is necessary to perform routine maintenance to keep the wearing surface and other exposed areas of the glulam timber girder bridge in good condition. It is also highly recommended that timber bridges be inspected every two years and any wood that is exposed be retreated every six years (Ritter, 1990). Retreatment can be done by spreading the preservative on the wood using a brush.

A.3 Glulam Timber Slab Bridges

Design and construction guidelines are proposed for different components of glulam timber slab bridges (Fig. A.18) including: (1) glulam deck panels, (2) glulam stiffeners, (3) wearing surface, (4) railing system, and (5) abutments. Those components, as well as the inspection and maintenance recommendations, are discussed herein.

Figure A.18 Typical Glulam Timber Slab Bridge

A.3.1 Glulam Deck Panels

Glulam deck panels shall be at least 6-in. deep as required by AASHTO (2013). The panel thickness shall be determined according to the AASHTO (2013) strength I limit state. The deck can be either sloped in one direction or crowned in the middle (Fig. A.19). The strong Southern Pine is recommended to be used for the deck panels due to high shear demand. All four edges of deck panels shall be cut and prepared with high precision to minimize the number and the width of fabrication joints.

(a) Slab Bridge with Single Cross Slope (b) Slab Bridge with Two Cross Slopes

Figure A.19 Cross-Section of Glulam Timber Slab Bridges

There would be a longitudinal joint directly at the center of the bridge when installing the bridge with two grades. The panel edges should be cut and prepared to minimize the gap at the joint. The gap should be filled with epoxy.

A.3.2 Glulam Stiffeners

According to current AASHTO (2013) standards, the product of the wood adjusted modulus of elasticity (E') and the moment of inertia (I) of a stiffener must be greater than 80,000 k-in^2. The minimum width of the stiffener is recommended to be 5 in. Each stiffener shall be made with the same material used in the deck panels.

Zinc-coated lag bolts shall be installed from the underside of the bridge to connect stiffeners to deck panels (Fig. A.20). The lag bolts shall not penetrate beyond 75% of the depth of the deck panels (Fig. A.20b) from underneath the deck. The lag bolts shall be at least 12 in. long with a diameter of 0.75 in. Two lag bolts shall be placed per panel on the stiffener.

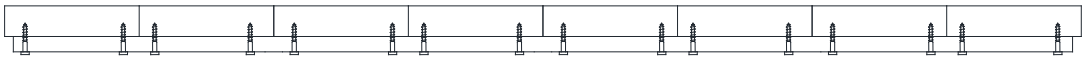

(a) Glulam Slab Timber Bridge Cross-Section

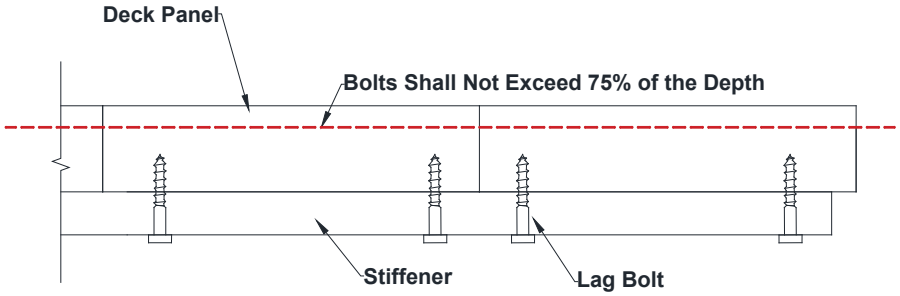

(b) Close-up of Two Panels

Figure A.20 Lag Bolt Requirements for Glulam Timber Slab Bridges

A.3.3 Wearing Surface

Refer to Sec. A.2.4 of the present report regarding the recommended wearing surfaces for timber bridges.

A.3.4 Railing System

Refer to Sec. A.2.5 of the present report regarding the recommended railing systems for timber bridges.

A.3.5 Abutments

Timber bridge abutments are typically constructed using either timber or concrete. The connections should be designed to resist appropriate design loads as required by AASHTO (2013). It is recommended that the existing abutments, if any, be modified for reuse to potentially save time and money. It is important that the abutment be completely flush with the deck panels to prevent point loads at the ends of the panels. Continuous bearing pads designed according to AASHTO (2013) shall be used for glulam timber slab bridges. The bridge panels shall be connected to the abutment using no more than two anchor bolts per panel, each with a minimum diameter of 0.75 in.

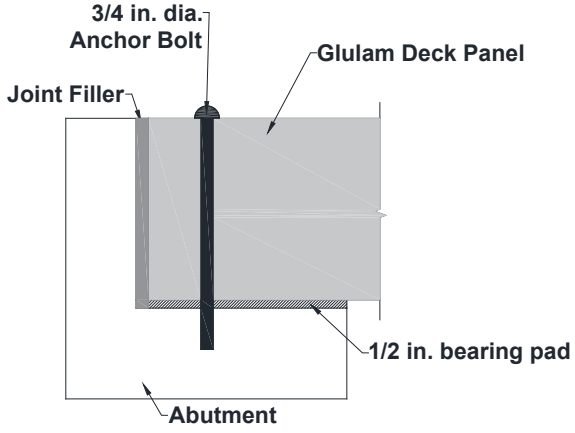

Figure A.21 Glulam Slab-to-Abutment Sample Connection

A.3.6 Inspection and Maintenance

Refer to Sec. A.2.7 of the present report regarding inspection and maintenance for timber bridges.